Réseaux de capteurs sans fils à faible consommation avec services de synchronisation haute précision et localisation

Thomas Beluch

THÈSE

En vue de l'obtention du

DOCTORAT DE L'UNIVERSITÉ DE TOULOUSE

Délivré par :
Institut National des Sciences Appliquées de Toulouse (INSA Toulouse)

Discipline ou spécialité :
Micro et NanoSystèmes

Présentée et soutenue par :
Thomas BELUCH
le : 2 avril 2013

Titre :

HIGH PRECISION SYNCHRONIZED MAC-PHY CROSS-LAYER DESIGNED WIRELESS SENSOR NETWORKS

JURY

Mme. Daniela DRAGOMIRESCU, Maître de Conférences - INSA Toulouse / LAAS CNRS
M. Christophe CHASSOT, Professeur - INSA Toulouse / LAAS CNRS
M. Jacques TURBERT, Ingénieur DGA

Ecole doctorale :
Génie Electrique, Electronique et Télécommunications (GEET)

Unité de recherche :
LAAS CNRS

Directeur(s) de Thèse :

Mme. Daniela DRAGOMIRESCU, Maître de Conférences - INSA Toulouse

Rapporteurs :
Mme. Nathalie ROLLAND, Professeur, IEMN / Université Lille1
M. Erchin SERPEDIN, Professeur, Texas A&M University

Thomas Beluch: *High Precision Synchronized MAC-PHY Cross-layer Designed Wireless Sensor Networks,*

Ohana means family.
Family means nobody gets left behind, or forgotten.

— Lilo & Stitch

Dedicated to the loving memory of Josette Beluch.
1926 – 2010

ACKNOWLEDGEMENTS

This is the place to express my thanks to many people without whom my doctoral thesis would not have been the same. First of all I want to express my thanks to Daniela Dragomirescu for her support and the excellent research environment she and all the MINC group provided. Next, I want to thank all the examiners for taking their time to read and evaluate my thesis. Thanks go also to the members of the characterization group, especially Alexandre Rumeau and Laurent Bary, for their help in building and using original test setups during the measurement campaigns and the sysadmin team (especially Marie Dominique Cabanne, Frederick Ruault and Julien Libourel) for their high responsiveness and competent help. A special thank goes to Eric Tournier for his help with the installation and use of the secure network. Thanks also go to people at CNFM, CMP and STMicroelectronics for making it possible for us to design, layout and tapeout top edge CMOS chips. My sincere thanks go also to all member of the MINC research group, especially the ones I were in closer contact with, for having made my almost four years at LAAS a pleasant experience. Thanks also for your practical help and the many technical discussions. Namely I want to mention the members of the Wireless Sensor Network team, which I worked with on a daily basis: Florian Perget, Mariano Ercoli, Vicent Puyal, Julien Henaut, and Aubin Lecointre . At the same I am grateful for the time I spent at INSA Toulouse during my entire cursus. Thanks to all I got to know there. Thanks also go to the different external project partners and suppliers I worked with, in particular CMP, CNFM, NXP Netherlands, STMicroelectronics, LeCroy, RedRapids, and many others. Furthermore, I want to acknowledge the principal source of nancial support of this thesis, namely the DGA. Finally, I want to thank my family for their support during these years, and for pushing me to put an end to this work. Special thank to those who nd themselves not on this list but deserve to be on it.

... and most importantly: Estelle, thanks for everything !

ABSTRACT

Wireless Sensor Networks have attracted mutch interest in the last decade, opening a new range of applications such as large area monitoring. However, a range of possible applications is still not satisfied due to strong blocking points remaining unsolved such as the lack of synchronization between measurements and low attainable data rates. This doctoral work aims at solving these two issues issue through the design of a Wireless Sensor node implementation. The proposed solution is based on cross-layer design and uses time-domain properties of UltraWide Band (UWB) to provide nanosecond-scale synchronization between nodes and high data-rate transmission. An ASIC implementation has been designed, and demonstrates a 2 ns synchronization error with IR-UWB modulation over a 1.5 GHz bandwidth. In this thesis, a cross-layer scheme named WiDeCS is proposed, and two proof of concept implementations are detailed.

Keywords: Wireless Sensor Networks, UltraWide Band, Synchronization, ASIC

RÉSUMÉ

Les réseaux de capteurs sans fil (WSN) ont attiré un grand intérêt dans la dernière décennie, et ont apporté des solutions dans un nombre croissant d'applications. Toutefois, certaines d'entre elles restent irréalisables en raison de forts points de blocage non résolus, comme un manque de synchronisation entre les prises de mesures, ainsi que des débits de données trop faibles. Ce travail apporte une solution à ces deux points majeurs via la conception d'un noeud communicant sans fil spécifique. Celle ci, basée sur la conception croisée, utilise les propriétés temporelles des modulations UltraLarge Bande (UWB) pour permettre une synchronisation très précise ainsi qu'un débit de données élevé. Notre démonstrateur ASIC basé sur ces travaux permet une précision de synchronisation de 2 ns pour une modulation IR-UWB sur une bande passante de 1,5 GHz. Cette thèse décrit le protocole de synchronisation WiDeCS et la conception de deux preuves de concept fonctionnelles sur FPGA et ASIC.

Mots clés : Réseaux de capteurs sans fil, Synchronisation, UltraLarge Bande, ASIC

CONTENTS

I COMMUNICATION IN WIRELESS SENSOR NETWORKS 21

1 INTRODUCTION TO COMMUNICATION IN WIRELESS SENSOR NETWORKS 23
- 1.1 Applications for Wireless Sensor Networks . . . 23
- 1.2 Communication for WSNs in an industrial context . . . 29
  - 1.2.1 Low data rate communications . . . 30
  - 1.2.2 High data rate communications . . . 32
  - 1.2.3 power-saving MAC protocols . . . 34
- 1.3 Services for WSNs . . . 38
  - 1.3.1 Clock synchronization and measurement trigger synchronization 38
  - 1.3.2 Distance evaluation for localization . . . 40
- 1.4 Conclusion . . . 43

2 UWB FOR WSN 45
- 2.1 Introduction to UltraWide Band Wireless communication . . . 45
  - 2.1.1 Main aspects . . . 45
  - 2.1.2 UWB modulation techniques . . . 45
  - 2.1.3 UWB channels: regulations and caracteristics . . . 47
- 2.2 IR-UWB . . . 49
  - 2.2.1 Principles and modulation techniques . . . 49
  - 2.2.2 IEEE 802.15.4a, a standard for IR-UWB communication for Wireless Sensor Networks . . . 51
  - 2.2.3 Low power implementations of IR-UWB transceivers . . . 55

II CROSS-LAYER DESIGN OF A HIGH DATA RATE SYNCHRONIZED WIRELESS SENSOR NETWORK COMMUNICATION INTERFACE 61

3 CROSS-LAYER DESIGN OF A UWB WIRELESS COMMUNICATION SYSTEM FOR WSN 63
- 3.1 System view: Cross layer considerations . . . 63
- 3.2 MAC Layer(s) . . . 64
  - 3.2.1 Fixed slot Time Division Multiple Access . . . 64
- 3.3 Specific Physical Layer Tuning . . . 65
  - 3.3.1 IR-UWB physical layer tuning . . . 65
- 3.4 Cross-layer services . . . 67
  - 3.4.1 Measurement trigger synchronization . . . 67

4 HARDWARE IMPLEMENTATIONS OF UWB COMMUNICATION SYSTEM FOR WSN 73
- 4.1 System Requirements . . . 73
  - 4.1.1 System for aircraft structure health monitoring . . . 73
  - 4.1.2 Reconfigurable tactical Impulse Radio UWB for communication and indoor localization . . . 74
- 4.2 Application specific improvements and simplifications . . . 75

4.3 Proposed system architecture . . . 76
4.4 Hardware simulations . . . 78
4.5 FPGA proof of concept . . . 81
4.5.1 Implementation details . . . 81
4.5.2 Measurement setup and results . . . 84
4.6 Mixed signal ASIC design flow . . . 87
4.6.1 Introduction and global view . . . 87
4.6.2 Input documents and data . . . 87
4.6.3 HDL implementation and behavioral simulation . . . 89
4.6.4 Synthesis and validation . . . 90
4.6.5 Floorplan design . . . 91
4.6.6 Place and Route and cell level DRC . . . 92
4.6.7 Layout operations . . . 94
4.7 ASIC proof of concept . . . 94
4.7.1 Implementation details . . . 94
4.7.2 Measurement setup and results . . . 97
4.8 Conclusion . . . 107

General Conclusion 111

Résumé en Français 115

2 INTRODUCTION AUX COMMUNICATIONS DANS LES RÉSEAUX DE CAPTEURS SANS FIL 3
2.1 Applications possibles . . . 3
2.2 Communications pour les WSN en environnement industriel . . . 4
2.2.1 Communications à bas débit . . . 4
2.2.2 Communications à haut débit . . . 4
2.2.3 Protocoles MAC à économie d'énergie . . . 5
2.3 Services pour les WSNs . . . 6
2.3.1 Synchronisation d'horloge et de prise de mesures . . . 6
2.4 Conclusion . . . 6

3 ULTRALARGE BANDE ET RÉSEAUX DE CAPTEURS SANS FIL 7
3.1 Introduction aux communications UltraLarge Bande (UWB) . . . 7
3.2 IR-UWB . . . 8
3.2.1 Principes et techniques de modulation . . . 8
3.2.2 IEEE 802.15.4a, la standardisation d'une modulation IR-UWB . . . 9
3.2.3 Implémentations faible consommation de transceivers IR-UWB . . . 10

4 CONCEPTION CROISÉE D'UN SYSTÈME DE COMMUNICATIONS UWB POUR WSN 11
4.1 Vue système et conception croisée . . . 11
4.2 Couche MAC à multiplexage temporel . . . 11
4.3 Optimisations dans la couche physique IR-UWB . . . 11
4.4 Services cross-layer : une synchronisation optimisée . . . 13

5 DÉMONSTRATEURS RÉALISÉS AUTOUR DE L'UWB ET WIDECS 15
5.1 Applications cibles . . . 15

5.1.1 Système pour le controle de santé des structures aéronautiques . 15
5.1.2 Radio tactique impulsionnelle UWB pour communication et localisation en intérieur . . . 15
5.2 Simulation matérielle . . . 16
5.3 Démonstrateur FPGA . . . 16
5.4 Preuve de concept ASIC . . . 17
5.5 Conclusion . . . 18

III APPENDIX 21

A FPGA IMPLEMENTATION FLOW 23
A.1 Introduction . . . 23
A.2 HDL Coding, and IP blocks implementation . . . 23
A.2.1 Conditions . . . 23
A.2.2 Signal versus variable . . . 25
A.2.3 On-chip buses . . . 25
A.2.4 chip's input / outputs . . . 26
A.3 Behavioral simulation . . . 26
A.4 Synthesis . . . 27
A.5 Place and Route . . . 27
A.6 In system debugging . . . 27

BIBLIOGRAPHY 31

LIST OF FIGURES

Figure 1 Example of a military oriented intrusion detection system 24
Figure 2 Example of a military oriented squad health monitoring equipment 25
Figure 3 Example of an in-flight testing context 26
Figure 4 Examples of monitored buildings 27
Figure 5 Example of a flood detection context 29
Figure 6 IEEE 802.15.4 cluster tree architecture 31
Figure 7 UWB versus narrowband 46
Figure 8 3.1 GHz - 10.6 GHz UWB regulations in selected regions 48
Figure 9 60 GHz band regulations in selected regions 49
Figure 10 Delay spread of IR-UWB signal 51
Figure 11 IEEE 802.15.4a UWB band plan 54
Figure 12 Proposed cross-layer system 64
Figure 13 Time Division Multiple Access channel occupation 65
Figure 14 IR-UWB transceiver 65
Figure 15 Piconet architecture 67
Figure 16 Latencies involved and flag positioning for WiDeCS 68
Figure 17 Exchange of timing information 68
Figure 18 Proposed system architecture 77
Figure 19 Hardware simulation setup 78
Figure 20 Full working synchronization and localization in hardware simulations 79
Figure 21 Effect of cluster tree architecture on synchronization 80
Figure 22 Hardware simulation of a fast changing channel's effect on Time of Flight (ToF) estimation 81
Figure 23 RF front-end for the FPGA demonstrator 83
Figure 24 Block diagram of the proposed FPGA demonstrator 84
Figure 25 Block diagram of the proposed FPGA demonstrator 85
Figure 26 Scope captures of the FPGA demonstrator 86
Figure 27 ASIC Flow 88
Figure 28 Chip floorplan with all pads and corner cells implemented 92
Figure 29 Chip floorplan with all pads and corner cells implemented 93
Figure 30 Floorplan of WIDEMACV1 chip 94
Figure 31 WIDEMACV1 chip 96
Figure 32 Probe station setup for transmitted signal analysis 98
Figure 33 Time domain DAC output of WIDEMACV1, scope display 99
Figure 34 Spectrum analysis of WIDEMACV1, scope display 100
Figure 35 Details of a data transmission occuring in a time slot 100
Figure 36 Setup for full connectivity check including PHY TX and RX, MAC, synchronization and localization 101

Figure 37 WIDEMACV1 test board . . . 102
Figure 38 Face to face test modes . . . 103
Figure 39 Histogram of delays between measurement triggers on master and slave nodes . . . 104
Figure 40 Synchronization stability versus clock drift between nodes (@3GHz base clock frequency) . . . 105
Figure 41 Power consumption versus clock frequency . . . 107
Figure 42 Comparaison bande étroite / UWB . . . 8
Figure 43 Etalement des échos sur l'IR-UWB . . . 9
Figure 44 Système proposé . . . 12
Figure 45 Délais successifs lors d'une transmission d'information sur un réseau sans fil . . . 13
Figure 46 Echange d'informations de délais . . . 14
Figure 47 Schema bloc du démonstrateur . . . 16
Figure 48 WIDEMACV1 - vue CAO . . . 18
Figure 49 FPGA Flow . . . 29

LIST OF TABLES

Table 1 Quantitative performance comparison of synchronization protocols 41
Table 2 IEEE 802.15.4a UWB frequency bands . . . 53
Table 3 State of the art UWB systems . . . 59
Table 4 Performance with face to face setup . . . 106
Table 5 Comparison with state of the art UWB systems . . . 108

ACRONYMS

ACK	Acknowledgement
ADC	Analog-to-Digital Converter
AEA	Adaptive Election Algorithm
AGC	Automatic Gain Control
AHB	Advanced High-performance Bus

AMBA	Advanced Microcontroller Bus Architecture
AoA	Angle of Arrival
ASIC	Application-Specific Integrated Circuit
ASK	Amplitude Shift Keying
B-MAC	Berkeley Media Access Control
BER	Bit Error Rate
BPSK	Binary phase-shift keying
CBR	Constant Bit Rate
CCA	Clear Channel Assessment
CCA	Clear Channel Assessment
CDMA	Code Division Multiple Access
CMOS	Complementary Metal Oxide Semiconductor
CNRS	Centre National de la Recherche Scientifique
COTS	Commercial Off-The-Shelf
CPU	Central Processing Unit
CS	Carrier Sense
CSMA-CA	Carrier Sense Multiple Access with Collision Avoidance
CSMA-CA	Carrier-Sense Multiple Access with Collision Avoidance
CSMA	Carrier-Sense Multiple Access
CTS	Clear To Send
DAC	Digital-to-Analog Converter
DDS	Direct Digital Synthesizer
DK	Design Kit
DSP	Digital Signal Processing
DSSS	Direct-Sequence Spread Spectrum
DVFS	Dynamic Voltage and Frequency Scaling
EHF	Extremely High Frequency
EIRP	Equivalent Isotropically Radiated Power

EMC	Electro-Magnetic Compatibility
EPP	Energy Per Pulse
FCC	Federal Communications Commission
FEC	Forward Error Correction
FFD	Full-Function Device
FFT	Fast Fourrier Transform
FPGA	Field Programmable Gate Array
GPS	Global Positioning System
GTS	Guaranteed Time Slots
GUI	Graphical User Interface
HART	Highway Addressable Remote Transducer
HD	High Definition
HDL	Hardware Description Language
I/O	Input Output
IC	Integrated Circuit
IEEE	Institute of Electrical and Electronics Engineers
IEEE	Inverse Fast Fourrier Transform
IP	Intellectual Property
IR-UWB	Impulse Radio UltraWide Band
ISM	Industrial, Scientific and Medical
LAAS	laboratoire d'Analyse et d'Architecture des Systèmes
LDPC	Low-Density Parity-Check
LEACH	Low Energy Adaptive Clustering Hierarchy
LNA	Low Noise Amplifier
LO	Local Oscillator
LoS	Line of Sight
LPL	Low Power Listening
LPL	Low Power Listening

LR-WPAN	Low-Rate Wireless Personal Area Network
MAC	Medium Access Control
MACA	Mobile-Assisted Connection-Admission
MB-OFDM	Multi-Band Orthogonal Frequency-Division Multiplexing
MCM	modulation, coding and multiple-acces scheme
MEMS	MicroElectroMechanical Systems
MIMO	Multiple Inputs, Multiple Outputs
MIT	Massachusetts Institute of Technology
MPC	MultiPath Component
MPW	Multi Project Wafer
NDA	Non Disclosure Agreement
NFER	Near Field Electromagnetic Ranging
NP	Neighbor Protocol
NTP	Network Time Protocol
O-QPSK	Offset Quadrature Phase Shift Keying
OFDM	Orthogonal Frequency Division Multiplexing
OOK	On Off Keying
OSI	Open Systems Interconnection
PA	Power Amplifier
PAMAS	Power Aware Multi Access with Signaling
PAN	Personal Area Network
PAPR	Peak-to-Average Power Ratio
PBTS	Perfectly Balanced Ternary Sequence
PCB	Printed Circuit Board
PHY	physical
PLC	Power Line Communication
PLL	Phase Locked Loop
PPM	Pulse Position Modulation

PR	Place and Route
PSD	Power Spectral Density
PSSS	Parallel Sequence Spread Spectrum
PTP	Precision Time Protocol
QAM	Quadrature Amplitude Modulation
QoR	Quality of Result
QoS	Quality of Service
RAID	Redundant Array of Independent Disks
RBS	Reference Broadcast Synchronization
RF	Radio Frequency
RFD	Reduced Function Device
RFID	Radio-Frequency IDentification
RM	Reference Methodology
RS	Reed-Solomon
RSSI	Received Signal Strength Indication
RTL	Register Transfer Level
RTS	Request To Send
S-MAC	Sensor MAC
SDR	Software Defined Radio
SEP	Schedule Exchange Protocol
SFD	Start Frame Delimiter
SHM	Structural Health Monitoring
SNR	Signal to Noise Ratio
SoC	System on Chip
SPI	Serial Peripheral Interface
SSD	Solid State Drive
T-MAC	Timeout MAC
TDMA	Time Division Multiple Access

TDoA	Time Difference of Arrival
TEDS	Transducer Electronic Data Sheet
TH-IR	Time-Hopping Impulse-Radio
ToA	Time of Arrival
ToD	Time of Departure
ToF	Time of Flight
TRAMA	TRaffic-Adaptive Medium Access
UPF	Unified Power Format
USA	United States of America
UWB	UltraWide Band
VCO	Voltage-Controlled Oscillator
VHDL	VHSIC Hardware Description Language
WiDeCS	Wireless Deterministic Clock Synchronization
WiDeLoc	Wireless Deterministic Localization
WLAN	Wireless Local Area Network
WPAN	Wireless Personnal Area Network
WSN	Wireless Sensor Network

PUBLICATIONS

Some ideas and figures have appeared previously in the following publications:

Awards and Honors

T. Beluch, F. Perget, J. Henaut;
Student Design Competition for Software Defined Radio;
IEEE Microwaves Theory and Techniques (MTT) division. IEEE International Microwave Symposium (IMS) 2012, Baltimore MD

T. Beluch, D. Dragomirescu, F. Perget, R. Plana;
Best Paper Award for Cross-layered synchronisation protocol for wireless sensor networks;
International Conference on Networks (ICN 2010), Menuires (France), 11-16 Avril 2010, pp.167-172 URL : http://dx.doi.org/10.1109/ICN.2010.36

International Journals

T. Beluch, F. Perget, J. Henaut, D. Dragomirescu, R. Plana;
Mostly Digital Wireless UltraWide Band Communication Architecture for Software Defined Radio;
Microwave Magazine, IEEE , vol.13, no.1, pp.132-138, Jan.-Feb. 2012 URL: http://dx.doi.org/10.110
status: Published

T. Beluch, D. Dragomirescu, V. Puyal, R. Plana;
Low power digital TTL command for 60 GHz RF MEMS phase shifter;
Microelectronics Journal (Elsevier), Volume 42, Issue 12, December 2011, Pages 1321-1326, ISSN 0026-2692, URL : http://dx.doi.org/10.1016/j.mejo.2011.09.014
status: Published

T. Beluch, D. Dragomirescu, R. Plana;
A sub-nanosecond Synchronized MAC - PHY Cross-layer design for Wireless Sensor Networks;
Ad-Hoc Networks (Elsevier); http://dx.doi.org/10.1016/j.adhoc.2012.09.010 ; status: Published online

International Conferences

D. Dragomirescu, M. M. Jatlaoui, S. Charlot, T. Beluch, P. Pons, H. Aubert, R.Plana;
Flexible integration techniques for wireless sensors network deployment: application to aircraft structure health monitoring;
International Workshop on Structural Health Monitoring (IWSHM 2011), Stanford (USA), 13-15 Septembre 2011, pp.1519-1526 status: Published

T. Beluch, A. Lecointre, D. Dragomirescu, R. Plana;
Reconfigurable tactical impulse radio UWB for communication and indoor local-

ization;
International Conference on Networks (ICN 2011), St Maarten (Pays Bas), 23-28 Janvier 2011, pp.235-240 status: Published

T. Beluch, D. Dragomirescu, F. Perget, R. Plana;
Cross-layered synchronisation protocol for wireless sensor networks;
International Conference on Networks (ICN 2010), Menuires (France), 11-16 Avril 2010, pp.167-172 URL : http://dx.doi.org/10.1109/ICN.2010.36 status: Published

T. Beluch, D. Dragomirescu, V. Puyal, R. Plana;
Actuation command circuit for 60GHz RF MEMS phase shifters;
International Conference on Electronics Computers and Artificial Intelligence (ECAI 2009), Pitesti (Roumanie), 3-5 Juillet 2009, pp.54-57 status: Published

National Conference

T. Beluch;
Architecture et modélisation de réseaux de capteurs sans fils synchronisés et localisée à faible consommation;
Journées Nationales du Réseau Doctoral en Microélectronique (JNRDM 2011), Paris (France), 23-25 Mai 2011, 4p. status: Published

GENERAL INTRODUCTION

Recent advances in MEMS design and wireless technologies have opened the way towards new sensing techniques. Usually, sensors are deployed in two usual manners. Sensors can be placed far from the actual phenomenon in order to reduce perturbations caused by the sensor itself. This method leads to heavy signal processing to extract actual data from noise caused by the distance to the phenomenon. Another way of measuring an actual physical event is to place sensors in the desired area, and to perform data processing elsewhere. The drawback of this solution is that conventional sensors are often connected individually to the processing unit through multiple long cables requiring long and expensive deployment tasks.

Sensor networks consist in a large number of sensing nodes densely deployed in the desired area. These nodes are connected to each other through wired or wireless links, and work together for sensing physical events, processing them, and transmitting data to a sink point.

These features enable their use in various domains. Commercially available systems are already in use in military operations for example with the sucessful replacement of mine fields for intrusion detection with a hardened Wireless Sensor Network (WSN) designed for detecting intrusions. Other applications, such as Structural Health Monitoring (SHM) for large structures are under development, and experimentations are currently performed for the monitoring of railroads, highways, and other large scale transportation facilities. Other applications are appearing in the field of house automation, and allow the seemless deployment of a domotic system in an existing house for example. More recently, a new set of possible applications has been an active subject of research. This set is composed of applications requiring a large amount of data to be transfered continuously over the network. Indeed, measurement systems, such as for vibration measurement, do require a large number of sensors to acquire measurements with sampling frequencies up to 50 kSps, and are often asked to synchronize measurement trigger for all the sensors. The amount of data generated by hundreds of sensors with sampling rates in tens of kilosamples per seconds does rise higher than 100 Mbps. The problems of trigger synchronization in WSNs and high datarate transceiver implementations for such networks are the two axis of work for this thesis.

For many years, high speed wired computer networks have concentrated a large part of the research about time synchronization. Network Time Protocol (NTP) and its improved variant: Precision Time Protocol (PTP) are widely recognized for use in wired networks. Performance attained by such protocols can reach a synchronization precision of 100 ns. These protocols, however, use a large amount of data sent on the network, which leads to a high power consumption that is not affordable in WSN. New protocols have been developed that take into account specific needs for usability in WSN. These protocol, mostly lightweight, are based on a small number

of synchronization steps. A sync packet can be timestamped when transmitted, thus providing an approximate date to the receiver. Other methods include an handshake in the scheme. However, these protocols are limited by a recurring drawback of the standard network interfaces. Indeed, the network layers are mostly non deterministic in terms of latency, and do not allow precise time-stamping of the events.

On the other side, low power transceiver implementations have been proposed for WSNs. Most of them are based on the IEEE 802.15.4 standard, and do implement protocol stacks similar to the ZigBee stack. Such implementations do offer very low power consumptions. However, the datarate achieved by such transceivers do rarely exceed 250 kbps. Academic researches have lead to low power transceiver implementations, using UltraWide Band (UWB) technologies, providing datarates up to 100 Mbps with energy per bit levels of 750 pJ/bit. A further improvement in the overall power consumption of UWB systems would allow longer lifecycles to WSN nodes during use.

The work presented in this thesis is aiming at designing and implementing a System on Chip (SoC) architecture for use in WSNs. Improvements compared to the state of the art have been targeted in the cross layer design, as well as during the implementation of a mixed signal SoC proof of concept. The cross-layer design proposes a simple yet effective Medium Access Control (MAC) layer for fixed networks such as measurement setups. This design also uses and improves an implementation of a Impulse Radio UltraWide Band (IR-UWB) modulation scheme designed by Aubin Lecointre in his thesis. Innovative services are also proposed for synchronizing measurement triggers among all the nodes of the network.

In the domain of implementation, and power consumption reduction, the implementation has been designed with the main objective of keeping the best data-rate and synchronization performance, with an energy consumption below the state of the art.

The first part of this thesis describes the potential uses for WSNs, as well as the state of the art in synchronization and implementations of IR-UWB transceivers. The context of WSNs is detailed in chapter 1. The use of UWB in such networks is analyzed in chapter 2, as well as the state of the art in low power IR-UWB transceivers.

The second part is focused on the design and implementation work proposed in this thesis. The chapter 3 describes the structure of the cross-layer designed system, and proposes WiDeCS as a solution for improving synchronization performance in WSNs. The implementations of the proposed system in FPGA prototype and ASIC are detailed in chapter 4. This last chapter also provides information about the specific test protocol developed for verifying the system's performance, and the results obtained are compared with state of the art low power implementation.

Part I

COMMUNICATION IN WIRELESS SENSOR NETWORKS

WSNs have been made possible thanks to innovations that have occured in the last two decades in the domains of microelectronics, integration, sensors, and energy harvesting. They are currently exploding in terms of usage and attainable performances, and improve the way of working in many contexts. Mine fields, for example, have been successfully replaced by efficient intrusion detection systems based on a large number of wirelessly connected autonomous elements. Other applications, such as railroad or building monitoring are being experimented around the world.

New modulation techniques, routing protocols, MAC schemes specifically developed for a use in WSNs have allowed their use in new domains of activity. This part details some of the most interesting wireless communication techniques and how they expand the number of possible applications by allowing them to use an adapted communication scheme. An introduction about WSN is first given. The different methods for transmitting data in such networks are then detailed, and specific new modulation techniques, called UWB are studied through an example: IR-UWB.

1

INTRODUCTION TO COMMUNICATION IN WIRELESS SENSOR NETWORKS

Wireless Sensor Network (WSN) is describing systems composed of sensing elements embedded with wireless communication ability and a variable part of autonomy. These Wirelessly connected sensor networks are often given functionality such as data gathering to gateway nodes also known as sink points, sensor heterogeneity or even actuation abilities. However, the possibilities of such sensor networks are not limited to these two functions. One can use a WSN to detect intrusions in a specific area, and trigger adapted alarm systems or even countermeasures. On the other side, the same technology can be used for monitoring a patient's vitals, and alert the medical crew when something goes out of chart such as an abnormal pulse rate, or epileptic ceasure. WSN is then a new basis for emerging products and applications. However, there is not a single solution for all applications, but rather a framework serving as a starting point for developing application specific solutions.

This chapter first describes some of the possible applications for WSN selected with regard to their interest for this work. Communication patterns used in WSNs are then studied in a second section. The last section of this chapter describes two services for WSNs necessary for the applications targeted in this thesis : synchronization schemes, and ranging and positioning methods.

1.1 APPLICATIONS FOR WIRELESS SENSOR NETWORKS

Sensor networks are not bound by standardization constraints. This expression actually describes every system composed of nodes with sensing capabilities communicating with each other in order to perform a task assigned to them. Applications linked to such systems are then possible in almost every domain of everyday's life. This section gives an overview of the possible applications, and points out the reason why WSN technologies can improve the way of working in this application.

1.1.0.1 *Military and security related applications*

- Intrusion detection: Sensor networks can be deployed over a surface to detect any movement of an unauthenticated target. The exact position of this target can also be assessed thanks to the positions of the nodes in detecting range of the target. Such systems are under experimentation as a replacement to mine fields for detecting an enemy presence in a demilitarized zone. Such a system, as presented in figure **??**, may be used for detecting an intrusion either by checking the status on site, or by means of remote monotoring.

- Impact damage assessment: Sensor networks are used as SHM equipments placed on a vehicle for assessing the status of a part that has taken damage

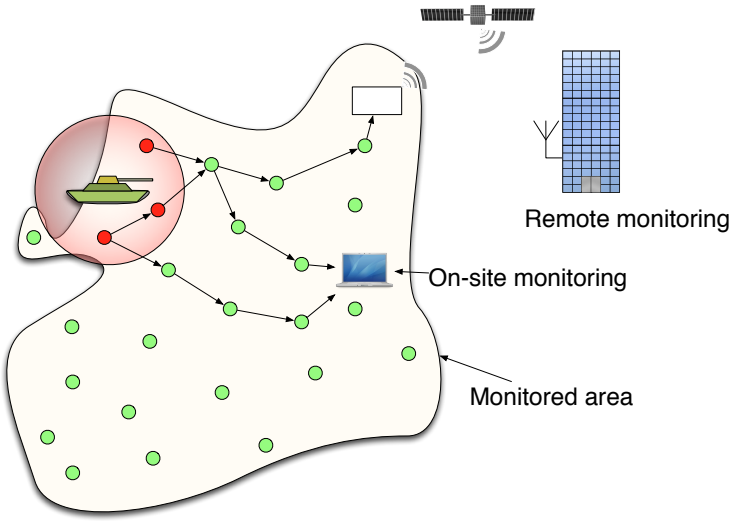

Figure 1: Example of a military oriented intrusion detection system

from an enemy shot [3]. Such systems help taking operational decisions thanks to the knowledge available concerning the overall damages taken by the vehicle.

- Mission reconnaissance: Sensor networks can be deployed prior to the mission in order to gather better information about the status of enemy troops and defense systems. Such deployment can be performed either by undercover agents or by means of sparse drop of SmartDust like motes. Such networks can then operate discretely and give useful information to plan a mission.

- Missile guidance and targeting: A Sensor network composed of multiple static nodes can help guiding a missile towards a moving target. The position of the moving target is obtained via conventional positioning schemes such as trilateration or triangulation of data obtained through a network of sensing elements such as passive and/or active radars, infrared video-cameras, vibration sensors or even motion detectors. Knowing the precise location of a missile allows real time flight parameter correction improving its accuracy.

- Detection of dangerous materials: Sensor networks can be deployed in critical buildings such as airports for detecting dangerous compounds. Gas or radiation detectors, embedded in every sensing node, increase the probability of detecting hidden explosive devices or radiating materials.

- Squad members health and location monitoring: Knowing the status of every team member is often a matter of life or death for the entire squad. Such applications can be found in military contexts such as urban warfare, where squad members are sometimes spread to better scour a building. Knowing where a squad member is located, as well as his or her status can be useful.

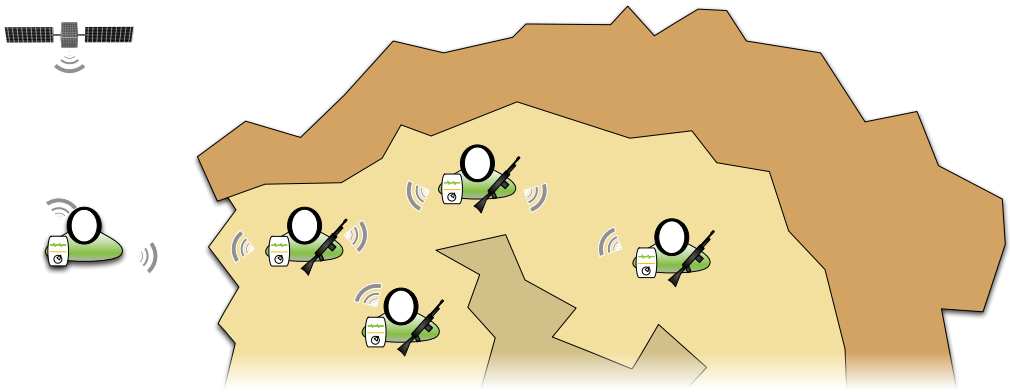

Figure 2: Example of a military oriented squad health monitoring equipment

It can indeed help in avoiding loosing a full squad in an ambush because a squad member has been silenced before he could warn the squad leader. These systems are planned to look like a PDA showing in real time the location of every squad member, as well as his vitals and his orders. The example in figure 2 shows an operation manager with a channel to a communication satellite exchanging data with a squad exploring a cave. Members of this squad each possess a PDA like apparatus logging their relative position, as well as vital parameters. This example then shows how communication and localization services can be brought to closed space with no need for a prior deployment of localization anchors.

1.1.0.2 *Industrial applications*

- Test and validation: Every item sold on the market must be tested for multiple reasons. The first and obvious one is to check the conformity of the product with its design. However, there are many other reasons for testing a product, each reason will require a set of test conditions and expected results. For example Federal Communications Commission (FCC) certification implies to verify the power radiated by a communicating device, as well as the power spectral density of the radiated signal. Such tests are usually made in an anechoic room and do use spectrum analyzers to qualify the measured spectrum with regulations. Other tests will require to check air pressure over and under a plane's wing to check its compliance with the requirements, as well as conformity to aeronautics related regulations. Such air pressure measurement is often performed using pressure sensors placed inside the wing and connected to the measurement site through a hose. Replacing this setup with thin wireless nodes providing similar results would divide the overall cost of installation and removal by four. For example, placing a pressure belt on a plane's tail allows a few tenths of sensors to be placed on the tail at the cost of more than one month of immobilization of the plane. Indeed, such pressure belts are extremely complex, and require a large number of

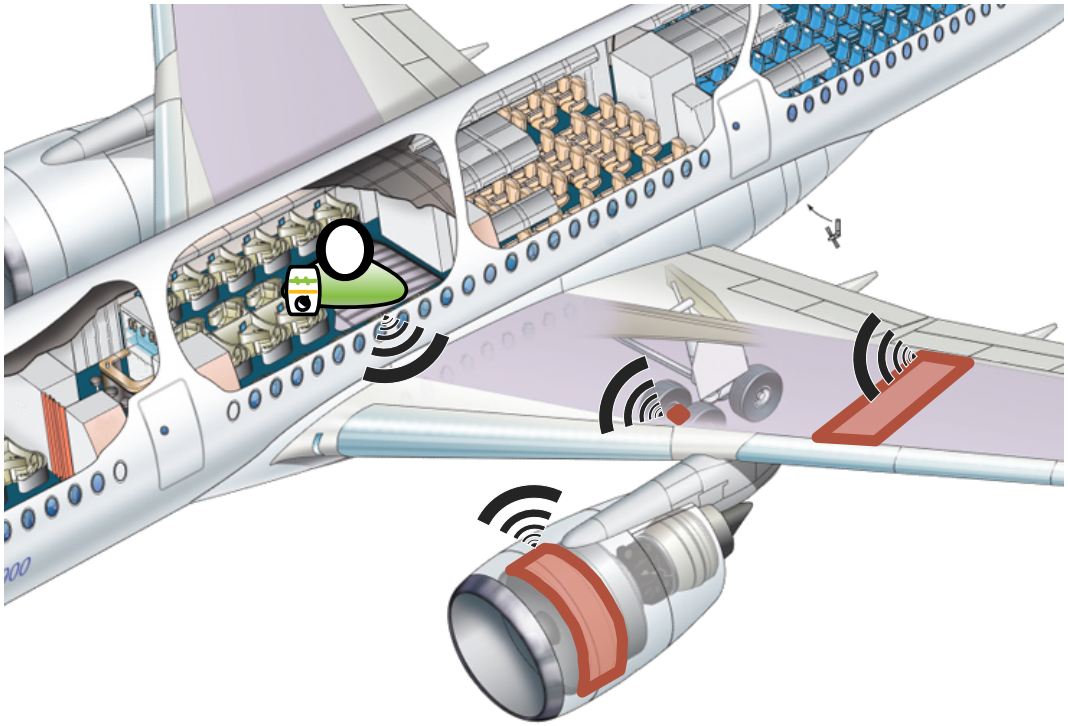

Figure 3: Example of an in-flight testing context

cables to be routed in the plane's structure to the cabin. The figure 3 shows various communicating modules placed at different places of a same plane which are communicating with an equipment inside the cabin. Such systems would allow aerospace industry to provide a monitoring equipment to a client for mounting on a suspected part of a plane during operation. Results of this monitoring would then be logged inside a computer in the cabin, and sent back to the support team for study of these logs. Such systems would drastically reduce the cost and duration of ground maintainance for planes.

- Building structural health monitoring: The complexity of building has been rising for the last decades, with higher towers, longer and thinner bridges, and other innovative buildings. Such improvements are often the result of a trade-off. Mechanical constraints computing has improved, and now allows lighter structures to be used. However, monitoring these vital points has become more important to the health of these new structures, as the overcompensation is nowadays much smaller. Sensors networks are more often deployed in newly built buildings, as well as in building that may be subject to problems with their structure. These sensors help in detecting fatigue cracks and deformations. These new techniques for monitoring the status of a building are often used for monitoring new building structures, especially when these structures represent a breakthrough in the technique, such as skyscrapers or unconventional buildings [79] (figure 4). However, building SHM systems,

(a) Burj Khalifa in Dubai (828 m) (b) Marina Bay Sands in Singapore (146 m)

Figure 4: Examples of monitored buildings

mostly based on fiber optics, have also been used in the more unexpected context of archeological buildings such as the Torre Aquila in Italy [28].

- Vehicle structural health monitoring: Recent vehicles such as cars and trucks do propose automatic diagnostic features, which are getting smarter with time rolling. WSN based SHM systems are opening the way to even better diagnostics based on the quantization of wear and tear on critical parts of an engine or even the early detection of damaged tires to avoid accidents. Such SHM is also seen as a promising solution to improve the reliability of airplanes, trains, and other public transport.

- Maintenance automation: The automated diagnostics based on WSNs can also be extended to ease maintenance by reporting parts that need to be changed to the mechanic.

- Energy optimization: Smart buildings are able to manage energy sources to reduce the consumption of commercial energy. Indeed, moving air between an area overexposed to sunlight and shadier areas helps in reducing power consumption related to air conditioning. WSNs help in performing these tasks by providing the best granularity available to the system.

- Inventory management: RFID tags have helped improving processes in logistics and inventory management. Tagging orders and parcels helps in keeping a constant knowledge about its location among the different storage centers and delivery trucks. However, sensing tags are at the limit between Identification tags, and intelligent nodes equipped with sensors. Such tags allow logging the temperature of a transported good, and give reliable information when this good is delivered to the end user. Such information can also be automatically

transferred from the goods to an inventory management unit which would be in charge of the status of every goods, and would advise the manager on his storage facilities.

1.1.0.3 *Health care applications*

- Physiological data monitoring: Sensors placed at the best spot on or in the patient's body are connected together and continuously send physiological data to a hub unit which relays this data to the medical crew [77]. Non invasive sensor networks reduce the constraints caused by a patient's condition when compared to a constant monitoring in a medical unit. Indeed, such equipment make it possible for a patient to go shopping while being remotely monitored and kept healthy.

- Patient identification, localization and personal data storage: The number of hospitals using RFID tags in constantly growing for patient identification. RFID techniques have allowed to improve patient management in hospitals in the last decade [49, 32, 65]. Current research are made towards smart identification tags coupling the physiological data monitoring with patient identification tasks [29].

- Automatic drug administration: Sensor networks can be used for constantly adapting the administration of a drug to a physiological data measured on the body, or even to a target dosage of the drug present in the patient's blood.

1.1.0.4 *Environmental applications*

Wireless Sensor Networks (WSNs) used for environmental applications are similar to each other. Indeed, most of them are deployed on wide areas, with no access to a conventional power source, and are required to regularly measure, analyze, detect and alert when abnormal measurement values are detected. Communications used in such applications are often long range and low data rate wireless transmissions.

- Flood detection: Sensors networks are used to protect areas presenting a high risk of flooding as shiwn in figure 5. Placed at strategic points for detecting a rise in the water level, they can provide early alerts in case the water level becomes abnormal[71].

- Fire detection: Gas or ultraviolet light sensing WSNs can be spread in a forest for detecting a fire outbreak as soon as it happens [26, 31].

- Pollution study: Pollution study stations are often heavy and costly boxes containing spread over a territory to monitor the presence of pollution related gases and volatile compounds. However, sensor networks are currently researched as a solution to improve the measurement granularity by increasing the number of sensing elements, and their dispersion in the monitored area through integration in vehicles [54].

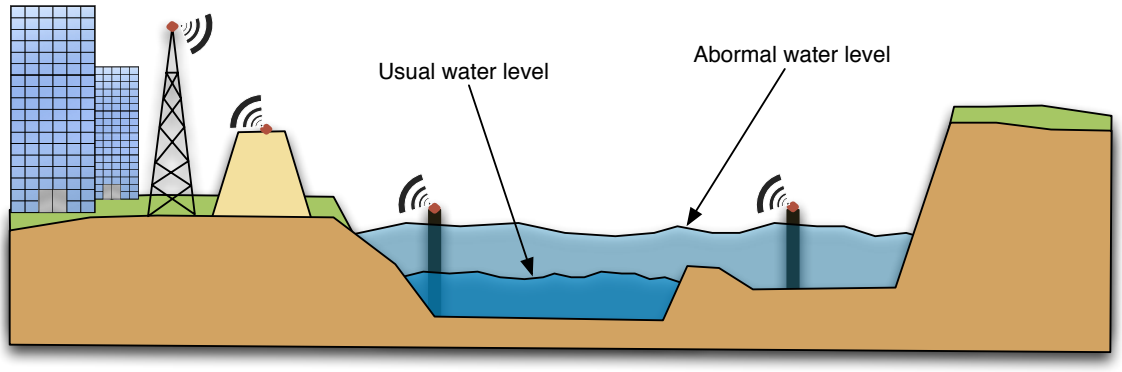

Figure 5: Example of a flood detection context

1.1.0.5 *Consumer use applications*

- Smart cars: Increasing the part of automation in a car is one of the keys to reduce the number of car crashes. Among the possible technologies for increasing the intelligence of a car, a network composed of cars in range of each other exchanging data about traffic conditions can improve the overall road safety. Inter-car communications are planned in most of the frequency allocation regulations, and are allowed on specific spectrum bands.

- Home automation: Automating a house in order to optimize its energy consumption while keeping it welcoming to its owner is a growing market. However, this market is ruled by a major parameter : the price of the equipment necessary to reach a satisfying behavior for such automation systems. Sensor networks can indeed be used to detect the presence of a person in a room in order to turn on or off the equipment present in this specific room. Shaders can be automatically opened to allow sunlight to enter the house during the day, and closed to prevent heat to leave the house through the windows during the night.

1.2 COMMUNICATION FOR WSNS IN AN INDUSTRIAL CONTEXT

Basebands for WSNs are designed with a specific range of applications in mind. Two types of requirements can be identified for sorting WSNs.

SHM applications often require a system to be installed for long periods on a monitored structure. Those systems aim at regularly checking physical measurements taken at relevant points of this structure and detect unusual changes in its mechanical parameters. In the case of a Sky-tower, it could mean to regularly monitor strain along the metallic core, as well as on a few selected floors.

These monitoring systems have to periodically take measurements, and dispatch them to a master unit. Considering that monitoring most of the common structures do rarely require sampling rates over 10 samples per second, it is often sufficient in such applications to transmit data regularly at second scale intervals. The corresponding system will be considered low data rate in the following thesis.

However, some structures, to be monitored, require the use of active monitoring systems. Applications for such systems include studying the propagation of seismic waves through a building, or detecting bullet impact on military structures, along with damage estimation.

1.2.1 *Low data rate communications*

Low data rate communications are often used in the case of low power nodes remaining idle for the major part of the time. These networks are often waiting for long periods between packet exchanges, and do require specific synchronization between the clocks to allow planning periods when every node has to be listening on the network. Such scheduling makes it possible to turn off every radio interface between these periods, and then save large amounts of power compared to usual always-on network architectures.

1.2.1.1 *IEE 802.15.4-2006, a Standard for WSNs*

The most spread standard for wireless communication aimed at WSN applications is IEEE 802.15.4-2006 [13]. This standard provide multiple physical (PHY) layer and MAC layer specifications for transmitting data with a low power consumption. This standard defines such communications in a Wireless Personnal Area Network (WPAN) context ranging up to 10 m, whereas many implementations demonstrate ranges up to 2 km. The proposed physical layers, as in the 2006 revision, include three variants of a Direct-Sequence Spread Spectrum (DSSS) modulation scheme based on Offset Quadrature Phase Shift Keying (O-QPSK), and a fourth modulation based on the combination of Binary phase-shift keying (BPSK) and optional Amplitude Shift Keying (ASK) based on Parallel Sequence Spread Spectrum (PSSS). These PHY layer allow channel data-rates up to 250 kbps in the 2006 release of this standard. Newer releases beginning with the IEEE 802.15.4a bring higher data rates, and are listed in the High data rate communication subsection.

The network interface described in the IEEE 802.15.4 standard are widely used in WSNs because of a low power consumption, and long transmission ranges. Applications have been developed in the field of SHM, with examples in bridge monitoring in the USA [50]. Home automation systems are currently sold using a ZigBee transmission system based on this standard for allowing the placement of various sensors at different places of a house without need for wiring them to the automation manager [5]. Actuators related to home automation, on the other side, are often interfaced through Power Line Communication (PLC) because most of the possible actuators do require levels of energy that cannot be achieved with batteries.

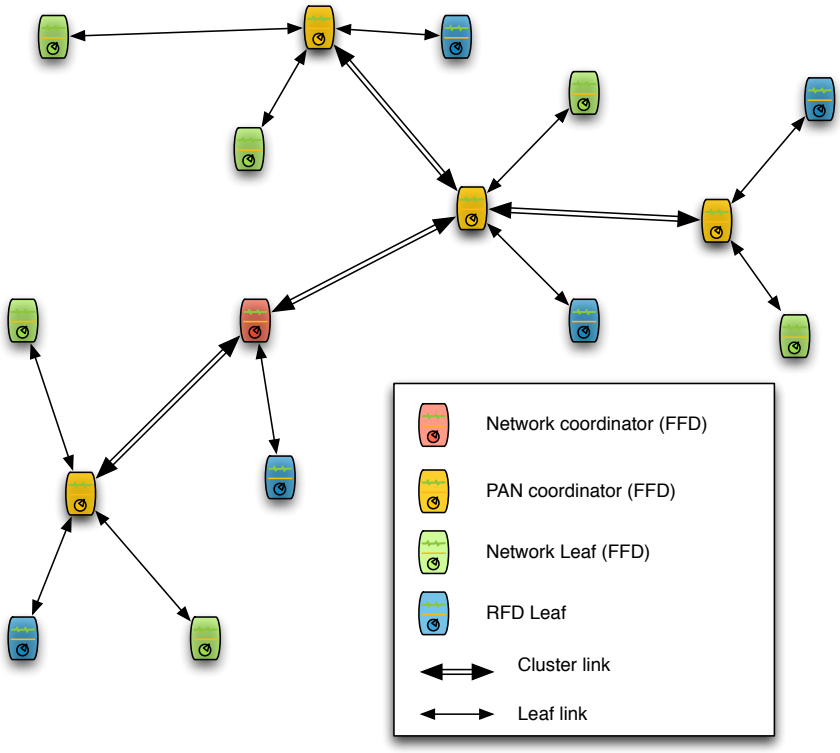

Figure 6: IEEE 802.15.4 cluster tree architecture

Many other applications with low needs in terms of quantity of data transmitted do use ZigBee as the main network interface.

The MAC layer described in this standard combines multiple MAC schemes. The choice of the used scheme is performed by a higher layer. A simple Aloha scheme is mandatory in the standard and does allow immediate transmission of new data with no regard to the channel occupation. This allows cheap Reduced Function Devices (RFDs) modules to communicate with Full-Function Devices (FFDs). A Carrier-Sense Multiple Access with Collision Avoidance (CSMA-CA) scheme is also described, as well as a super-frame structure for permanent slot allocation. The described MAC layer then allows the simpler devices to communicate at low data-rates, whereas FFDs have the possibility to bring order to the used channel and then improve the data-rates. The usual structure for implementing a IEEE 802.15.4 network is a heterogenous cluster tree network composed of FFDs and RFDs. FFDs can be acting acting either as network / Personal Area Network (PAN) coordinators, or as network leafs. RFDs, on the other side, can only act as leafs on the network. An example of a IEEE 802.15.4 cluster tree architecture is shown in figure 6. The possible uses for each type of node in this network architecture is displayed in this schematic.

This standard, however, has served as the basis to many of the most known low cost low power radio interfaces such as ZigBee [2], MiWi [74], and other constructor specific implementations.

1.2.1.2 *WirelessHART*

Highway Addressable Remote Transducer (HART) protocol is a digital industrial automation protocol based on field-bus. Its main uses are in the field of industrial process automation by providing a reliable data transmission interface for linking the different elements used in an industrial process to the control unit. Among the elements that can be linked to the control unit are sensors for measuring parameters during the process' execution, and actuators for executing the process itself. The performance in terms of data rate is relatively low when compared to other wired networks. However, this open protocol has an optimized packet structure, and do produce a reduced overhead.

WirelessHART is an implementation of the HART protocol over a wireless link. The radio interface chosen for this wireless implementation is IEEE 802.15.4. A HART compliant network management protocol in implemented on top of the wireless interface to allow seamless integration in a usual HART compliant network. WirelessHART sensors and actuators can be added in a HART industrial control system by adding a WirelessHART adapter on the HART network.

This protocol, along with the wired HART protocol, do provide industrial grade communications with reliable data transmission and optimized packet structure. However, none of the implementations proposed are suitable for high data-rate applications.

1.2.1.3 *IEEE 1451*

IEEE 1451 standard[14] is not a wireless communication standard. However, this standard describes smart transducer interfaces for connecting transducers (including sensors and actuators) to instrumentation units, and process control and management units. The interfaces described by this standard include network independent communication interfaces for connecting these transducers. The main point of this standard resides in the Transducer Electronic Data Sheet (TEDS) format description, which aims at integrating a digital data-sheet inside every transducer. This TEDS contain transducer identification, calibration, correction data, and manufacturer-related information. The main goal of the IEEE 1451 is to allow access to the TEDS with no regards to wether the network is wired or wireless. As IEEE 1451.5 version of this standard, TEDS are compliant with four wireless network interfaces including 802.11 WiFi, Bluetooth, ZigBee, and 6LoWPAN. RFID access to TEDS has been added with the 2010 version of the standard.

1.2.2 *High data rate communications*

High data-rate communications are necessary in applications in which the amount of data to be transmitted between the nodes becomes higher than 10 Mbps, or when the number of nodes required to send data simultaneously rises up to hundreds of nodes. In this case, it is no longer useful to plan sleeping periods. However, energy management and routing protocols become important if the energy is not provided by a reliable source. In this case, most of the systems described above do

not comply with these specific requirements. Zigbee is limited to 250 kbps in most of its use cases. IEEE 802.15.4 was also limited to 250 kbps in its 2006 version [13] until a newer version, allowing higher throughput was released under the name IEEE 802.15.4a or 802.15.4-2011 [18]. As of 2008, the only systems commercially available for use in Wireless Sensor Networks (WSNs) were limited to 250 kbps. Since then, multiple paths have been tried to propose a low-power high-throughput radio interface for WSNs

Methods for improving the data-rate of a wireless network vary and include channel binding, Multiple Inputs, Multiple Outputs (MIMO) channel separation, UWB communications, Orthogonal Frequency Division Multiplexing (OFDM) based modulations, and the use of Extremely High Frequency (EHF) frequency bands. However, most of these technologies do imply a rise in power consumption due to more complex computing, wider band modulations requiring higher functioning frequencies, and higher propagation loss due to increased free space loss and molecular resonance. The following paragraphs does study the most promising solutions for performing high data-rate communications. Their respective complexity is also studied, and their use in the case of WSNs is studied.

1.2.2.1 *IEEE 802.11 WiFi*

WiFi networks have evolved from the first standard versions allowing 11 Mbps PHY data-rates in the 802.11b version [7] of the standard, up to 6.93 Gbps with the 802.11ac version [4] of this standard in MIMO with channel binding and 256 Quadrature Amplitude Modulation (QAM) modulation. This wireless network standard is the most widely used for communications between computers, handheld devices, and more recently set top boxes. The main advantages of WiFi has always been the compatibility between devices implementing different versions of the same standard, as well as high data-rates. Indeed, an access point compatible with 802.11n version, is supposed to be able to communicate with 802.11b devices, if the configured security protocol remains compatible with the older device. On the other hand, this compatibility has a main drawback in the fact that the whole data-rate of the wireless network is determined by the highest data-rate attainable by every node connected to the same access point. An active 802.11b device connected to a 802.11g access point does limit the whole data-rate to 11 Mbps instead of "g" version's 54 Mbps. The other advantage is the extremely high data-rates, which are reaching 6.93 Gbps in the 802.11ac version of this standard.

However, this rise in data-rate, as allowed by the latest version of this standard comes with strong drawbacks. The first and foremost among them is the high system complexity needed for reaching such data-rates [4]. Indeed this version requires multiple antennas on both the transmitting and receiving sides in order to increase the data rate through MIMO multi-chaneling. The size and power consumption of a WSN node would become unacceptable in most of the application schemes. Moreover, these data-rates are reserved to systems such as laptop, computers, and wireless routers and access points. Handheld devices are only allowed lower

data-rates, which is mostly due to a smaller number of integrated antennas for MIMO, as well as complex computations needed for receiving data correctly [4].

1.2.2.2 *UWB modulations*

UltraWide Band (UWB) modulations are technologies which have known a growing interest in the last decade. Foundry technologies have improved the maximum frequency attainable for digital Application-Specific Integrated Circuits (ASICs), thus opening the way to wider band modulations. Indeed, UWB modulations are often seen as a way to simply improve the throughput of a channel. An example is the ECMA 368 standard [37], which is mostly based on OFDM modulation. These systems do offer higher data-rates, thanks to their higher bandwidth. However, this increase in throughput is countered by new requirements in terms of working frequency, algorithm complexity, and power consumption. Lower complexity implementations of UWB modulations have been proposed for use in measurement WSNs [53]. On the other side, the power consumption remains too high for autonomous nodes. Other UWB modulations based on IR-UWB exist, and are listed in section 2.2. These solutions, on the other side, have been a growing subject of interest from scientists, but they require deep developments for implementing, and have only been standardized recently in the IEEE 802.15.4a (see section 2.2.2).

The work presented in this thesis is mostly based on the use of IR-UWB PHY layers presented in A. Lecointre's thesis, in which modifications were made for supporting Time of Arrival (ToA) measurement.

1.2.3 *power-saving MAC protocols*

This section lists the major MAC protocols used in the case of WSNs. Medium Access Control (MAC)is an important technique that enables the successful operation of the network. Medium Access Control in the case of wireless sensor networks has been a very active research area in recent years. The usual wireless medium access control protocols such as 802.11 WiFi protocol is not suitable for such network applications because of a high complexity, as well as multiple different possible computations depending on the heterogeneity of the network. Considering that WSNs are composed of battery or super-capacitor powered nodes, such complex MAC protocols must be replaced by new less complex protocols with no requirement for high speed processing units [58].

The MAC protocol used then has to address the following energy related issues:

- Collisions: Collisions occur when more than a single node are transmitting at the same time. The resulting signal present on the channel is then a combination of the signals transmitted by both the emitting nodes. The result of a collision is lower Bit Error Rate (BER) performance, and often the complete loss of the information transmitted by the colliding nodes. This causes an energy loss due to the need of resending the information, and to the cost in energy of the useless collided transmission. Collision avoidance is then a mean to reduce the energy consumption of a WSN node.

- Overhead: Overhead refers to the data transmission required for assuring a proper Medium Access Control (MAC). This data is not related to the application itself, but it is necessary for the network to setup properly, and to avoid collisions. The reduction of the overhead improves the efficiency in terms of energy per bit of application related data. However, lower overhead may reduce the stability of the network, and cause packet loss, collisions, and overhearing.

- Overhear: A cause of energy loss in wireless networks is the fact for a node of receiving data which is not intended to it. Consequences are more visible in wireless networks than in wired networks because of frequent preambles which are necessary for synchronizing the receiving PHY layer to the modulated signal. Simple overhear reduction techniques such as stopping the reception after having checked a destination MAC address is then not appropriate for every network.

- Idle listening happens when a node is listening on the channel, waiting for a possible data to receive. Listening to the channel has a cost caused by the combination of two causes. The first cause is the time being actually lost while listening on the channel, and waiting. The other cause for the cost is the actual power consumption of idle listening. Reducing either one or another of these causes will reduce the overall cost of idle listening.

- Complexity: As we stated in the introduction of this section, the complexity of a protocol causes multiple effects at different moments of the use of this protocol. A complex protocol will require more computing capabilities from the communicating node. This causes a higher power consumption of the Integrated Circuit (IC) chip because of larger areas required, as well as higher operation frequencies.

Successfully solving these issues with regard to requirement specific to the target applications is the main goal of WSN oriented MAC protocols. The MAC protocols proposed for WSNs can be divided into two categories namely Contention based and Schedule based.

Schedule based protocol can avoid collisions, overhearing and idle listening by scheduling transmit and listen periods. However, these protocols have strict time synchronization requirements and do often require a higher complexity logic for synchronization purpose.

The contention based protocols, on the other hand, relax time synchronization requirements. These protocols are based on Carrier-Sense Multiple Access (CSMA) techniques, which are more adapted to changing network topologies, due to a high tolerance to new nodes joining the network, or to the ones leaving it. Their complexity is also often lower than schedule based protocols. However, they underperform in terms of solving the above listed energy related issues. Indeed they present higher costs for message collisions, overhearing, and idle listening.

Among the existing MAC protocols, the following protocols represent a panel of various MAC protocol types and implementations.

1.2.3.1 *Sensor MAC (S-MAC)*

The Sensor MAC (S-MAC) protocol was introduced to solve the energy consumption related problems of idle listening, collisions, and overhearing in WSNs using only one transceiver [59]. S-MAC considers that nodes do not need to be awake all the time given the low sensing event and transmission rates. A contention based S-MAC protocol is based on Carrier-Sense Multiple Access with Collision Avoidance (CSMA-CA). Energy conservation and selfconfiguration are primary goals, whereas latency and determinism are considered less important. The S-MAC protocol reduces energy loss due to collision, overhearing, packet overhead and idle listening by turning the radio on and off based on the fixed duty cycles. The main drawback of S-MAC is that the use of fixed duty cycles can waste considerable amounts of energy since the communication subsystem is activated even though no communication will take place.

1.2.3.2 *Timeout MAC (T-MAC)*

Timeout MAC (T-MAC)[98] is a MAC protocol based on the S-MAC protocol possessing an adaptive timeout instead of a fixed duty cycle. Each slave node goes to a sleep period if no activation event has occurred for a defined duration. Such an event can be reception of data, start of listen/sleep frame time etc. The T-MAC protocol introduces the idea of having an adaptive active/inactive (listening/sleeping) duty cycle to minimize the idle listening problem and improve the energy savings over the classic CSMA and S-MAC fixed duty cyclebased protocols [59]. The T-MAC protocol, however, may often make the slave nodes oversleep, and then miss a data transmission that was occuring during a sleeping period. This oversleeping can highly increase the overall latency between the time a packet is being put on the network, and the time it is well received by the target node. This protocol is then better suitable for event based low data-rate WSNs with low requirements in terms of latency.

1.2.3.3 *Berkeley Media Access Control (B-MAC)*

The Berkeley Media Access Control (B-MAC) protocol [59] is a CSMA based MAC protocol for WSNs. B-MAC introduces several interesting mechanisms and features. One mechanism is the Clear Channel Assessment (CCA) for effective collision avoidance, which takes samples of the media to estimate the noise floor. B-MAC also utilizes a preamble sampling like technique called Low Power Listening (LPL) to minimize the idle listening problem. Finally, B-MAC includes the use of ACK frames for reliability purposes and throughput improvement. Moreover, B-MAC is able to function with B-MAC mechanisms, such as the CCA, acknowledgments, and LPL disabled to tradeoff power consumption, latency, throughput, fairness or reliability. The main drawback of this protocol is the stringent requirements in terms of PHY layer adaptations that need to be implemented for the mechanisms such as CCA and LPL to function.

1.2.3.4 *Low Energy Adaptive Clustering Hierarchy (LEACH)*

The Low Energy Adaptive Clustering Hierarchy (LEACH) protocol [52, 59] includes several ideas to reduce the energy consumption in WSNs. First, LEACH includes the idea of clustering but without including any powerful node as the cluster head. Second, in order to save additional energy in the nodes, LEACH utilizes a Time Division Multiple Access (TDMA) schedulebased MAC mechanism for intracluster communications. By allowing nodes to turn themselves ON and OFF at appropriate times (given by the schedule), a TDMA MAC protocol avoids problems such as collisions, hidden and exposed terminal problems, overhearing and idle listening problems [59]. In LEACH there is no intercluster communications, instead cluster heads are meant to transmit directly to the sink node. In order to avoid collisions, LEACH utilizes Code Division Multiple Access (CDMA) for cluster headsink communication, so cluster heads can transmit simultaneously to the sink without colliding with each other. It has some drawbacks. First, the cluster heads have to perform very computationally difficult and energy consuming tasks, such as preparing and managing the TDMA schedule, fusing and aggregating the data, and transmitting directly to the sink node. Second, LEACH needs synchronization, so that the TDMA scheme can actually work. Lastly, LEACH lacks multihop routing capabilities, which limit its applicability to small spaces.

1.2.3.5 *Power Aware Multi Access with Signaling (PAMAS)*

The Power Aware Multi Access with Signaling (PAMAS) protocol [59] is based on the Mobile-Assisted Connection-Admission (MACA) protocol but includes a separate signaling channel to avoid the collisions and overhearing problems. All nodes utilize the signaling channel to exchange Request To Send (RTS)Clear To Send (CTS) frames and therefore gain access to the media. All nodes know who has gained the media and for how long, information that nodes use to turn themselves off. The other channel is used exclusively to transmit data frames, which is collisionfree. The main disadvantage of PAMAS is that it needs an additional radio for the signaling channel, which adds to the cost of sensor network devices.

1.2.3.6 *TRaffic-Adaptive Medium Access (TRAMA)*

The TRaffic-Adaptive Medium Access (TRAMA) protocol [85] is a distributed TDMA mechanism that allows for flexible and selfmotivated scheduling of time slots. TRAMA provides the energysaving advantages of schedulebased mechanisms without the disadvantages of having a node as the main controller. TRAMA consists of three components that assign time slots only to stations that have traffic to send while being implemented in a distributed fashion. Further, it performs better than contentionbased mechanisms because the slot assignment avoids collisions. TRAMA nodes use the Neighbor Protocol (NP) and the Schedule Exchange Protocol (SEP) to send their transmission schedules along with information related to the current time slot, one and two hops away node identifiers, and traffic interests. Then, the Adaptive Election Algorithm (AEA) uses this information to determine

the transmitters and receivers for the current time slot and derive the nodes sleep schedule.

1.2.3.7 *Wise MAC*

The Wise MAC [40] protocol combines both TDMA and CSMA techniques. It also proposes a dynamically adapted preamble size for better adaptation to changing situations. The preamble sampling technique used in Wise MAC performs better than one of the S-MAC variants [59]. The main drawback of Wise MAC is that decentralized sleep scheduling results in different sleep and wakeup times for each node in the network. This is important regarding the idle-listen issue, especially in the case of broadcast communications. In addition, the hidden terminal problem comes along with Wise MAC model as in the spatial TDMA and CSMA with preamble sampling algorithm. That is because Wise MAC is also based on a non persistent CSMA. This problem will result in collisions when one node starts to transmit the preamble to a node that is already receiving a message from a hidden node.

1.2.3.8 *DMAC*

Convergecast is the most frequent communication pattern observed within sensor networks. Unidirectional paths from sources to the sink could be represented as data-gathering trees. The principal aim of DMAC [70] is to achieve very low latency for convergecast communications, but still be energy efficient. DMAC could be summarized as an improved Slotted Aloha algorithm in which slots are assigned to the sets of nodes based on a data gathering tree. During the receive period of a node, all of its child nodes have transmit periods and contend for the medium. Low latency is achieved by assigning slots to the nodes that are successive in the data transmission path.

1.2.3.9 *Conclusion on MAC protocols for WSNs*

The MAC protocols listed above do provide various services for various applications. Contention based protocols are more adapted to large scale evolutive sensor networks, with a low amount of data being transmitted simultaneously on the network. On the other side, Schedule based protocols do provide a better throughput, but suffer from scaling, and evolutions in the network such as nodes entering and leaving it. The specific adaptations listed above tend to reduce the drawbacks of these solutions. However, the whole world of applications related to WSNs cannot be addressed with a single MAC protocol, but rather with multiple MAC protocols better suited for each situation.

1.3 SERVICES FOR WSNS

1.3.1 *Clock synchronization and measurement trigger synchronization*

As explained above, schedule based MAC protocols are more appropriate for continuous transmissions, due to the predictability of the channel occupation. Moreover,

when it comes to clock synchronization, a Time Division Multiple Access (TDMA) MAC protocol is based on time to divide the channel, and then is pre-adapted to measurement of Time of Arrival (ToA) events. The induced determinism is then only limited to the knowledge of variable events occurring at MAC level and below. Such non determinism include channel coding, scrambling, RF front-end jitters, and propagation time. Research on time synchronization has been made for many years, mostly on traditional computer networks. This is due to the importance of synchronization in various domains such as process automation, high precision multi sensor measurements, and detection of events which must be dated precisely. In the case of need for high precision synchronization, a standard, IEEE 1588 Precision Time Protocol (PTP), has been proposed for synchronizing wired network interfaces by statistically modeling the entire path between the two computers which must be synchronized. Although this protocol enables sub-microsecond synchronization, it uses a large number of packet to reach such performance. That is why it is not adapted to wireless networks.

More recently, research efforts have been concentrated on WSNs. The cost of such networks is continuously falling due to the reduction of manufacturing costs. Such networks can cover a wider range of applications than the ones possibles using wired networks. Synchronization protocols for WSN include Global Positioning System (GPS) time synchronization, useful when the nodes are moving, or are rarely in range for transmitting data but costly in terms of processing resources. Protocols based on communication between nodes are more widely proposed. The following protocols represent an overview of the published synchronization protocols specific to WSN.

First synchronization protocols which have been presented by Ping et al. [83] were mostly based on a master / slave model. A timestamp is merged in the packet emitted by the master. The slave, on the other hand captures the date at the beginning of the reception. These protocols allow short initial synchronization in the sensor network along with reduced use of the network link. However, it is not easy to obtain synchronization under 15 μs. A similar protocol has been developed by Ganeriwal et al. [44] and provides a more precise clock synchronization owing to bidirectional use of the link. Both the master and the slave send messages including timestamps.

Other protocols allow receivers to be synchronized to each other by the means of a synchronization beacon sent by a master. Synchronization is not guaranteed between the slaves and the master. However, the slaves are synchronized to each other due to similar receivers and propagation times between them. Reference Broadcast Synchronization (RBS) is the most known protocol developed using these techniques. Improved protocols based on RBS have been proposed by PalChaudhuri et al. [80] and Maróti et al. [72]. IEEE 1588 PTP and its ability to perform very precise synchronization offset of hundreds of nanoseconds has also been adapted to Wireless Local Area Network (WLAN) networks with success [33], attaining 600 ns clock offsets. However this implementation is not adapted to the field of WSN due to its complexity and its induced power consumption.

In the field of Wireless Sensor Networks (WSNs), theoretical studies have obtained convincing results in terms of convergence speed, as well as absolute mean square error[30]. The proposed protocols, however, are based on the main assumption that the propagation time is stable. The best attainable error is then limited by the evolution of medium related parameters. Indeed, fast changing Time of Flight (ToF) won't allow statistical studies to obtain a good estimator.

Table 1 summarizes the existing protocols up according to the comparison framework described by Sundararaman et al. [95]. These proposed synchronization protocols do not fit with the context of industrial test measurement which often require measurements to be taken at different places with delays below 100 ns between them.

1.3.2 *Distance evaluation for localization*

Distance evaluation, also known as ranging, is another main subject of research in WSNs. Indeed, these systems are often deployed without knowledge of the location of every node either because the nodes have been dropped randomly over the area, or because nodes are fixed to moving objects or persons. Knowing the position of a node therefore requires the use of a specific method. A patient in an hospital, a fireman in operation , and even a military in a urban war context have in common the fact that knowing data about the person's physiology is not sufficient. Knowing the position of the person whose data is off the charts is also necessary for helping that person in time.

Location of a node can be either determined regarding to a global coordinates system, or to local systems centered around each node. Location of a node in global coordinates is performed thanks to its relative position regarding reference static nodes called 'anchors' whose locations are known with respect to a global coordinates system -i.e. GPS-. Relative positioning is useful when none of the nodes have access to their coordinates in a global system. This occurs when firemen or military are in operation in closed spaces such as tunnels, caves, or building complexes. In such cases, knowing the relative position of an other node is more important than knowing its absolute position.

Whatever the context is, the process of locating consists of two stages:

1. Ranging and/or angle measurement
2. Computation of position of the devices based on data acquired in step 1.

The three most widely spread methods for computing localization are [55]:

- Triangulation uses one distance and 2 angle informations to compute the position of a node when the 2 reference base stations have known positions. Its advantages are the small number of base stations necessary to determine the position coupled with no necessary synchronization between base stations. However, a high accuracy of the measured Angle of Arrival (AoA) is necessary.

Table 1: Quantitative performance comparison of synchronization protocols

Protocol	Precision	Piggybacking	Complexity	Network size
RBS [39]	$1.85 \pm 1.28\,\mu s$	N/A	High	2-20 nodes
Ganeriwal et al. [44]	$16.9\,\mu s$	No	Low	150-300 nodes
Ping [83]	$32\,\mu s$	Yes	Low	Unknown
PalChaudhuri et al. [80]	*Unknown*	Unknown	High	Unknown
Maróti et al. [72]	$1.5\,\mu s + 5\,\mu s$ / hop	No	Low	50 - 60 nodes
Cooklev et al. (IEEE 1588 over WLAN) [33]	$600\,ns$	No	High	2 nodes (ad-hoc)

- Trilateration is a method similar to triangulation with the difference that it uses a ratio between distances measured relatively to at least three base stations. This distance can be estimated from the ToA. However, a high synchronization is required between all the stations.

- Multilateration is derived from trilateration. Instead of using absolute ToA to determine the distance, the Time Difference of Arrival (TDoA) works similarly with no synchronization required between the node and the base stations. Those base stations, on the other side, still need to be synchronized.

This section focuses on the part consisting in determining a distance between two nodes, as well as the AoA of a packet for a fast and rough estimation of the relative position for military applications.

Ranging operations can be performed owing to four main methods. These methods include Received Signal Strength Indication (RSSI), Time of Flight (ToF), Time Difference of Arrival (TDoA), and Near Field Electromagnetic Ranging (NFER).

- Received Signal Strength Indication (RSSI) is based on the measurement on the attenuation of a signal through the wireless channel to estimate the transmitter-receiver distance. Although this method's simplicity has made it the most implemented in WSNs, reliable results remain extremely hard to obtain due to large errors caused by multi-path recombinations which often limit the method's accuracy [67].

- Time of Flight (ToF), also called ToA on the other side, involves the measurement of the transit time of the signal between two nodes to determine the distance between them. It is much more precise in multi-path environment thanks to a measurement performed on the first occurence of a specific event [47]. Performance of ToF measurement has been proven with UWB implementations [57, 42, 48]. The main drawback of this method is that the precision of ToF measurement is directly related to the precision of clock synchronization between the network's nodes. A 1 ns precise clock synchronization directly allows 30 cm ranging precision.

- Time Difference of Arrival (TDoA) is similar to the ToA method. The Time of Arrival (ToA) of a message transmitted by the blind node is measured on every anchor. The blind node's location is then computed on the basis of the difference between the ToAs at every anchor rather than based on ToF estimation. This method does not require a precise synchronization between the blind node and the anchors [42, 43].

- Near Field Electromagnetic Ranging (NFER)involves the measurement of the phase change of a signals magnetic and electric component to estimate distance. NFER operates on very low frequencies (i.e AM broadcast band 530-1710 kHz). However this technique broadens the used bandwidth , and can interfere with other systems therefore the FCC limit the maximum transmission power. For this reason, NFER ranging method are used for ranges up to 60 m [88].

Coupling one of the ranging methods with a Angle of Arrival (AoA) measurement allows hybrid computation using both distances and measured AoAs. AoA involves the use of complex antenna arrays names smart antennas to measure the arrival angle of a received signal. The requirement of complex antenna arrays used to make AoA an impractical solution for sensor nodes due the physical size of those antennas. However, higher frequency bands such as the 60 GHz Industrial, Scientific and Medical (ISM) band allow antenna sizes down to 5 mm. Moreover, static anchors, the main drawback of current localization system, are no longer required for hybrid computations. Indeed, the map's orientation can be determined thanks to these AoAs.

1.4 CONCLUSION

This chapter presented Wireless Sensor Networks (WSNs) as the solution to problems in multiple domains, from environmental monitoring, to military squad member localization. However, bringing a solution to such various applications and domains of applications does require either extremely tunable systems, or specific implementations and network architectures. One of the goals being an operation without access to reliable power supplies, the existing systems aiming at operating in a WSN context, such as IEEE 802.15.4 based ZigBee are limited to a part of the possible applications, and do reach their best performance in an even smaller part. Other application subjects, such as military applications, or industrial measurement have been a subject of specific researches. Indeed, the specific stringent requirement linked to such domains make such systems more difficult to make. The data-rate is higher than the existing systems, security of communications has to be enforced, and services, such as localization and synchronization between measurements have to be provided to the application layer.

This thesis is then addressing this specific problem of bringing WSNs to the industrial measurement and military world by proposing a baseband solving two major requirement specific to these domains: achievable data-rates, and synchronization and ranging capabilities.

2

UWB FOR WSN

2.1 INTRODUCTION TO ULTRAWIDE BAND WIRELESS COMMUNICATION

2.1.1 *Main aspects*

UltraWide Band (UWB) is a radio technology which aims at occupying an ultra large portion of the radio spectrum for wireless communications. The use of ultra-large bandwidth opens a wide range of new possibilities for communication systems, as well as new constraints. These constraints include relatively low maximum Power Spectral Density (PSD) to avoid interferencing with other regulated systems that use narrow bands included in the used UWB channel. The new possibilities are, for most of them, making use of the time-domain properties of UWB modulations. Indeed, narrow band modulations occupy narrow bandwidth in the frequency domain. However, In order to respect the narrow allocated bandwidth, every change of any parameter of the carrier wave for data transmission purpose is by definition long in the time-domain. On the contrary, UWB, owing to the large spectrum band used, allows modulations and reception techniques based on short time-domain events and large frequency domain bandwidth.

This major difference between narrowband modulations and UWB modulations is shown in figure 7 with a ASK narrowband modulation being compared with a IR-UWB BPSK modulation. In the frequency domain, the example ASK narrowband modulation only uses a 200 kHz frequency bandwidth and transmits with a PSD of 10 dBm/MHz. On the other side, the IR-UWB modulation occupies a 500MHz bandwidth with a PSD of -41.3 dBm/MHz. The overall emitted power by the narrowband ASK modulation is 10 mW, whereas the power emitted by the UWB modulation is of 8.7 dBm or 7.4 mW. Radiated power is the similar between those two technologies. The difference is then that narrowband modulations are based on short frequency ranges, whereas UWB modulations focus on short time domain events.

2.1.2 *UWB modulation techniques*

Such differences between narrowband technologies and UWB technologies do require different signal shape and modulation techniques. Properties of UWB modulations can be used for serving two opposite goals.

- Increased data-rate: One can indeed use the UWB as a set of joint narrow bands, and increase the data-rate by parallelizing narrow band modulations such as in Multi-Band Orthogonal Frequency-Division Multiplexing (MB-OFDM). MB-OFDM modulation fill the communication channel with a chosen number

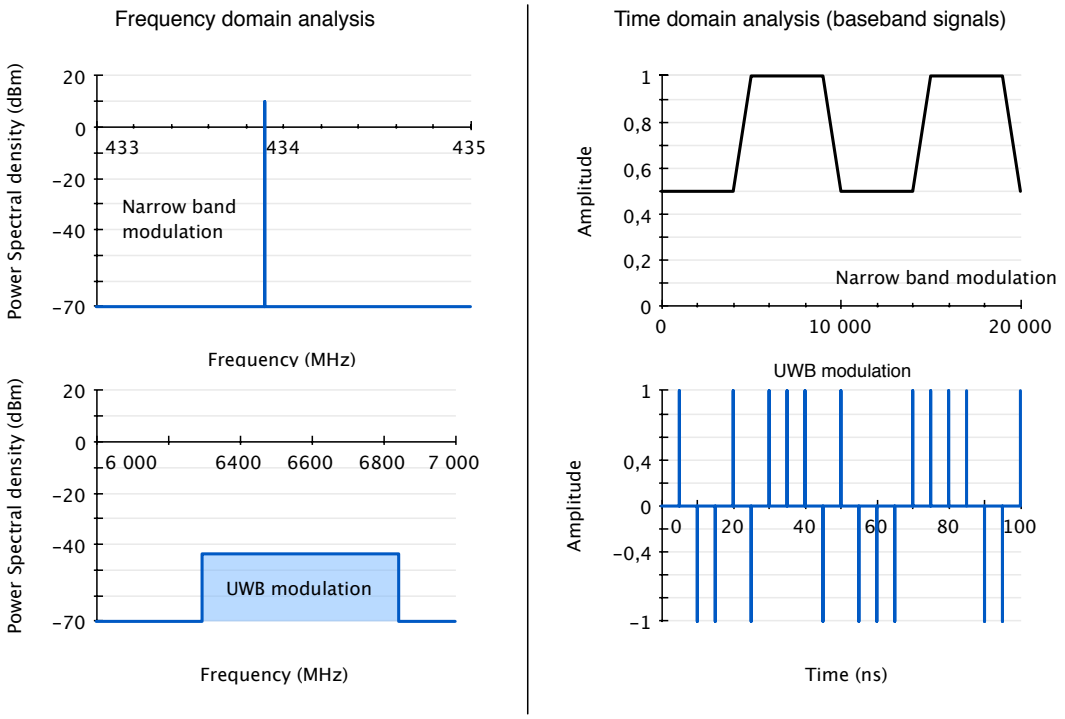

Figure 7: UWB versus narrowband

of orthogonal frequency carriers. Most of the carriers are used for data-transmission and are modulated with usual QAM modulations, whereas other carriers are used for channel modeling and equalization, as well as Medium Access Control (MAC) related tasks. Although the resulting spectral efficiency is much lower than narrow band OFDM techniques, these method allow data-rates up to 480 Mb/s data-rates in the 3.1-10.6 GHz ISM band[37, 51]. Wireless USB[17], a high data-rate cable replacement technology uses a MB-OFDM modulation standard ECMA-368 [37] also known as WiMedia UWB for providing data-rates up to 480 MB/s over 3 m, and 115MB/s over 11 m.

- Low power consumption: An other possible use of UWB is to allow lower power modulation techniques for a use in Wireless Sensor Networks (WSNs). Most of the WSNs send data during short time with long silent periods between transmissions. Owing to this technique, a WSN node can be used to monitor slow events, such as structural fatigue in a bridge or land area intrusion, without needing a power line supply, or a daily battery change. The principle of a sleep mode used to cut-off power supply to the wireless network interface during silent periods can be extended to power some parts relative to the modulation only during short pulses. Impulse Radio UltraWide Band (IR-UWB), as an example, is a modulation scheme, detailed in 2.2, which is based on the transmission of nanosecond scale pulses with a period going from 4 ns to a few microseconds [41, 94, 24] depending on the specific goals. This Impulse Radio UltraWide Band (IR-UWB) modulation in the 3.1-10.6GHz ISM band has

been included in the IEEE 802.15.4a standard [18] since 2011, and is aiming at low power low data-rate transmission over medium-range distances (see 2.2.2 for more details). The low power consumption and small form factor of such wireless communication system makes it a good competitor to other narrow-band low data-rate transceivers.

Whatever the main reason is for using UWB techniques, opportunities related to the time domain properties of UWB also include precise synchronization and ranging. Indeed, these two services can make usage of sudden events existing in UWB technologies to determine the ToF as well as clock offset and clock drift between nodes of a WSN.

UltraWide Band (UWB) technologies are also chosen for high datarate wireless communications in the 57-64 GHz ISM band. This EHF band, unlicensed by most of the regulation authorities, is divided in 1.7 GHz wide channels over a 7 GHz spectrum. Such a channel width allows data-rates up to 7 Gb/s [82, 16] for each channel with 512 carrier UWB-OFDM modulations [38]. This 60 GHz band has known a growing interest for the last 5 years owing to the high data-rates that can be achieved by using OFDM modulations with a high number of carriers on such high bandwidths. The applications taking advantage of 60 GHz communications are mostly multimedia applications for transmission of HD video streams from a set-top box to a HD display. For these purposes, the 60 GHz band is used by some commercial standards for transmission of such video streams. Among them, the ECMA 387 standard [38] is derived from the Wimedia ECMA 367 standard [37] and is improved with an increased number of OFDM carriers. Other systems such as WiGig alliance / IEEE 802.11ad [82], IEEE 802.15.3c [16], Wireless HD [1] and WHDI do also propose high data-rates in the 60 GHz frequency bands.

2.1.3 *UWB channels: regulations and caracteristics*

2.1.3.1 *3.1 GHz - 10.6 GHz UWB ISM band*

In 2002, the FCC introduced a UWB regulation for a 3.1 GHz - 10.6 GHz unlicensed band. Communications in this band are allowed with a minimum bandwidth of 500 MHz and an allowed Equivalent Isotropically Radiated Power (EIRP) of -41.3 dBm/MHz. Such power densities are in the same order of magnitude than the noise level allowed for electronic devices [19]. Since then, the other regulation authorities have proposed similar regulations. European and Asian countries for example have reduced the allowed band to approximately 3 Ghz bands whereas Canada has a more relaxed regulation comparable with the one in the USA. Regulations from selected regions for this 3.1-10.6 GHz band have been summarized in figure 8. Green bands are allowed for any UWB emission below -41.3 dBm/MHz, whereas devices willing to transmit in the bands colored in red must implement detect and avoid systems in order to avoid perturbation of devices functioning in these bands. This chart emphasizes the small amount of spectrum allowed all around the world between 7.2 GHz and 8.4 GHz. Systems then either have to be set-up depending on the country of use, or are limited to an extremely small amount of spectrum, only

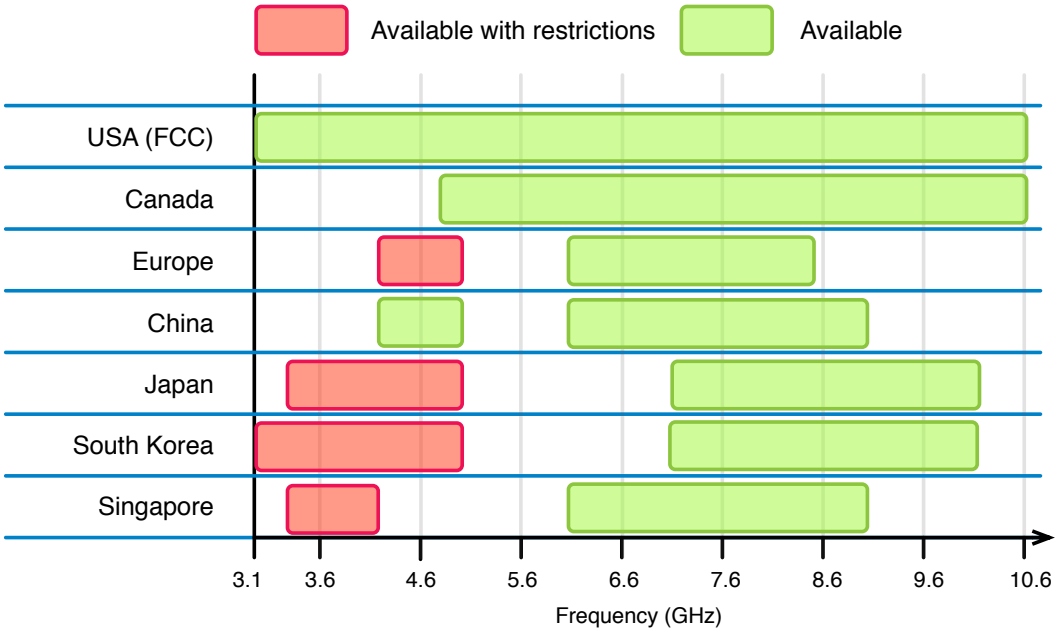

Figure 8: 3.1 GHz - 10.6 GHz UWB regulations in selected regions

allowing the use of two 500 MHz channels over the 16 possible ones for the entire FCC band.

IEEE has identified a task of modeling the UWB channel during the process of standardization of the "a" revision of the IEEE 802.15.4 standard [75, 76]. This channel model [75] has served as a basis for evaluating proposed UWB PHY layers for inclusion in the 802.15.4a WPAN standard. This channel model shows the frequency selectivity of the path-loss, and provides stochastic interarrival times of the MultiPath Components (MPCs). In the case of pulse based modulations, the UWB channel can be considered free of multipath fading as multipath reflexions do not overlap the pulse itself. However, multi path reflexions, and inter-pulse interferences must be taken into account when designing a physical layer.

2.1.3.2 *57 GHz - 66 GHz UWB ISM band*

The improvements in silicon technologies developped in the late 1990s have opened the way to cheaper and faster ICs for communications. Thanks to these innovations, faster technologies allowed simultaneously larger bandwidth complex modulations to be used, as well as higher carrier frequencies. One of the consequence of that was the idea that 60 GHz communications could be used for short range high datarate wireless communications. Following these improvements, the FCC has opened an unlicensed 57 GHz - 64 GHz band for ISM devices in 2001[9, 11]. The choice of

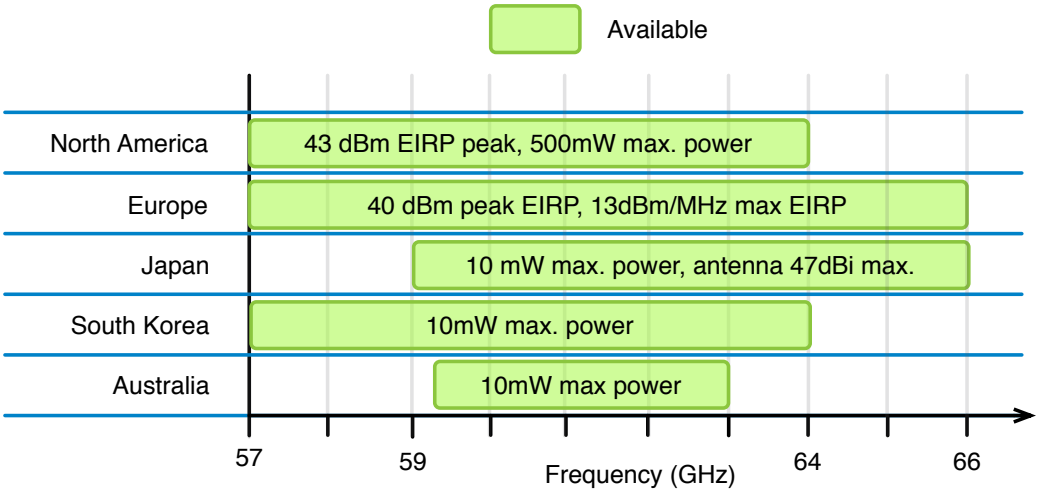

Figure 9: 60 GHz band regulations in selected regions

this frequency band is partly due to the absorption of RF signals around 60 GHz by oxygen molecules, which prevents long range propagation of such signals. Since then, other regulation authorities have followed this way, and a band around 60 GHz is available for short range communications in most countries (see figure 9). Standards have been issued, allowing for most of them multi-gigabit per second transmission of data. Among them, the IEEE 802.15.3c splits the 57 GHz - 64 GHz band in four 1.76 GHz wide channels whose center frequencies are spanned with a 2.16 GHz pitch [21]. The PHY level modulations are mostly based on OFDM with up to 512 carriers in each channel coupled with Low-Density Parity-Check (LDPC) codings. Such design allows datarates up to 5.7 GB/s over distances up to 5 m. Single carrier modulations are also made possible, especially in the application case of media kiosks where smartphones shall download high amounts of data while keeping a decent battery life[21].

The other standards in the 60 GHz band, such as IEEE 802.11ad [82] or ECMA 387 [38], are based on the same OFDM modulation or its SC-FDMA variant coupled with strong coding capabilities. However, such systems do require 512 point FFTs and IFFT!s for modulating and demodulating the signal. As a consequence, the power consumption of such transceivers prevents their use in the context of a Wireless Sensor Network (WSN).

2.2 IR-UWB

2.2.1 *Principles and modulation techniques*

Impulse Radio UltraWide Band (IR-UWB) is a communication scheme based on transmitting data through the emission of short UWB pulses at specific time intervals. The transmitted energy is then gathered in nanosecond scale time events with time intervals specifically decided depending on environment related parameters. Multi-paths and reflections, with this technique, result in pulses being received

multiple times at the receiver side. This channel delay spread (see figure 10) causes a pulse that has been sent at once by the transmitted to be received multiple times at the receiver side. The time interval, also called chip duration, is then to be determined with regard to the channel's specific delay spread and to the power levels of the multi-paths.

These pulses carry the information over the wireless link and can be modulated in many different ways depending on the required power consumption, BER, and the desired data-rate. The following modulation schemes are the most common modulation schemes for IR-UWB transmission:

- Pulse Position Modulation (PPM): A delay between the pulse's usual time of arrival and the actual one means either a 0 or a 1 value. Other PPM modulations imply the position of a pulse burst inside a two-slot symbol, as in IEEE 802.15.4a (2.2.2).

- Amplitude Shift Keying (ASK): This modulation is based on the amplitude of a pulse compared to other pulses from the same burst. This modulation has poor BER performance compared to other modulations due to its sensitivity to changing channel characteristics. However, the complexity of transmitters and receivers using this modulation is extremely low. A simple envelope detection is often enough when followed by comparators. A variant of ASK modulation is On Off Keying (OOK) modulation based on the transmission of a pulse or its absence. This variant is actually much more used than common ASK modulation because of the possibility of designing even simpler receivers based on analog or digital energy detection modules for deciding wether the received information is a 0 or a 1. A simple energy detector ran with a period corresponding to the modulation's chip time outputs the demodulated data directly.

- BPSK: This modulation uses positive and negative pulses to transmit data over a wireless link. The detection of a Start Frame Delimiter (SFD) is performed on the basis of both the actual SFD and its contrary. If the inverted SFD is detected, then the rest of the decoded bits will be inverted as well to decode the correct data. This modulation requires simple yet more complex receiving coherent algorithms than Amplitude Shift Keying (ASK) or Pulse Position Modulation (PPM) modulations which can use non-coherent receiving techniques. This is why it is often used for transmitting complementary error correction codes for improving attainable data-rates for faster devices, while keeping the possibility for reduced functionality devices to still function on the same network.

The IEEE 802.15.4a standard, which describes a IR-UWB interface for WSNs, uses a combination of BPSK modulation and PPM modulation. Such combination of an easily detectable /acPPM modulation, with a more robust, yet more complex BPSK modulation do allow Reduced Function Devices (RFDs) to communicate with Full-Function Devices (FFDs)

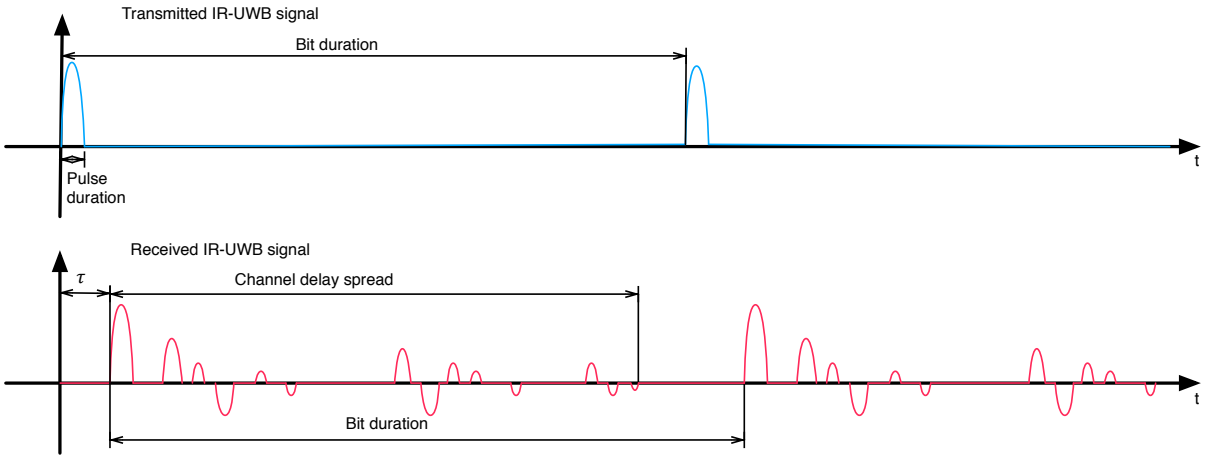

Figure 10: Delay spread of IR-UWB signal

The following section describes the IEEE 802.15.4a, a standard for designing WPAN targeted radio interfaces with IR-UWB as one of the possible modulations. This section is inspired by the analysis of this standard published by Zhang et al. [103].

2.2.2 *IEEE 802.15.4a, a standard for IR-UWB communication for Wireless Sensor Networks*

The IEEE 802.15.4a standardization group was established in 2004 and was assigned the development of a new PHY layer for WSN and other WPAN applications. The main goals of this standard are to improve the 802.15.4 standard with enhanced communications and node distance evaluation for enabling geolocation. This standard is oriented towards a use in a WPAN context. An example is Bluetooth, another technology developed towards WPAN applications, which proposes a radio range up to 10 meters [12].

The final draft for P802.15.4a standard was approved in March 2007, and published in June 2007 [15]. It describes details of the PHY layer, including modulation/coding schemes, multiple access and ranging related waveforms, as well as MAC layer related modifications to the IEEE 802.15.4-2006 standard.

2.2.2.1 *PHY layer design*

The 802.15.4a standard details two options for designing the PHY layer. Among them, the UWB Low-Rate Wireless Personal Area Network (LR-WPAN) option is designed to provide robust data communications and to improve the ranging precision thanks to Time-Hopping Impulse-Radio (TH-IR).

In order to reach these goals, the UWB PHY provides the following features:

- Low Power Spectral Density (PSD). Regulations concerning UWB in different parts of the world define PSD levels up to -41.3 dBm per MHz in the best case scenarios.

- Multiple bands and operating frequencies within each band. Devices may need to avoid using an occupied band or a band that is forbidden in the specific country where the device is being used.

- Reconfigurability. The devices should be able to modify the symbol timing, as well as the pulse's shape in order to either make a more efficient use of the channel with good transmission conditions and a high number of communicating nodes, or to allow coexistence with other spectrum users. This reconfigurability is managed through specific command for allowing higher layers to perform reconfigurability tasks.

Communication can be done between any UWB device and a coordinator or in a peer-to-peer way between coordinators. In order to allow this, a 850 kb/s mandatory data-rate is provided, along with optional variable data-rates such as 110 kb/s, 1.70 Mb/s, 6.81 Mb/s and 27.24 Mb/s.

WSNs are heterogenous by definition, i.e. formed by nodes with different capabilities and requirements (Section III-D, 802.15.4a standard [15]). Considering this, the network must have at least one FFD, i.e. one device implementing all the optional features of the standard. These FFD are less cost sensitive because of their reduced number, and are usually connected to a permanent power supply. Owing to these particularities, these devices are often configured to perform network coordination and other complex tasks the other nodes may not be able to perform. Sensors, on the other hand, are usually Reduced Function Devices (RFDs) and do often have stringent limits on complexity and energy consumption. The standard PHY layer is designed so that FFDs and RFDs achieve optimum performance through flexible modulation, coding and multiple-acces schemes (MCMs). A FFD may indeed use a more power consuming reception method based on coherent reception, whereas the RFD would use a simple energy efficient non-coherent receiver based on energy level detection. Moreover, such a flexible MCM does almost keeps intact the possible performance of the FFD, i.e. the performance of FFD with flexible MCM is almost as good as with a fixed MCM.The rest of this section (III-D) describes in better detail some specific features and designs of the 802.15.4a standard.

The frequency and bandwidth of the UWB signals are the result of a tradeoff between performance for FFDs and low complexity for RFDs. A larger UWB band allows higher transmit powers and more granularity in delay for time-hopping. However, the receiver's design complexity rises with larger bandwidths. Indeed, non-coherent receivers favor more narrow bandwidth, since the receiver cannot efficiently combine resolved multi-path components. For a coherent receiver, recombination is possible through the use of a correct number of Rake fingers as stated by Cassioli et al. [27]. The last parameter taken into account for this tradeof between performance and compatibility is the clock frequency which raises with the signal bandwidth and causes higher energy consumption, especially in Rake receivers. These consideration led the IEEE 902.15.4a to favor a 500 MHz bandwidth for all mandatory modes. Optional modes may use bandwidth up to 1.3 GHz by bonding three 500 MHz channels. Table 2 lists the different UWB bands defined in IEEE 802.15.4a standard along with the regulatory domains where these bands

freq.	Band center freq. (MHz)	BW (MHz)	Allowed in		
			USA	EU	JPN
0	499.2	499.2	X		
1	3494.4	499.2	X	X	
2	3993.6	499.2	X	X	X
3	4492.8	499.2	X	X	X
4	3993.6	1331.1	X	X	X
5	6489.6	499.2	X	X	
6	6988.8	499.2	X	X	
7	6489.6	1081.6	X	X	
8	7488.0	499.2	X	X	X
9	7987.2	499.2	X	X	X
10	8486.4	499.2	X		X
11	7987.2	1331.2	X		X
12	8985.6	499.2	X		X
13	9484.8	499.2	X		X
14	9984.0	499.2	X		X
15	9484.8	1354.9	X		

Table 2: IEEE 802.15.4a UWB frequency bands

are admissible. All the center frequencies listed in this table can be derived from existing 13 MHz or 19 MHz crystal oscillators. The 5 GHz ISM bands have been kept empty because of possible interference with narrow-band systems such as 802.11n WiFi. The repartition of these bands is summarized in figure 11 (in the 3.1 GHz to 10.6 GHz unlicensed ISM band).

The IEEE 802.15.4a standard is designed to work with both coherent and non-coherent receivers. In order to achieve this objective, a hybrid modulation scheme based on Time-Hopping Impulse-Radio (TH-IR) , BPSK and Pulse Position Modulation (PPM) has been chosen [91]. Every bit is coded in a pulse burst that is either sent in the first half or in the second half of the PPM period. A non-coherent receiver will integrate the signal and detect wether the pulse was in the first or second half of the PPM period. A coherent receiver, on the other side is able to perform a correlation with the awaited pulse burst and then improve the Signal to Noise Ratio (SNR) by a factor of N, where N is the number of pulses in a burst. Multiple-access is allowed through time-hopping. the burst waveform is sent in a different slot of the PPM half-period. The time-hopping sequence is pseudo-random and is unique to each node. A second multi-user separation technique is used by coherent receivers, and is based on the burst waveform, which is also unique to each node. This hybrid modulation, coupled with the time-hopping multiple access, allow both FFD and

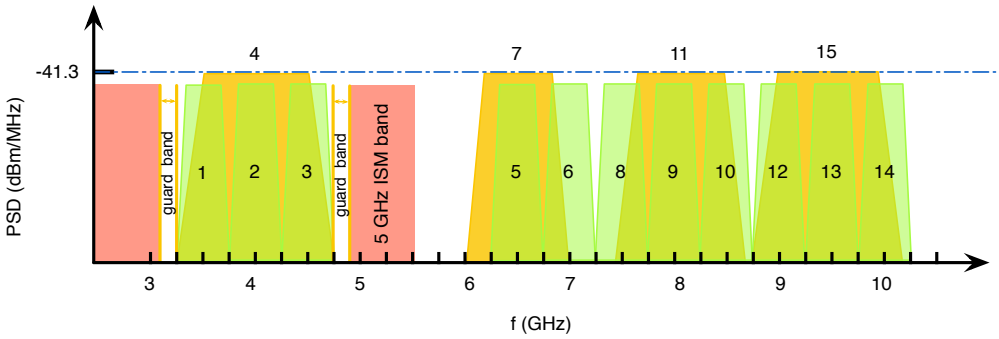

Figure 11: IEEE 802.15.4a UWB band plan

RFD to send and receive message to and from each other with no knowledge about the fact that the other node is a FFD or a RFD.

A systematic Reed-Solomon (RS) code is used for improving the performance of the transmission [45]. A 1/2 convolutional code then encodes the data in two modulation schemes: the Systematic bit is sent through PPM, and the Parity bit is sent through BPSK with the phase of the burst waveform. Different levels of decoding can be implemented in a receiver. The simplest receiver will neither decode the RS encoding, nor the BPSK convolutional parity check. The most complete receiver, on the other side, will be able to use turbo decoding with an exchange of soft information between the two decoding units.

The last part of the PHY layer described in the IEEE 802.15.4a standard is dealing with preambles and synchronization. The hybrid modulation scheme leads to specific needs for the preamble and synchronization part. Perfectly Balanced Ternary Sequences (PBTSs) are proposed as the solution to this issue. Thanks to the use of Perfectly Balanced Ternary Sequences (PBTSs), all the receivers are able to synchronize to the incoming message, whereas the coherent receivers takes benefits from its more complex specific synchronization and gain 3 dB more than the non-coherent receiver. The preamble sequences are either 31 bit , or 127 bit long, and all the allowed sequences are defined in the standard. Every network has to use a different preamble sequence in order to avoid interference between multiple networks using the same standard.

2.2.2.2 *MAC layer design*

IEEE 802.15.4a standard allows different Medium Access Control (MAC) schemes. The ALOHA scheme is presented as a mandatory scheme for any type of node. ALOHA is a scheme not needing any check before transmitting. Whereas this scheme allows even simpler nodes to be designed, an optional TDMAMAC protocol is proposed, especially for star networks up to seven nodes plus the controller. A PAN coordinator is then in charge of the attribution of permanent time-slots to nodes making the specific request to join the TDMA super-frame. One drawback for this TDMA mode is that the super-frame may only allow a number of Guaranteed Time Slots (GTS) up to seven. An other task of the PAN coordinator is to guarantee

synchronization to the TDMA super-frame. Carrier Sense (CS) based optional MAC schemes are also defined in the standard for reducing the chances of a non TDMA compliant node interfering with a TDMA frame. This scheme is based on the use of specific preambles which are multiplexed with the data and periodically inserted in the payload. A Clear Channel Assessment (CCA) scheme will then listen for this specific preamble, and delay the transmission if it detects one occurrence of this preamble.

This standard then describes one mandatory extremely simple ALOHA MAC scheme. A more complex TDMA based scheme is also proposed for better performance with a growing number of nodes. A simple CS optional scheme is also described for avoiding interferences from a RFD in a TDMA coordinated channel.

2.2.2.3 *Ranging*

As ranging is becoming a common issue in WSNs, the IEEE 802.15.4a standard proposes a frame for ranging. However, the ranging calculations are left to each implementation.

A two way ranging scheme is allowed through a set of specific packets. The requesting node "A" sends a $\text{RFRAME}_{\text{REQ}}$ packet to a node "B", and stores the timestamp of this packet's transmission. The node "B", on its sides, sends back a $\text{RFRAME}_{\text{ACK}}$ embedding the time spent between arrival of the request packet, and departure of the acknowledgement packet. The node "A" then receives this acknowledgement and timestamps it. The ToF estimation can then be performed by computation. The time between the request is sent by the node A and its acknowledgement is received is measured, and then the delay measured between the moment the request is received, and the transmission of an acknowledgement on the node "B" is subtracted. The resulting value is twice the ToF between the two nodes. This two way ranging may have performance varying with different parameters such as the precision of timestamps on both sides, and the computation itself[47, 48].

In order to improve time-stamping performance in both the receiving and transmitting sides of the PHY layer, a Start Frame Delimiter (SFD) is present in the frame after the preamble and before the actual data. This SFD is useful to determine the precise ToA of a frame. Indeed, the preamble may not be detected from the exact beginning, and it is much easier to detect a standard sequence as the beginning of each packet than to assume it from the end of a preamble. Owing to this SFD, one can concentrate on this moment to perform quality time-stamping.

The last point about ranging, that is treated in the standard, is private ranging. Indeed, ranging may be a strategic need in some cases such as many military applications.

2.2.3 *Low power implementations of IR-UWB transceivers*

IR-UWB transceiver have different implementations than other usual narrow band transceivers do. For example, Phase Locked Loops (PLLs) circuits are no longer

reliable when it comes to synchronizing transceivers. Indeed, Short pulses cannot be used for training such systems. On the other side, a precise timing synchronization is required to properly decode PPM modulations, as well as to receive data from a single transmitter in a multi-user channel where other transmitters may be transmitting pulses at the same time.

This subsection is detailing specificities of implementations of IR-UWB transmitters and receivers. In the same time, it is also listing some of the most remarkable IR-UWB implementation selected with regard to specific requirements targeted in the present thesis. The major points of interest are the power consumption, the attainable data-rate, and the synchronization or ranging performance. These parameters are then the base for comparing reference in both this subsection, and at the end of chapter 4.

2.2.3.1 *Transmitters*

When designing a narrowband transmitter, Power Amplifiers (PAs) are often the most critical blocks, since their power consumption usually dominates in the global consumption. However, in the case of IR-UWB transmitters, the use of short pulses allow PAs to be turned on and off between two pulses, thus making its consumption fall to the same order of magnitude than the rest of transmitter blocks [89]. Pulse shaping circuits are then a major point of interest when building a low power IR-UWB transmitter. These transmitters can be designed with a variable amount of digital logic in the design.

Analog pulse generators can be built on very distinctive forms. Some of them are using derivative functions on a digital signal to form pulses [89, 68, 69]. The derivation is performed through LC oscillators schitched by short current spikes. The main drawback of this pulse generation technique is the lack of configurability, preventing the use of BPSK modulations. Other implementations, allowing BPSK modulations, are using mixers to build Gaussian pulses [102, 20]. These Gaussian pulse are obtained by exploiting the transcient behavior of a custom designed mixer. The BPSK functionality can be obtained by passing a baseband digital pulse either in the positive input or in the negative input of an amplifier circuit [102]n or by putting a Digital-to-Analog Converter (DAC). More recently, researchers have proposed the use of gaussian and sinusoidal phase-to-amplitude converters to build high speed Direct Digital Synthesizer (DDS) that could be used for generating pulses [25]. The main interest of this technique is the range of possible pulse configurations in terms of width and shape.

Mostly analog transmitter implementations have been proposed for their low power consumption, as well as their small form factor. Most of these implementations consider that the functionality required for transmitting the pulse at the right moment is performed in a preceding block.

Other implementations, making a greater use of digital logic have been proposed, which also allow reconfigurability of the pulse shape and amplitude. Some of the designs cited below include the pulse form generation, as well as timing logic for performing the transmission of the pulse correctly.

Among mostly digital implementations, there are two main ways of performing pulse generation. The first one focuses on designing a combinatory circuit for creating pulses with a pulse width far below the digital system's clock frequency [93, 78, 101]. This can be obtained through the use of a chain of logic inverters causing a sub-nanosecond delay between a rising signal and its delayed image. A XOR function between the original and the delayed signal then creates a pulse shorter than the clock period.

The other way of forging pulses requires fast logic latches, as well as a fast Digital-to-Analog Converter (DAC). Its purpose is to compute the shape of the pulse in a digital circuit, and then convert it through the DAC [63, 62]. The main drawback of this technique is the fast clock speed required for forming sub-nanosecond pulses. However, such designs allow reconfigurability in terms of pulse shape and amplitude.

Owing to the variety of features proposed in each implementation, a comparison in terms of power consumption with regards to data-rates is not as reliable as it shall be.

2.2.3.2 *Receivers*

Implementations of IR-UWB receiver interfaces can be sorted through the proportion of analog circuit in the detection and correlation processes. Mostly analog implementations will provide a bit value information, and do rarely use Analog-to-Digital Converters (ADCs) and DACs because a 0-1 information is provided by an analog correlator. A good example of a working IR-UWB receiver has been proposed in 2006 by Tamtrakarn et al. [96]. Recent analog implementations are often lower power than digital based implementations thanks to circuitry that is specifically designed for the task of detecting or generating pulses [35]. An analog front-end receiver for IR-UWB transmissions, proposed by Van Hellepute et al. [100] provides pulse detection and a conversion gain up to 50 dB for pulse rates up to 39.065 Mbps with a power consumption of 70pJ/pulse in 130 nm CMOS. However, the reconfigurability of such devices is rarely possible due to a specific implementation, optimized for a specific pulse shape, and a specific pulse rate. Other implementations have been proposed containing an increased part of digital computing. For example, a mostly digital implementation, including an analog front end front-end [73, 34], has been proposed by Prof. Chandrakasan's team at Massachusetts Institute of Technology (MIT).

A recent receiver implementation, proposed by Van Hellepute et al. [99] is a mostly digital implementation coupled with specific analogue signal processing for ToA estimation and ranging applications. This receiver, which is fully and independently working, shows a reduced power consumption of 108 pJ per received bit. As of 2011, this implementation was the least power consuming high data-rate /acIR-UWB receiver implementation. The lowest power consuming complete transceiver was the implementation proposed by Terada et al. Terada et al. [97]. Although this implementation provides ranging service with a precision down to 2.5 cm, the proposed data-rate remains very low when compared to our goals.

Full transceivers, containing both transmitter and receiver functionalities, have been proposed and allow for more reliable comparisons.

State of the art receiver and transceiver systems detailed above are listed for comparison in table 3.

Ref.	Tech.	Freq.	Features	Pulse rate	Min EPP	Ranging acc.
Tamtrakarn et al. [96]	0.15μm FD-SOI CMOS	0-960MHz	RX only	25 k	12000 pJ	n.a.
Terada et al. [97]	0.18μm CMOS	0-960MHz	Transceiver	1 M	4000 pJ	2.5 cm
Lee et al. [66]	0.18μm BiCMOS	3-10GHz	RX only	100 M	750 pJ	n.a
Lachartre et al. [60]	0.13μm CMOS	4-5GHz	Transceiver	31 M	1100 nJ	30 cm
Mercier et al. [73]	90nm CMOS	3.5-4.5GHz	Full BB	16 M	300 pJ	est. 30 cm
Daly et al. [34]	90nm CMOS	3.5-4.5GHz	RX only	16 M	500 pJ	30 cm
Zheng et al. [104]	0.18μm CMOS	3.1-5.5GHz	Full Baseband (w/o ADC)	1 M	6220 nJ	n.a.
Van Helleputte et al. [99]	0.13μm CMOS	0-960MHz	RX only	39 M	108 pJ	1.4 cm

Table 3: State of the art UWB systems

Part II

CROSS-LAYER DESIGN OF A HIGH DATA RATE SYNCHRONIZED WIRELESS SENSOR NETWORK COMMUNICATION INTERFACE

The following part explains the cross-layer design of a WSN baseband including a UWB PHY layer and a specific TDMA MAC layer with services such as synchronization between nodes, and distance evaluation for localization purpose. The chapter 3 explains the system design through the advantages of a cross-layer design when the specific needs are challenging in regard to the state of the art in every domain. The design of a small complexity TDMA MAC layer is detailed. Services specific to WSN are studied from algorithm design and implementation to error analysis in chapter 3.4. The last chapter of this part (chapter 4) shows two implementations of the same MAC layer and services for two different applications. A first design is optimized for high data-rate long range data transmission of synchronized measurements in mostly Line of Sight (LoS) conditions. A custom mixed signal ASIC flow developed for implementing the second design is presented. Finally, the second design presented is optimized for highly reflective channels, and high precision relative positioning of moving nodes.

3

CROSS-LAYER DESIGN OF A UWB WIRELESS COMMUNICATION SYSTEM FOR WSN

3.1 SYSTEM VIEW: CROSS LAYER CONSIDERATIONS

The requirements mentioned above are not reachable when using the common Open Systems Interconnection (OSI) model for networks. Such models are designed for common applications, and limit the overall performance and determinism at tolerable levels when developing general purpose applications. This application, however, is constrained in almost every direction, and allows no tradeoffs, which are necessary when using the OSI model.

The proposed solution solves this issue with the use of cross layering. The proposed cross-layer system is shown in fig 12. An Ordonancer, coupled with the system timer, runs the different tasks with regard to the schedule. A frame cycle time is set up to stick to the required refresh rate. By doing this, the system is always aware of the time remaining before the next refresh event occurs.

This cycle time then gives the information about the expected measurement date. This cycle time can then be used as the main TDMA frame, and is static through time. Measurements can be taken with the same refresh rate, and are sent to the master by the way of the TDMA MAC. However, it is necessary to synchronize the nodes to a master clock, not only to synchronize measurements, but also to synchronize the slaves' transmitting periods to not overlap.

The Wireless Deterministic Clock Synchronization (WiDeCS) scheme solves this problem, and gathers signals from different layers of the interface Beluch et al. [23, 22]. The figure 12 shows the transversality of the scheduler and the implementation of WiDeCS scheme.

Existing standards describing PHY layers for wireless communications do not implement precise Time of Departure (ToD) and Time of Arrival (ToA) measurement techniques. The ToD and ToA measurements are currently based on time-stamping in higher layers such as application layer, and less frequently in the MAC layer. The proposed scheme uses flags implemented inside the PHY layer. The dependency of WiDeCS scheme over these flags makes it incompatible with most of commercially distributed PHY layers. It is then necessary to modify an existing IR-UWB PHY layer to include those flags. The WiDeCS scheme is then advised for application specific development, especially when a precise synchronization between captured events is a strong requirement.

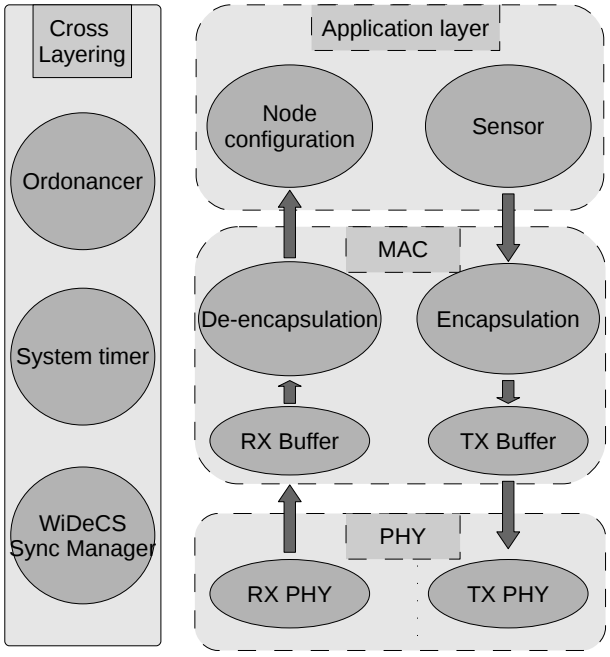

Figure 12: Proposed cross-layer system

3.2 MAC LAYER(S)

3.2.1 *Fixed slot Time Division Multiple Access*

A MAC layer has been designed specifically for WSNs aiming at taking measurements continuously from a fixed number of sensors. Such a network does not have any need for a complex MAC protocol. Instead, the cross-layer services do need a MAC respecting the following requirements. The network has to be deterministic in order to precisely plan the date of transmission of each frame. Indeed, a precise synchronization is possible with a reduced amount of transmitted data when a part of the information required is implicit by means of the protocol. A fully deterministic MAC layer would allow each node to know when the other nodes are expected to transmit data.

The other requirement that was taken into account to design this MAC layer was to build a system with the lowest possible power consumption .

The network architecture that could host a huge number of nodes and reach the requirements above is a cluster tree network. A cluster is formed between a Base Node and a set of relays. Each relay has a dual wireless interface, and acts as a slave to the Base Node, and as a Master to the connected sensing nodes.

A fixed slot TDMA MAC layer fits perfectly to these requirements. A master node manages a fixed set of slave nodes. Each one of these slave nodes transmit a fixed amount of data containing either sensor data, or setup and monitor related data.

Time is divided as in fig.13. The master node sends a beacon frame, addressing to all of its cluster's slave nodes. This beacon is formed with the network ID (i.e. the ID of the cluster this node is managing), the source ID, here a master node ID, and

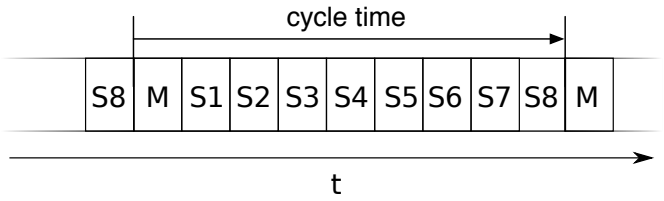

Figure 13: Time Division Multiple Access channel occupation

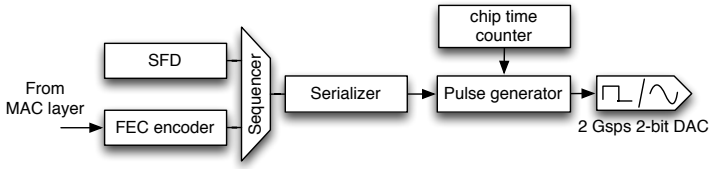

(a) transmitter

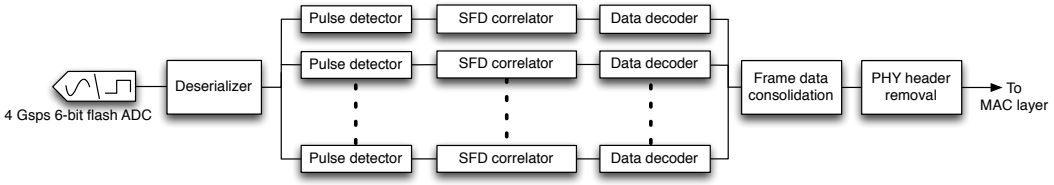

(b) receiver

Figure 14: IR-UWB transceiver

service related data. This service related data is used to help in performing clock synchronization of the slaves with the master node.

3.3 SPECIFIC PHYSICAL LAYER TUNING

3.3.1 *IR-UWB physical layer tuning*

The strong synchronization required by aeronautic and space applications do induce some requirements at physical level. An UWB modulation scheme, with its very fast changes in time domain, allows more precise time-stamping than narrowband modulations. The proposed system is based on a BPSK Impulse radio UWB modulation. This modulation can be summarized to the transmission either of a positive pre-defined pulse or a negative pulse with the same shape. The low complexity of this modulation is strengthened by the fact that these pulses are transmitted with the same bit-time whatever their phase is.

The transmission module is composed of a Forward Error Correction (FEC) encoder, a chip time counter and a pulse generator (Fig 14a). Each time the counter reaches its overflow value, a pulse is transmitted with the correct phase according to the input value. In order to allow proper synchronization of the receiver to the transmitted frame, a SFD is introduced at the beginning of each frame.

A rake receiver as proposed by Lecointre et al. [61] is implemented on the receiver side, and allows decoding each multi-path separately (Fig 14b). The values captured by the ADC are first compared to a positive and a negative pulse. The most probable result is then passed as a 0 or a 1 to the rake decoder. In this decoder, the timeline is deserialized into a vector containing at least a full chip time.

This reception method strengthens the receiver owing to its capacity of using the multi-path effect to improve the quality of reception instead of trying to avoid it.

The frames sent by this physical layer are composed of :

- Pulses for training the Automatic Gain Control and improving reception performance.
- a Start of Frame Delimiter, which is used for training the PHY level synchronization at receiver side.
- the effective data, given by the MAC layer on transmitter side, and passed to the MAC layer on receiver side.
- a Forward Error Correcting hash for correcting transmission errors.

Modifications have been applied to this physical layer in order to take advantage of the side-effects of this modulation. The fact that a high sampling rate is required for UWB modulation can also be used to improve the time-stamping performance. Indeed, the physical level synchronization protocol used for matching the signal sampling to the received data is modified, and outputs a pulse when the first pulse of the first effective bit of the frame is being received. Delays between detection and triggering are compensated owing to the predictability of this precise event thanks to the PHY level synchronization.

The resulting performances are reception triggers with errors below the ADC sample period. Performances attained in triggering the reception of a frame at receiver side will be determined according to the ADC sampling frequency Fs, usually more than twice the used bandwidth. The achievable timestamp accuracy ϵ, in seconds, of the receiver is defined by:

$$\epsilon[s] = \frac{1}{F_s} \tag{3.1}$$

A similar flag is triggered by the transmitter part of the physical layer when the same first bit of effective data is transmitted. The two triggers are passed to the MAC layer for time-stamping purposes.

3.4 CROSS-LAYER SERVICES

3.4.1 *Measurement trigger synchronization*

3.4.1.1 *Identification of the major blocking points*

Most wireless network interfaces rely on flexible and scalable MAC protocols, thus generating randomly distributed delays in the MAC layer. A frame provided to the MAC layer by the network layer does often wait for an undetermined time before it is being put on the channel. State of the art synchronization systems try to compensate this unknown delay by means of a statistical analysis based on a big number of frame exchanges. However, such protocol rarely adapt well to the moving node problem. The goal is then to determine precisely most of these delays, in order to provide better synchronization performances and refresh rates.

3.4.1.2 *Algorithm design*

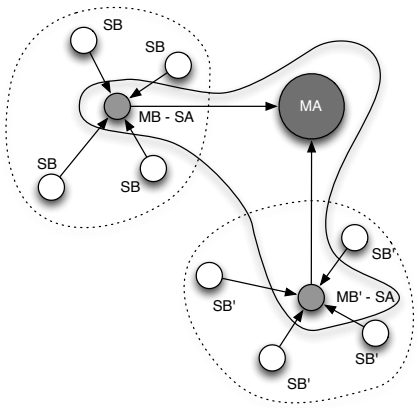

Figure 15: Piconet architecture

The Wireless Deterministic Clock Synchronization (WiDeCS) protocol is based on the planning of transmissions, and the respect of this planning. It is designed for propagating the master clock of a star network to all the slaves. The cluster tree is organized as stacked levels of star networks named pico-nets. Each piconet is composed of a master node and up to eight slaves (fig 15). This protocol then propagates the clock information to slaves of these networks. These slaves then repeat the operation with levels below.

The figure 16 details sources of delays in the network link. Delays are measured on the first effective bit (events linked to preambles and serialization have to be de-embedded). Current synchronization protocols tend to determine these delays by the means of time stamping.

Efforts have been made to place this time stamping as close as possible to the effective channel, thus reducing uncertainties on the characterization of the propagation time on the channel. However, none of the known protocols for WSN uses time

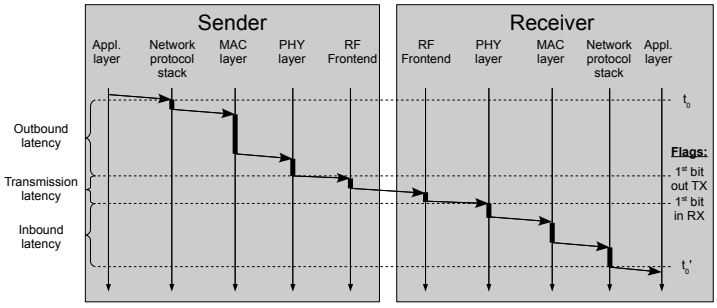

Figure 16: Latencies involved and flag positioning for WiDeCS

stamping at levels as low as physical (PHY) layer. Time-stamping in the PHY layer has been proposed in 2005 by Kannisto et al. [56]. However, their implementation of the synchronization protocol is performed on a classic IEEE 802.11 WLAN network interface. The performances claimed by Kannisto et al. in their paper's abstract are as low as 1.1 ns mean error and 3.1 ns² variance. WiDeCS uses similar time stamping at the time of the first effective bit at the output of the PHY layer in emission, and the first effective bit in input of the PHY layer in reception. Owing to the TDMA MAC layer, each node of the network is supposed to talk at precise moments. Measuring delays between expected receiving times and actual ones helps determining the clock offset and the propagation time. WiDeCS Synchronization protocol uses possibilities relative to time division to determine the clock offset between each node and the master. The figure 17 shows the different informations gathered on different sides, and sent to the slaves by the master.

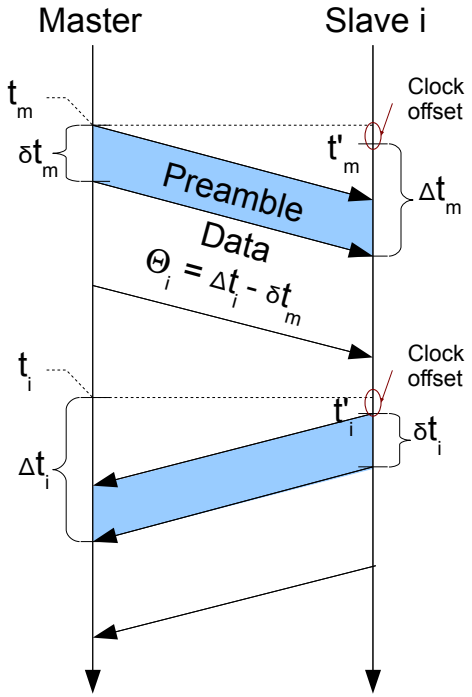

Figure 17: Exchange of timing information

The complete synchronization is based on 2 steps.

Phase 1: Pre-synchronization

This step is performed by every slave when joining the network.

The master (the router) has the same communicating hardware the slaves have, along with other network interfaces to communicate with higher levels of hierarchy. The function of the master is to create, and regularly send a preamble for the frames of its piconet. The slaves, when reset, or desynchronized, switch to reception only mode, and wait for the master node to indicate the beginning of the frame. When this message is detected, the slave resets its *frame counter* to a predefined reset value in order to begin transmitting data in the dedicated slot. When this step is passed, the slave switches to phase 2 of the synchronization process.

Phase 2: Fine-synchronization

Once pre-synchronized, the nodes have a clock offset of 1 μs relative to the master clock.

This step consists in determining the offset with the greatest precision possible. When the slave is allowed to transmit data, it does it at one precise moment t_i of the slot. This date is coded in the protocol and is known by every slave, and more importantly by the master. Data is sent to the PHY layer when$t = t_i$ and a capture of the timer is done when the TX_ONGOING flag is set. t_i is then subtracted to this date, and the result is stored as δt_i. Note that small deltas (δ) are used for delays in transmitted packets, whereas capital deltas (Δ) are for delays in received packets

$$\delta t_i = t(\text{TX\_ONGOING}_{slave}) - t_i$$

The master, on its side, capture the date when RX_ONGOING is set, waits for the packet to be passed through the layers to the applicative part, and deducts t_i from the captured date. The result, Δt_i, is then stored and linked to the correct node.

$$\Delta t_i = t(\text{RX\_ONGOING}_{master}) - t_i$$

When the master slot begins, the master start the transmission of a standard preamble to the TDMA frame, and includes delay informations concerning the slave nodes and measured deltas. The information transmitted is named Θ_i and is defined as follows:

$$\Theta_i = \Delta t_i + \delta t_m$$

Δt_m is measured while transmitting the packet and is stored for the next frame. This approximation can be avoided if TX_ONGOING rises before the transmission of data to the PHY layer has ended.

$$\delta t_m = t(\text{TX\_ONGOING}_{master}) - t_m$$

The number of bits used in packets transmitted by the master for the complete set of Θ depends on the number of bits used for the encoding of each Θ. The higher this number is, the faster the synchronization will be optimal. The slaves, when receiving the message from the master, determine Δt_m:

$$\Delta t_m = t(\text{RX\_ONGOING}_{slave}) - t_m$$

Considering t_p the propagation time almost symmetrical. The clock offset can be determined with these equations.

$$\Delta t_{clk} = t'_m - t_m$$

$$\Delta t_{clk} = \delta t_m + t_p - \Delta t_m$$

for packets from the master node, and

$$\Delta t_{clk} = t'_i - t_i$$

$$\Delta t_{clk} = \Delta t_i - t_p - \delta t_i$$

for packets from the slave node. By adding those two equations, we obtain

$$2 \times \Delta t_{clk} = \Delta t_i - \delta t_i + \delta t_m - \Delta t_m$$

and then

$$\Delta t_{clk} = \frac{(\Delta t_i + \delta t_m) - (\delta t_i + \Delta t_m)}{2} \tag{3.2}$$

$$\Delta t_{clk} = \frac{\Theta_i - (\delta t_i + \Delta t_m)}{2} \tag{3.3}$$

The correction offset is applied to the timer, forcing rollback if necessary. Consequences depend on the date chosen to apply this correction, as well as on the actions other clock dependent processes may be performing at this moment.

WiDeCS can be used in every frame to maintain a clock as precisely synchronized as possible for all the length of the measurements. Another possibility is to train the slave with an optimal number of frames, and then turn the reception module in sleep mode for as long as blindness is allowed in the network.

3.4.1.3 *Error Analysis*

The errors relative to WiDeCS protocol can be sorted in two major types :

Time sampling errors

WiDeCS massively uses time capture to reach a view as deterministic as possible of the whole system. The major drawback of this is the fact that time sampling is limited by a major element: the clock speed. Indeed, it is impossible to tell precisely the date of a digitally captured event. Captured values have a ± 0.5 clock period uncertainty. When spreading this to the equations, we obtain $\Delta(X)$ the value of uncertainty of X($\Delta t_{spl} =$ is the time sampling uncertainty)

$$\Delta(\Delta t_{clk}) = \frac{(\Delta(\Delta t_i) + \Delta(\delta t_m)) + (\Delta(\delta t_i) + \Delta(\Delta t_m))}{2}$$

$$\Delta(\Delta t_{clk}) = \frac{2\Delta t_{spl} + 2\Delta t_{spl} + 2\Delta t_{spl} + 2\Delta t_{spl}+)}{2}$$

$$\Delta(\Delta t_{clk}) = 4\Delta t_{spl} \tag{3.4}$$

By combining equations 3.3 and 3.4, we obtain the complete evaluation of the correction to be applied to the timer.

$$\Delta t_{clk} = \frac{\Theta_i - (\delta t_i + \Delta t_m)}{2} \pm 4\Delta t_{spl}$$

$$\Delta t_{clk} = \frac{\Theta_i - (\delta t_i + \Delta t_m)}{2} \pm 2t_{clk} \tag{3.5}$$

RF front-end asymmetry and evolution of the channel

The other major source of uncertainty is the asymmetry existing between two RF front-ends. Although both RF front-ends should share the same hardware, slightly different clock speeds could cause unexpected asymmetry between the propagation time among the nodes.

The other phenomena causing unexpected effects on the propagation time (t_p) is a fast evolution of the communication channel. This evolution is compensated during the next two cycles happening after the evolution. Moreover, considering the context and the requirement for frames of a few tens of microseconds, it seems unlikely that it will cause a failure in synchronization.

4

HARDWARE IMPLEMENTATIONS OF UWB COMMUNICATION SYSTEM FOR WSN

4.1 SYSTEM REQUIREMENTS

4.1.1 *System for aircraft structure health monitoring*

Structural Health Monitoring (SHM) has been a growing field of research in the last decade. Nowadays, innovative constructions are being monitored to check how materials age. This is also done with unstable monuments for improving their lifetime by preventing failures. Although this market is constantly growing, a set of very constrained applications poses problems that remain unsolved. Aeronautics and Space SHM applications demand performances yet unattained. Indeed, the context specific to this range of applications is often combining requirements on the Quality of Service (QoS) with higher precision synchronization, and advanced functionality such as defect localization. Moreover, the number of nodes in a volume unit is higher than usual WSN applications, and the propagation channel is often a metallic chamber. Innovative SHM systems, using acoustic wave transmission and reflexion inside the structure, have been proposed to detect and locate defects. The type of defect and its location in the structure can be determined owing to delay measurement between the reception on different nodes along with waveform study. However it is necessary, in order to determine precisely the position of the defect, to have a shared clock reference for allowing trilateration based on the propagation of the wave through the structure and ToA. All the nodes involved in such tests have to be synchronized to a same reference clock.

A similar system is also needed to evaluate a system's compliance with its specific requirements, Hardware system testing is conducted on a complete and integrated system. In the final phase of the development of an airplane, flight-test equipment gathers and analyzes data during flight to evaluate evolution of parameters of the aircraft and to validate its design including safety aspects. Such systems, intensely used by aircraft manufacturers, currently use wired communication systems. Sensors, placed all around the plane, are wired to calculators inside the cabin. Although good performance is observed in terms of measurement accuracy and synchronization, these systems show strong drawbacks. The two most troublesome ones are the weight of the system and its installation. The weight of all the cables passing through the wings modifies its behavior, and can introduce false errors to the testing process. These cables also represent a challenge during the installation of the measurement setup and increase the cost of installation of such systems. These points and the complexity of such systems do not allow a great number of measurement points. For all these reasons, research has been conducted [53] on a wireless measurement system based on WSNs over UWB channels.

From the context described before, we can extract required parameters the MAC layer and synchronization protocol have to reach.

- Continuous emission: Measured data has to be provided to the data logger continuously. Measurements are taken every few tens of microseconds and sent to the data processing unit.
- Correlation possible in 3D models: A correlation is performed on simultaneously measured data to extract informations about defects in real time. To perform such correlation, the exact positioning of every sensor has to be configured during the development of the calculation tool. This requirement enables a simplification of the whole network which will require it to be pre-defined and fixed through time.
- Precise synchronization of the measurements through the entire system: This requirement is the reason for the development of the proposed synchronization protocol. In the literature, no proposed protocol allows precise synchronization between measurements from hundreds of sensors with a maximum tolerated offset under the microsecond.
- Tunable sensing parameters: Considering the wide range of possible uses in the same context, the data processing unit requires the possibility to act on parameters of the sensing elements.

All these requirements represent a challenge for the design of a synchronization protocol. The proposed protocol described below has to meet all these requirements, while using simple mathematic operations to keep a low power consumption.

4.1.2 *Reconfigurable tactical Impulse Radio UWB for communication and indoor localization*

The proposed tactical radio interface is aiming at providing to infantry means to communicate efficiently health related data, as well as relative position between members of a same squad. This data has to be refreshed regularly in order for each member of the squad to know the positions of his squad-mates with an acceptable delay. Military operations do require such services including positioning in closed spaces such as buildings or caves. Conventional positioning system, usually requiring a direct LoS with multiple reference stations. In the case of GPS, the satellites act as reference stations whose exact locations are determined precisely at every moment [36]. Radio-Frequency IDentification (RFID) based positioning, as well as other indoor localization schemes, allows positioning inside buildings. However it requires the installation of a high number of static stations in every room in order to locate a node efficiently [81, 84, 92].

Because of the lack of pre-deployed reference stations in enemy buildings or caves, military related constraints cannot be satisfied with existing protocols.

The proposed solution involves measuring the ToF between the team's member to quickly aggregate a database containing ToF between nodes, and build up a map

of these nodes. The orientation of this map can be determined by adding the AoA information along with the ToF when building this database. A fast rough estimation is possible by means of these two informations, and determine the direction in which the friend nodes possibly are.

The requirements for localizing nodes in a tactical context are then propagated to the baseband as:

- Highly directive wave propagation : for determining precisely the AoA.
- Sub-nanosecond scale time synchronization and ToF evaluation : for localization precision up to 15 cm.

4.2 APPLICATION SPECIFIC IMPROVEMENTS AND SIMPLIFICATIONS

A network is usually composed of nodes coming and leaving the network. The number of nodes changes with time. In the contexts described before, the network is planed and parametrized before its deployment. In the aeronautical context, the nodes are deployed inside and on the external surfaces of the structure. On the other hand, in a military context, squads are defined before a mission, and network communication can be divided in a fixed cluster tree network architecture. Simplifications are then allowed by these two application contexts without risking uncontrolled behavior. The simplifications used in this paper are listed below, and reasons are given for their existence.

- Fixed number of nodes per piconet and pre-programmed time slots:

  As we explained before, the network architecture is fixed, and planned before deployment of the communication system. The number of nodes for each piconet is then a tradeoff between attainable uplink bit rate, desired bit rate, and uplink occupation based on these 2 parameters.

- No jamming between neighboring pico-nets:

  The UWB unlicensed band is divided in sub-bands. The placement of pico-nets on the surfaces can be designed to avoid jamming between channels. This consideration enables the use of one TDMA master per piconet, and then allows the whole developed protocols to work correctly. In the case of moving nodes such as military squads, bands are attributed to squads and stay this way until the end of the mission.

- Symmetrical links:

  Every node of the network is fabricated using the same hardware. Delays in Radio Frequency (RF) front-ends are then similar from one node to another.

As described in section II, some modifications are implemented inside the existing PHY layer. These modifications improve time-stamping performances by avoiding unknown delays. They also allow, along with the simplifications allowed by the application specific requirements and permissions, a simple yet performant Wireless communication interface for WSN.

4.3 PROPOSED SYSTEM ARCHITECTURE

In this case, sensor and nodes are disposed at many different positions of the monitored structure. Such a monitoring system, sampling measurements from all over a structure, helps in validating design simulations. This is done by giving enough data to virtually replay the test sequence, and check the structure's behavior through time. In order to acquire reliable data, the sampling frequency has to be high enough to respect the Shannon-Nyquist sampling theorem[90]. Moreover, the delay between the measurements from all nodes has to be as small as possible. This is necessary for every space-time correlation of data acquired from all the sensors. Determinism and clock synchronization are keys in controlling wether the small detectable events measured by different sensors on the same structure can be correlated as parts of a same event or not.

The proposed system is based on a cluster tree network as in fig 18. A gateway is in charge of gathering data collected by every sensor in the network. This gateway is composed of

- A storage unit: large enough to store the data coming from all the sensors during a full test campaign. access to it also has to be fast to allow data from all the sensors to be written simultaneously.
- A reporting software: Used to generate real-time reports for test engineers. Has a fast access to stored data.
- A clock reference: obtained either through GPS or through a IEEE 1588 PTP [10]compliant network. This clock is used as the reference for time-stamping measurements.
- A top-level master wireless interface: This wireless network interface acts as the top node or the cluster tree network.

The cluster network, generated by the wireless interface contains a fixed number of relay nodes, or sensing nodes. In this case, the number chosen for this application has been fixed to 4 relays. This number is set this way in order to keep a low overhead, and a high data-rate.

A relay, composed of two network interfaces, is used to extend the capacity of the network. Every relay acts as a slave for the main cluster network, and is a master to its own cluster network. In this cluster network, a fixed number of 4 sensing nodes is connected to the relay node.

A sensing node gets results from up to 8 sensors with a 16bit resolution and 25KHz sampling rate. It is possible to allow a higher resolution or more sensors by acting on the number of bits allocated to each sensor.

Considering that measurement trigger synchronization is a major requirement for obtaining reliable data, the WiDeCS protocol is used to synchronize slave nodes to the master nodes in this cluster tree network.

When compared to the Gateway relays possess the following measurement trigger error (t_1 is the error between the relay and the gateway, t_{std} is the synchronization error of WiDeCS protocol):

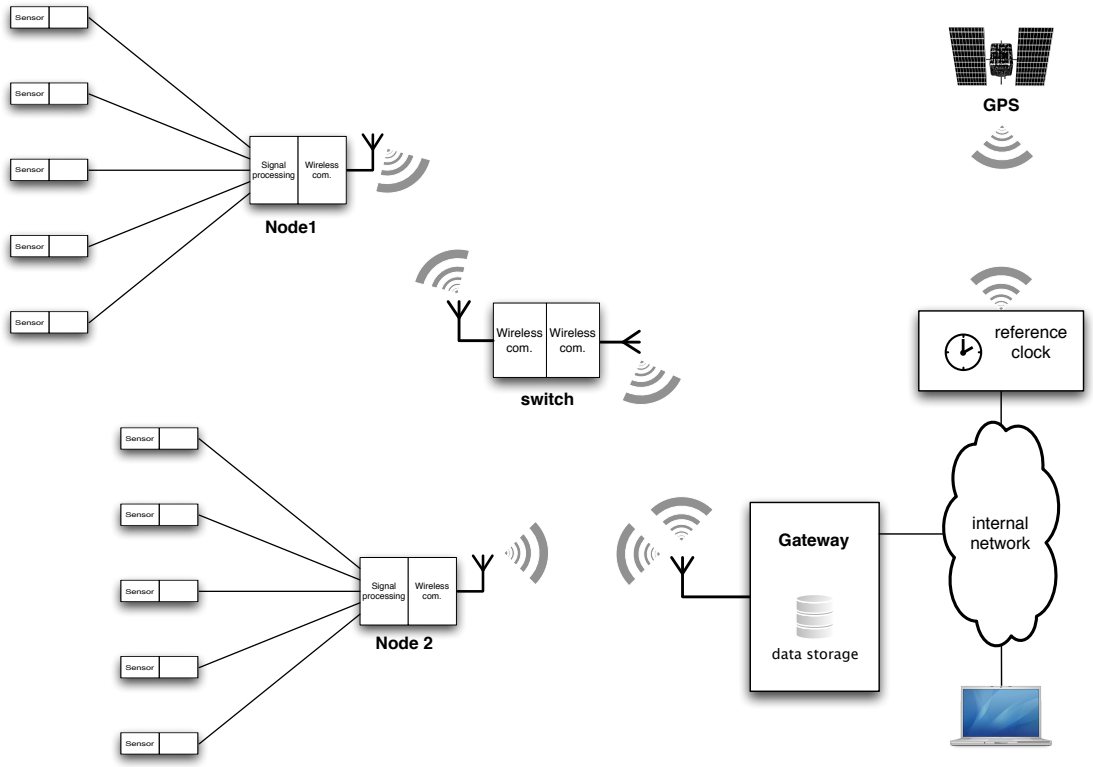

Figure 18: Proposed system architecture

$$t_1 = t_{std}$$

Sensing nodes have the same error compared to their relay.

$$t_2 = t_1 + t_{std} = 2t_{std}$$

This network is then a 2-hop cluster tree network, and proposes a synchronization error of $2 \times t_{std}$

The data captured by the sensors is assembled in a frame sent to the relay every 40 μs. The relay bundles the frames received from its slaves, and sends it to the gateway.

Concerning the communication over a wireless link, WiDeCS MAC protocol has been chosen to keep determinism and allow clock synchronization. A UWB OFDM physical layer implementation has been made in the research team, and has been modified to work with WiDeCS as explained in chapter 3. The baseband described above is implemented along with specific IP for each part of the network.

The sensing nodes contain Serial Peripheral Interface (SPI) Input Outputs (I/Os) for obtaining data acquired through Commercial Off-The-Shelf (COTS) ADCs. A queue is then added at the input of the MAC layer to sort data coming from different sensors in the right order.

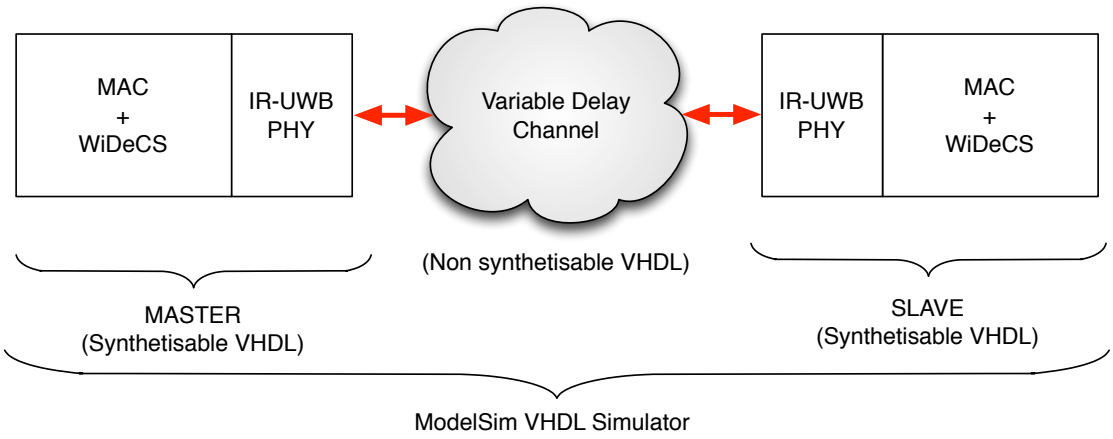

Figure 19: Hardware simulation setup

In the relay node, a first master instance of the baseband is implemented, then a queue is implemented to concatenate frames received from the different nodes. The resulting frame is sent on the higher level cluster through a slave instance of the baseband described above. The clock information is shared between the two basebands so that when a correction is applied with respect to the gateway's orders, the reference for the relay's slaves changes accordingly.

The gateway uses a master instance for managing the entire wireless network. The clock module is modified to take the reference clock as an input. Data coming from all the nodes in the network is received, and timestamped with the date corresponding to the moment it was really taken. This is done owing to the clock synchronization protocol which also provides the same trigger to the gateway. Data gathered from every sensor of the WSN, is then stored in a storage unit composed of Solid State Drives (SSDs) in RAID 5 configuration . This storage unit, when composed of 3 256 GB SSD drives, is capable of recording 512 GB of data at 75 MB/s.

The data gathered in the gateway is then processed by report generation tools, and submitted to the user through either an application specific bus, or a remotely connected monitoring computer.

This whole system can be used in many different applications without needing heavy modifications at hardware level. Specific data-rates, sensor resolutions, sensor types and linearity corrections will be implemented at software level to allow client-specific modifications, as well as performance improvement and bug correction with lower costs.

4.4 HARDWARE SIMULATIONS

The proposed system has first been tested in hardware simulations with the simulation setup presented in fig. 19. The whole system including the nodes, the channel, and the test-bench are developed in VHSIC Hardware Description Language (VHDL). This Hardware Description Language (HDL) language allows

Figure 20: Full working synchronization and localization in hardware simulations

describing the behavior of any time and event based system. Only subsets of this languages can be converted in Register Transfer Level (RTL). This is due to the fact that implementing time-based instructions present in VHDL is not possible. These time-based instructions do not have any equivalent in digital logic considering that digital logic is event-only based. The result of an instruction is either continuously processed, or processed at precise events on input signals. The system's clocks act as the triggers for most processes. In this case, only the nodes are built using only synthesizable instructions and programming style. The ADC, DAC, channel model, and test-bench are developed in non synthesizable VHDL. This allows to add various delay to the channel, as well as noise and multi-path reflexions. The test-bench generates clock and input signals for each of the tested nodes.

The figure 20 shows a standard IR-UWB BPSK communication between a master and a slave node. The master, on the left transmits a frame containing synchronization related data, and standard application related data. The slave, on the right transmits data corresponding mostly to measurement data, as well as informations about the node's status. Those frames are sent by each of the nodes in their respective time slots. The synchronization between measurements on different nodes is being checked by measuring the delay between the pulse on the master's trigger output, and the pulse on the slave's output. Synchronization performances can then be computed from this measured delay and sum up to the mean delay, the standard

deviation, and the range measured for 95 to 98% of the values. The results in simulation with a variable delay channel are a mean delay of 0.5 clock period, and a range of +0 ; +2 clock ticks. The reason of this result is the simplicity of the channel model, combined with lossless data transmission.

The synchronization performance obtained with the synthesizable IR-UWB physical layer are relevant with the ones obtained with the generic PHY when the channel delay is kept constant for two frame exchanges. A $\Delta t_{clk} = \pm 2ns$ maximum delay is measured with slow changes in the channel's delay, as well as a mean initial convergence time of $25\mu s$ (i.e. 5 times the TDMA frame duration). The transient state shows a synchronization error below the variation in delay. As explained in section 3.4, the variation in delay has no common measure with the refresh period of the synchronization scheme, and is then irrelevant in the target applications. This allows application in networks with nodes moving relatively to and from each other. Requirements specific to the SHM applications do not require the network to accept new nodes dynamically, and to deal with a node leaving the network during operation. The proposed system does not take these two elements into account, even though it is feasible with no major modification to the MAC protocol.

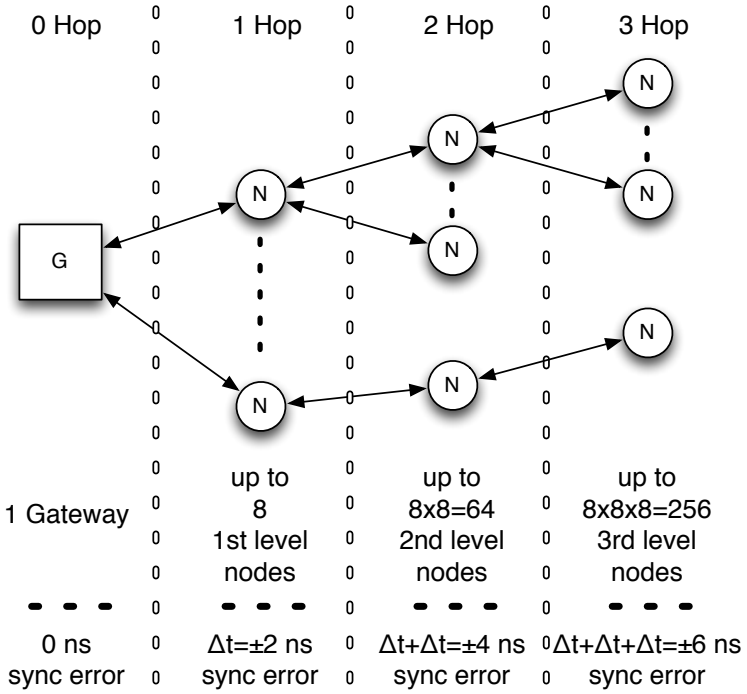

Figure 21: Effect of cluster tree architecture on synchronization

These simulations show a precise synchronization of time reference between a master node and slave nodes of a piconet under 2 ns. The scale factor is achieved by stacking levels of piconets working on different channels for avoiding interference. The expected architecture and performance are shown in figure 21. 2 ns is the maximum synchronization error between a master node of a piconet and a slave

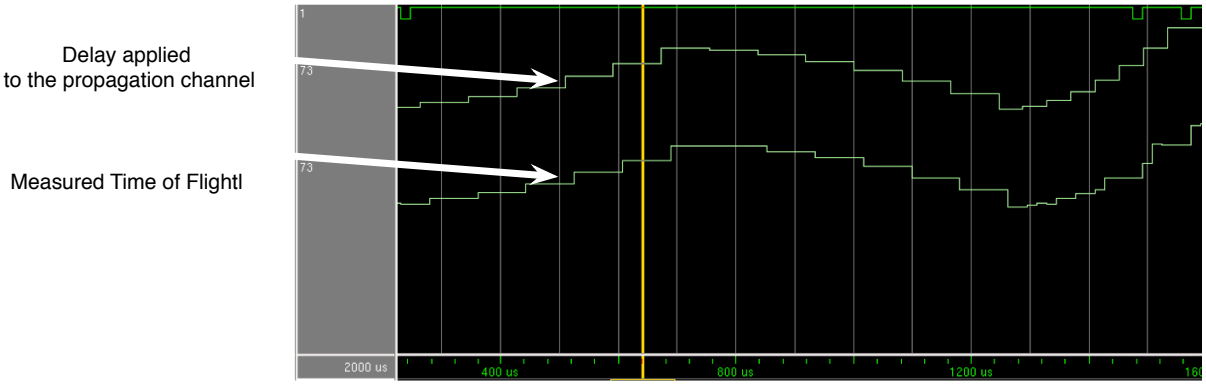

Figure 22: Hardware simulation of a fast changing channel's effect on Time of Flight (ToF) estimation

of this same piconet. We can expect the maximum error to add-up with every hop necessary to communicate with the network gateway acting as the absolute clock reference. The limit in terms of attainable number of nodes for the entire network is related to the number of available channels, and to a possible spatial division multiplexing for reusing channels.

The Time of Flight estimation pursuit is tested in figure 22 with a changing channel in terms of delay. The upper curve shows the ToF between the master and the slave. The curve below is the estimation computed in the simulated system. These values fit perfectly with a small delay under $30\mu s$ between delay change and its effect on the ToF estimator. The tested demonstrator proposes a pursuit on changing channel delays over 10 ns every cycle. With a $16\mu s$ cycle configuration, this represent nodes moving towards each other or separating from each other with a relative speed of $v = \frac{tolerance}{refreshrate} * v_{propagation} = 187km.s^{-1}$. This calculation is performed for data transmission in free space with the speed of light as the propagation speed of the wave. In the facts, the propagation speed will never be as high as the speed of light. However, the order of magnitude of the maximum speed tolerated by the algorithm will still be in the same range which is not attainable by common ground vehicles.

These simulation have proven the functioning of our whole implementation of the protocols and services proposed in chapters 3 and 3.4 in hardware simulation with changing parameters.

4.5 FPGA PROOF OF CONCEPT

4.5.1 *Implementation details*

Best synchronization and localization performances are attained with IR-UWB modulation. However, a Field Programmable Gate Array (FPGA) implementation of a 2GHz UWB transceiver requires a development board providing along with a FPGA,

a 2 GSps DAC, and a 4 Gsps ADC. Such a development board is extremely rare and expensive. For this main reason, the FPGA implementation of the MAC layer and services has been developed alongside a OFDM physical layer developed by Julien Henaut in his thesis work. He made the necessary modifications to his proposed OFDM implementations to provide the necessary signals for time-stamping incoming and outgoing frames.

The implementation of this demonstrator was performed on a board including a FPGA and fast ADC and DAC. The RedRapids 365 [86] boards include a Virtex 5 SX50T FPGA along with the Texas Instruments ADS5474 14-bit ADC and 16-bit DAC5682 DAC. A specific version of this board, clocked at 500MHz is used for this demonstration. The RedRapids board is connected to the analog RF front-end composed of connectorized circuits. A separate external power supply is used to power the RF front-end modules The block diagram of the whole demonstrator is shown in Figure 47. This section presents the design of each part of our demonstrator except for the PHY layer details, which are the subject of Julien Henaut's thesis. This paper is organized as a bottom-up explanation from the RF front-end to the MAC layer of the challenges we faced during the assembly of this system.

4.5.1.1 *Analog RF front-end*

The goals of the RF front-end design for this contest were simplicity and size. Indeed, we planned to use connectorized RF components to build a RF front-end. The number of elements included in our front-end had to be as small as possible for demonstration purpose. For this reason, we chose a direct conversion transmitter and receiver architecture, as they use a small number of components, while still providing good performance and the flexibility needed by the ongoing design of the other parts of the system. The adopted architecture is pictured in figure 23.

The transmitter shown in figure 23a receives the signal from the DAC on the left and mixes it with a Local Oscillator (LO) signal generated by the Voltage-Controlled Oscillator (VCO) at the top for the up-conversion. The PA then boosts this signal before sending it in the air by the antenna. In this direct up conversion architecture, the LO signals falls into the RF signal band, and thus cannot be filtered afterwards. This is why we chose a balanced mixer, which provides a high LO-to-RF isolation. Furthermore, the UWB-OFDM modulation used in the physical layer has a high Peak-to-Average Power Ratio (PAPR) because of the high number of subcarriers used [8]. Therefore, we chose a passive mixer for its high output linearity whose conversion gain is -7dB.

At the receiver shown in figure 23b, the signal received by the antenna on the left is amplified by a Low Noise Amplifier (LNA) and then mixed with another LO for the down-conversion. This signal is then fed to a passive low pass filter followed by two cascaded baseband amplifiers, which boost the signal until it reaches the full scale of the ADC. A digital low pass filter is also implemented inside FPGA in order to narrow the 250 MHz digitized signal to the actual 125 MHz bandwidth. The requirements for the antenna were a very large bandwidth (5 to 10 GHz), a moderate to high gain (between 5 dBi and 15 dBi) and a small size. This led us to

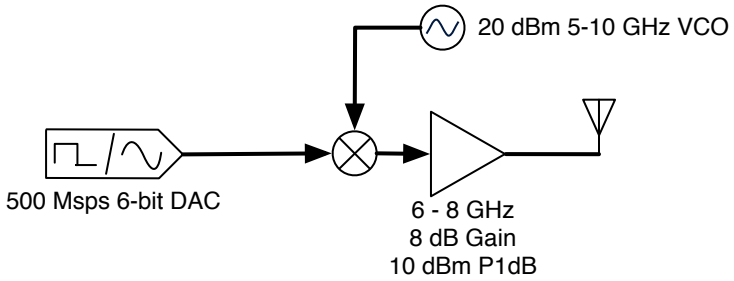

(a) TX part

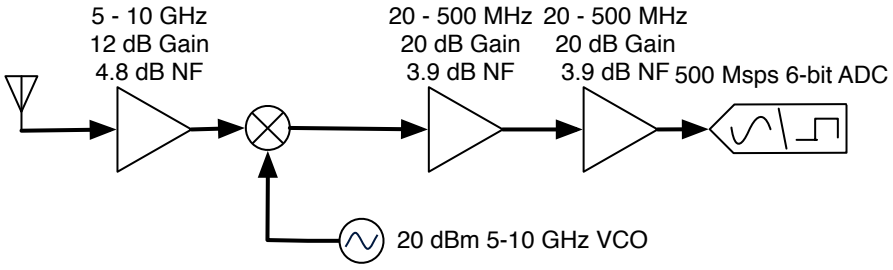

(b) RX part

Figure 23: RF front-end for the FPGA demonstrator

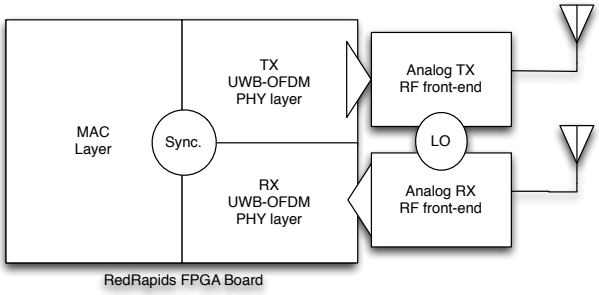

Figure 24: Block diagram of the proposed FPGA demonstrator

choose a micro-strip-fed Vivaldi slot antenna design [46, 6], as it can be made with both a high gain (in our case 9 dBi) and a large bandwidth. This receiver has a gain of 45dB and a noise figure of 6.15dB as calculated in the following equation.

$$NF_{Rx} = NF_{A1} + \frac{NF_{MIX}}{G_{A1}} + \frac{NF_{LPF}}{G_{A1} + G_{MIX}} + \frac{NF_{A2}}{G_{A1} + G_{MIX} + G_{LPF}} + \frac{NF_{A3}}{G_{A1} + G_{MIX} + G_{LPF} + G_{A2}}$$

This receiver front-end still lacks Automatic Gain Control (AGC) and thus requires manual tuning by spacing the antennas appropriately to guarantee full scale at the input of the ADC. However, for the purpose of the demonstration, this operation can be performed when the demonstrator is operated.

4.5.1.2 *UWB OFDM physical layer*

The PHY modules have been developed on Matlab Simulink using Synopsys model compiler Digital Signal Processing (DSP) toolset. Owing to this development method, heavy signal processing modules became easier to build and to debug using Matlab Simulink simulations capabilities. Testing on hardware is also made possible by means of High Level Synthesis compilation functionality. This compilation transforms the graphically designed PHY modulator and demodulator in fully synthesizable HDL modules. VHDL has been chosen to improve integration speed between the two major parts of this FPGA demonstrator. The VHDL coded MAC layer and services are interfaced with the PHY modules by means of black box insertion in Synopsys Model Compiler. This method also allows a full test of the FPGA baseband demonstrator in Simulink simulation.

Owing to this joint implementation, the MAC layer protocol is demonstrated on a FPGA development board.

4.5.2 *Measurement setup and results*

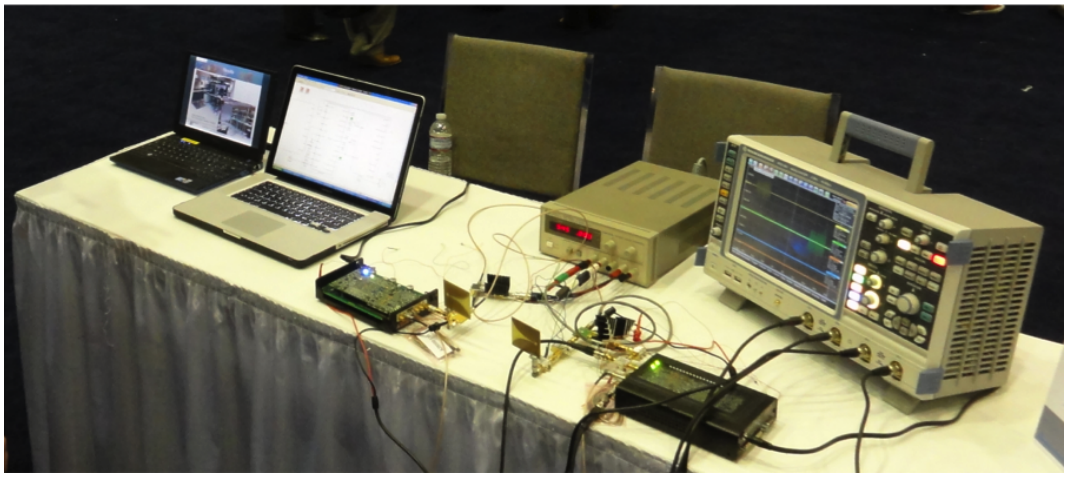

Figure 25: Block diagram of the proposed FPGA demonstrator

The complete demonstration setup has been built and tested in a lab room. Two Vivaldi antennas are connected to the master and slave nodes, and are facing each other with a 20 cm space between them. The Figure 25 shows the complete demonstrator proposed for the Student Design Contest, section Software Defined Radio (SDR) at IMS 2011 - Baltimore conference. It includes two Red Rapids boards mounted in two Acquisys eInstruments-DAQ Node boxes. The RF front-end, composed of connectorized circuits, is plugged at the DAC output and ADC input of these cards. The measurement below are performed with a LeCroy SDA 813Zi [64], and the demonstration performed at IMS used a 4 GHz Rhode & Schwartz RTO oscilloscope [87]. The scope is used for the measurement trigger signals on a digital IO of the Red Rapids boards, the baseband signal at the analog output, as well as RF signal at the input of the antenna.

The Figure 26a shows the baseband UWB-OFDM spectrum composed of individual carriers gathered in sub-blocks. Unused carriers appear in the spectrum analysis as gaps between used carriers. The two demonstrated nodes are both transmitting data in their respective slot. This proves that the entire transceiver is working enough for the slave to reach the master-created TDMA frame.

In figure 26b, The display on top of the capture shows the channel between the two nodes. This view shows the working TDMA MAC protocol. The second display shows measurement triggers probed on both nodes, and allows trigger delay measurement. A histogram of the measured offset between these triggers is computed to determine the performance of this system. These two checks have been gathered in a single scope display for the purpose of the demonstration. This histogram logs the delay values recorded over 1h time. The measured delay is below 60 ns for 95% of the measurements for a clock period of 125 MHz.

The FPGA demonstrator shows, after hardware simulations, the proof that the concepts designed in chapters 3 and 3.4 do work in real world context. However, the protocols are designed to work with a 2 GHz bandwidth IR-UWB physical layer. It is

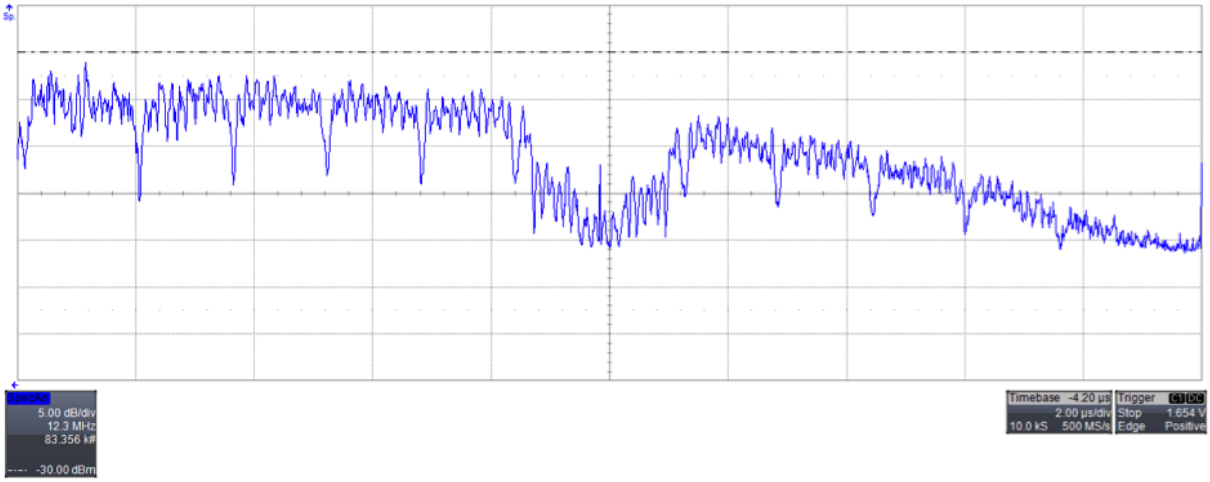

(a) Spectrum of the signal transmitted at the output of the DAC

(b) Channel occupation, measurement triggers, and trigger delay statistics

Figure 26: Scope captures of the FPGA demonstrator

then necessary, in order to test this assumption, to design an ASIC implementing the work presented in this thesis.

4.6 MIXED SIGNAL ASIC DESIGN FLOW

4.6.1 *Introduction and global view*

The ASIC implementation flow presented in this section aims at implementing mixed signal SoCs containing both a digital core along with its dedicated I/O pads and custom analog IP provided by another team member. The flow presented in figure 27 has been built during this thesis work and is based on design automation scripts named Reference Methodology (RM) and provided by Synopsys. The green colored steps are manual and coding tasks, the yellow ones are verification steps, whereas tasks in red are performed by customized versions of the RM scripts.

4.6.2 *Input documents and data*

This section lists input documents and data required to perform the ASIC flow.

4.6.2.1 *Fully tested HDL behavioral model*

This HDL model should have also been implemented and tested on FPGA prior to this flow in order to improve the chances of obtaining a working ASIC. In the present work, this model contained all the algorithm description, and was exempt of any part of implementation dependent code.

4.6.2.2 *User Constraints*

Files describing user constraints have to be provided as input at different steps of the flow, and do contain information such as the expected clock frequency, expected power consumption and die/core sizes. Although information about clock frequency is mandatory for an efficient synthesis process to happen, the expected power consumption and die size can be obtained through the synthesis process. Another piece of information that is provided as an input, and used at different steps of the flow is the list of required pads, as well as the type and parameters for each of them.

4.6.2.3 *Custom Analog IP block*

A commercial analog or digital Intellectual Property (IP) block is, in most of the cases, delivered in three different parts.

- The simulation model is delivered for implementing the IP in the HDL files. This simulation model also helps in simulating the correct functioning of the system including every IP implemented in it.

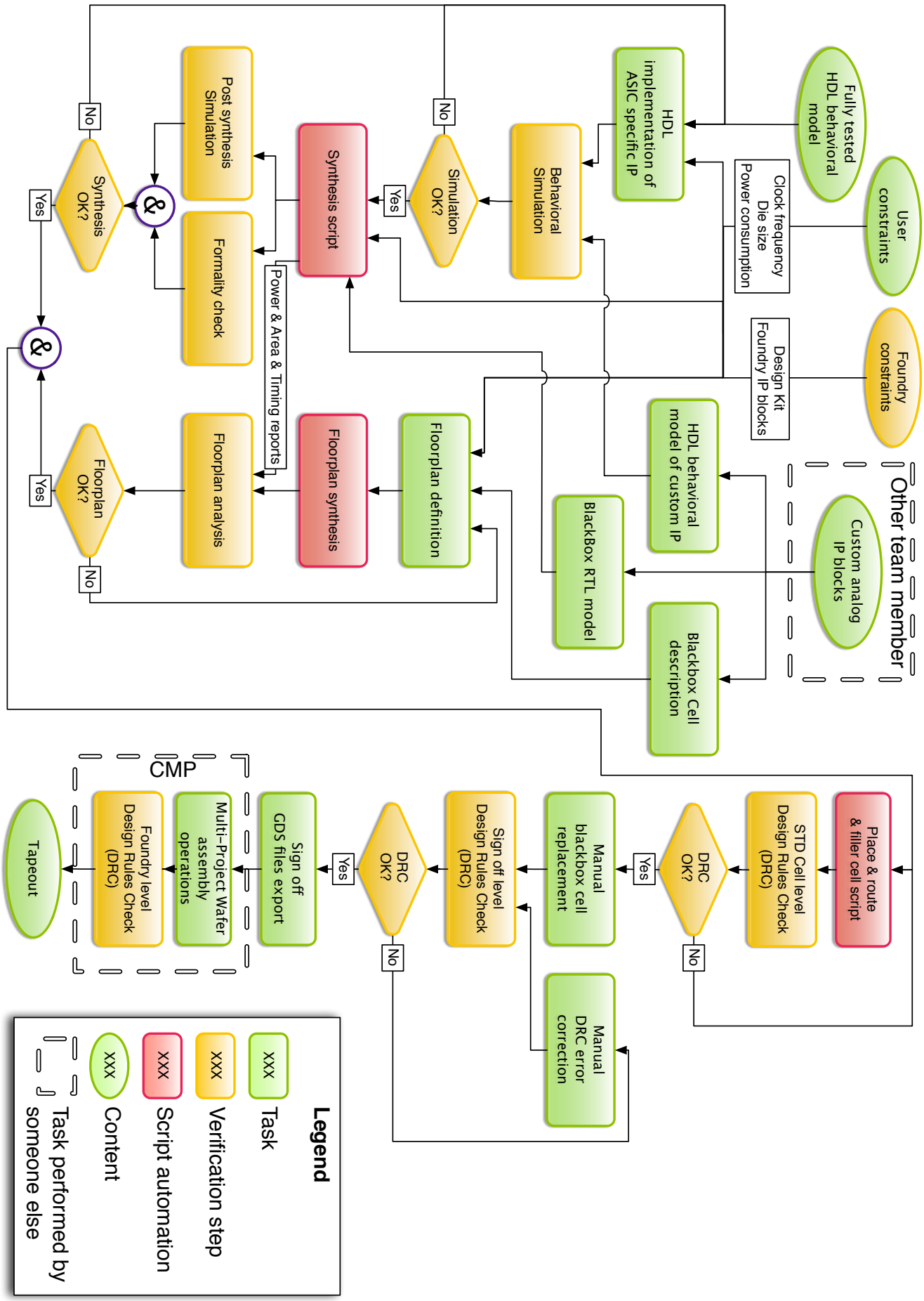

Figure 27: ASIC Flow

- Black box descriptors are files containing information about the size of the IP block, as well as the list of I/O ports and their respective behavior. This behavior will be modeled through main aspects such as the capacitive load connected to the port, a maximum delivered power, and dynamic aspects such as switching speed.
- The last part delivered by an IP provider is either a layout cell for implementation during the layout step, or in some cases a blackbox cell when it occurs that the IP provider will process the layout before tapeout.

The analog IP implemented in the demonstrator chip is an internal development. Owing to this, all of the models and boxes described above weren't available, and had to be developed as a part of this work.

4.6.2.4 *Foundry constraints and Design Kit*

Foundries provide Design Kits (DKs) containing different amounts of documentation, models, libraries and analog IPs. In this case, the technology used was CMOS 65 nm technology from ST Microelectronics. The contents and information about the design kit used for this work are under a Non Disclosure Agreement (NDA) and canot be disclosed.

4.6.3 *HDL implementation and behavioral simulation*

There is a major difference between HDL code for simulation, code for FPGA implementation, and finally for ASIC implementation. Indeed, code for FPGA implementation has to implement specific IP blocks for compensating an underperforming standard synthesis of common procedures such as Fast Fourrier Transform (FFT) by replacing it with a specifically designed blackbox.

In the ASIC world, everything has to be specifically designed and implemented for the desired foundry technology. Every pad, analog IP, or even black box IP such as a Central Processing Unit (CPU) for example shall be implemented in the HDL code before synthesis. This operation provides information to the synthesizer software about delays, loads, fan-outs of the implemented blocks, and improves the synthesis performance while providing an early overview of the attainable performance. Coding af all work described in this thesis has been done using the Sigasi HDT editor which is based on Eclipse, and provides an on the fly HDL syntax checker.

In the case presented in this work, custom analog IPs have also been implemented in this step. However, IP black-box descriptors are required at this step for the sythesizer to work correctly and to not prune an apparently useless blackbox.

Behavioral simulation has been performed using Synopsys VCS simulator for its efficiency, as well as for the support of all DesignWare IPs provided by Synopsys and implemented in this project.

4.6.4 *Synthesis and validation*

Synthesis step as presented in this flow is actually a meta task containing a large number of actions required for obtaining a RTL logic implementation of the desired algorithm. Thanks to reference methodology scripts provided by Synopsys, I was able to customize these scripts in order for them to work with the ST CMOS 65nm design kit libraries. This step is performed in the Synopsys Design Compiler (DC) software. DC aims at providing an environment for design synthesis, and makes use of a large library of optimized implementations and IPs named DesignWare.

Configuring the synthesis script requires providing the following information in its config file.

- Design HDL files including all the design files, as well as optional soft IP blocks delivered as HDL libraries. Simulation models for libraries also provided as black boxes is forbidden, as their compiled form conflicts with the blackbox cell.
- Target library files, with the .db extension, are files listing standard cells for subsets of the technology. These libraries contain all the standard cells allowed for replacing HDL instruction with logic cells. A large number of standard cells are available, providing various performance in terms of setup delays and power consumption. In this work, we targeted the least power consuming standard cell library which had Low Power and High Treshold Voltage markers. However, for some parts of the design to pass the high frequency requirements, we added a faster Standard Treshold Voltage library for allowing the synthesizer to pick latches when absolutely necessary.
- Additional link library files, with the same .db extension, contain black box descriptors of the implemented IP blocks. These libraries are not intended to be used for replacing HDL instructions during synthesis.
- A set of files describing the technology itself named TLU-Plus files. These files list the different layers, as well as their respective resistivity, minimal size and other process related information. These files are not required for the synthesis step itself. However, they are used during a side step of this task which is Milkyway library creation.

The Milkyway library can store different views of the same design, from RTL logic view, to signoff layout. This library is created by the synthesis script during its first step, and facilitates the import action in the place and route step. For these purposes, the MilkyWay library has to include links to every standard cell library used in the design, with all of their respective views. Views required in the Milkyway library for any blackbox cell or standard cell are a FRAM or CEL view providing information about the size of a cell, the location of its ports, and layer occupation masks for avoiding routing conflicts.

Outputs of the synthesis step are:

- RTL logic view of the design containing only standard cells and black-box implementations, as well as wiring between all of them. This view is provided in two formats: Milkyway library for continuing to the place and route steps, and back-annotated Verilog format for post-synthesis simulation.
- Report files containing information about timing, power and area of the synthesized module. The quality of result of the synthesis step is assessed owing to these report files.

4.6.5 *Floorplan design*

Building a correct floorplan during the design of an ASIC chip is, to me, the most difficult task in the whole implementation flow. Indeed, a floorplan that is ready for place and route operations is built through multiple manual steps requiring an advanced knowledge of both the design itself, but also the foundry technology itself and the provided design kit. This task has been performed in the Synopsys ICC software, which aims at providing tools for place and route of digital designs.

Parts of this task can be performed through custom scripts. However, manual interventions vere unavoidable for repairing incorrect automatic operations when the Quality of Result (QoR) is correct elsewhere.

The first step towards a correct floorplan is floorplan initialization. This step builds a grid for digital logic standard cell placement, as well as it sets up the cell orientation, as well as distance and form factor for the final chip. A unit cell file is required for the grid to be generated correctly. This file, provided in the DK contains information about the standard height of all digital cells provided in the DK, as well as a width unit for spacing cells correctly with regards to spacer sizes.

Once the floorplan is initialized, power and ground lines are declared, including lines for pad power supply (usually named VDDE). The design, synthesized before is imported to place the pads it implements, as well as for preparing a pre-place operation. After this importation, only digital related pads are imported. The next step is to script the implementation pads for power supply, as well as corner cells for propagating a power ring inside the pad ring itself (figure 28). Other signals such as digital pad level compensation cells may be required depending on desired pad performance in terms of voltage stability. One must keep the rules related to pads for the target foundry technology in mind. A VDDE pad will often be enough for supplying power to a limited number of I/O pads. This, along with other pad related rules implies the necessity to implement not only one pad for each power supply and ground inputs, but rather a higer number of pad for each of these inputs.

Once pads have been implemented in the design, a script must be written to sort the pads on the different sides of the die. Every pad is given a destination side, as well as an order number, which will define its final placement on this specific side. In this mixed signal design, we decided to implement custom pads inside

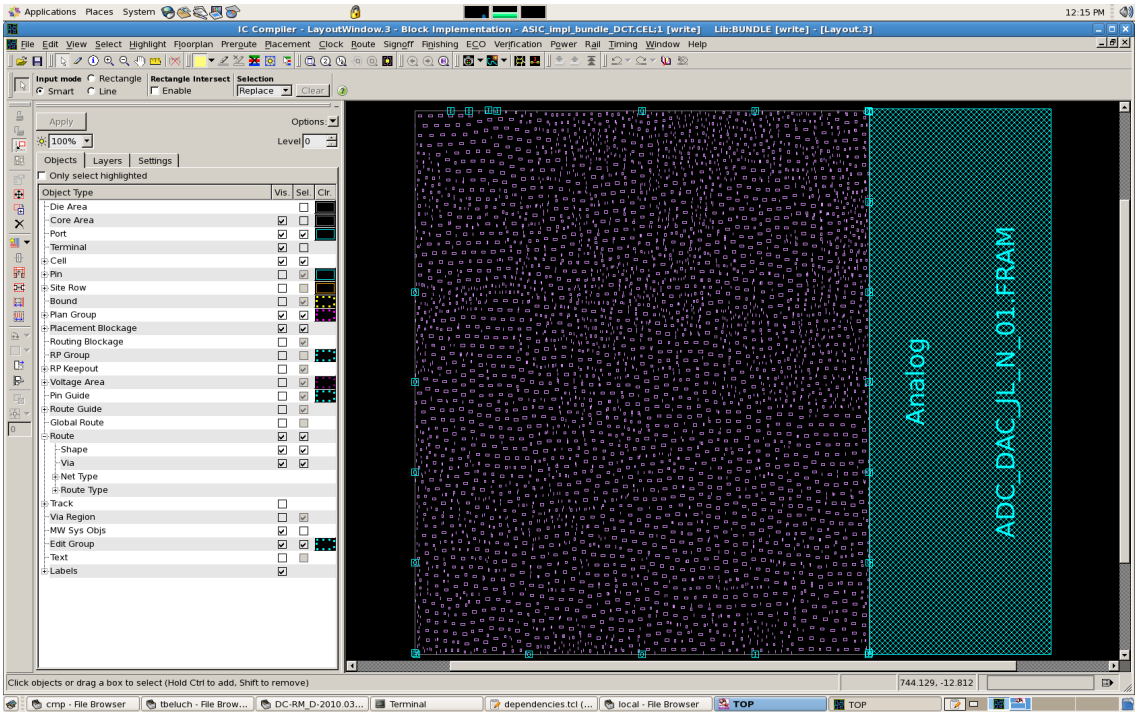

Figure 28: Chip floorplan with all pads and corner cells implemented

the analog IP block, and then forbid the use of east side of the chip in the pad placement script where the analog IP block was manually placed (figure 29). Power supply pads for the analog IP block, however, have been implemented in this step, and were to be connected manually to the IP in the final layout edition step.

The last setup task to perform before floorplan synthesis is to configure the power rings and power grids. These steps require that the design is loaded in the ICC environment in order to process a correct power consumption evaluation. Owing to foundry related information coupled with design related constraints, the power grid synthesis builds a grid with dimensions adapted to the design. Reports allow to verify the voltage drop in the grid, and to check that electromigration will be contained through time. This operation includes a pre-place step, which consists in placing standard cells inside the core to estimate voltage drop and electromigration correctly.

Whel all these configuration and commit steps have been performed, a floorplan design is issued as shown in figure , ready for place and route of digital logic.

4.6.6 *Place and Route and cell level DRC*

Place and route operations are performed sequentially by a script derived from Reference Methodology issued by Synopsys. The MilkyWay library passed from the

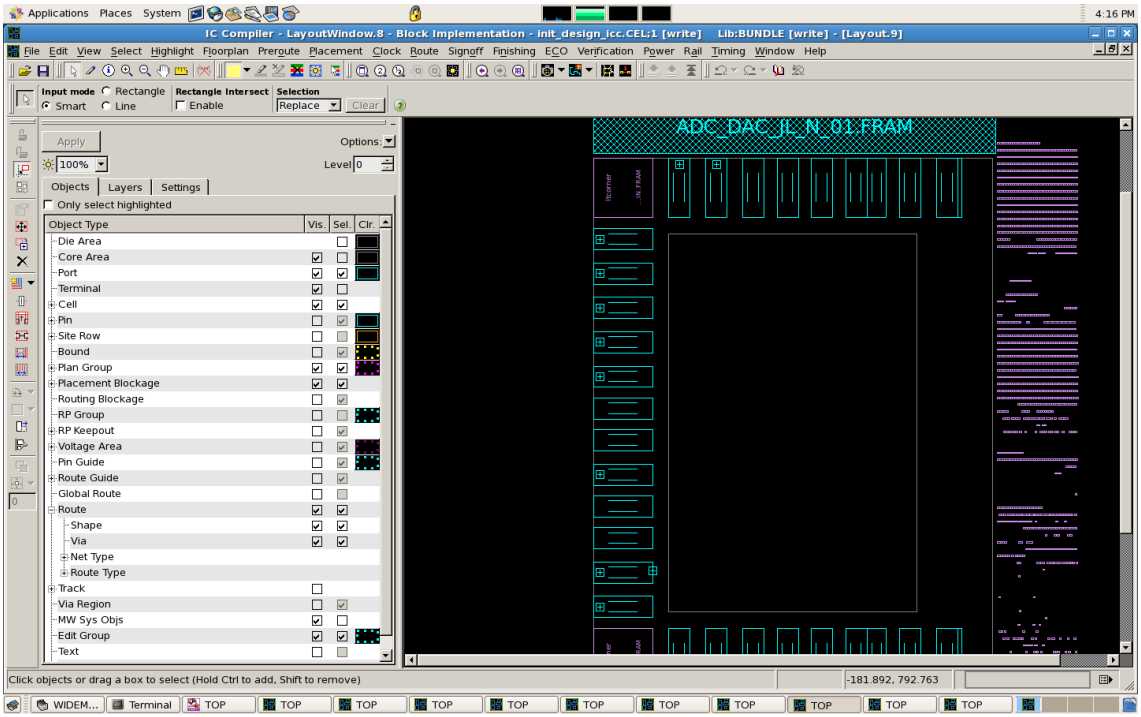

Figure 29: Chip floorplan with all pads and corner cells implemented

output of the synthesis process to the input of this task also links to FRAM views for every cell implemented in the design. This leads to a mostly automatic process providing a placed an routed design at the output. Reports about DRC violations in the placement of cells or in the routing of nets are issued. Timing checks are performed based on technology, net lenghts, and the metal layers used for routing the nets. Filler cells, as well as metal filler are also placed during this step. This avoids mechanical and Electro-Magnetic Compatibility (EMC) constraints in the chip with respect to the design rules.

The outputs of this process are:

- A design, ready for cell replacement, converted in a Cadence library format for layout steps.
- Reports allowing to check the timings, power consumption, and potential DRC violations.
- A backannotated HDL model, usually exported in verilog format and including all the delay information about the design. These delay informations include cell related delays, as well as wiring related delays due to capacitive and resistive parasitics presents in such dense metal routings.

Validation of this step is performed through DRC result check, and proper functioning of the chip can be checked in a post place and route simulation. Backannotated HDL file is passed to the VCS simulator and simulated. This helps in determining the real final maximum operation frequency depending on technology related parameters. One can estimate the effect of process variations and a high temperature on the maximum frequency.

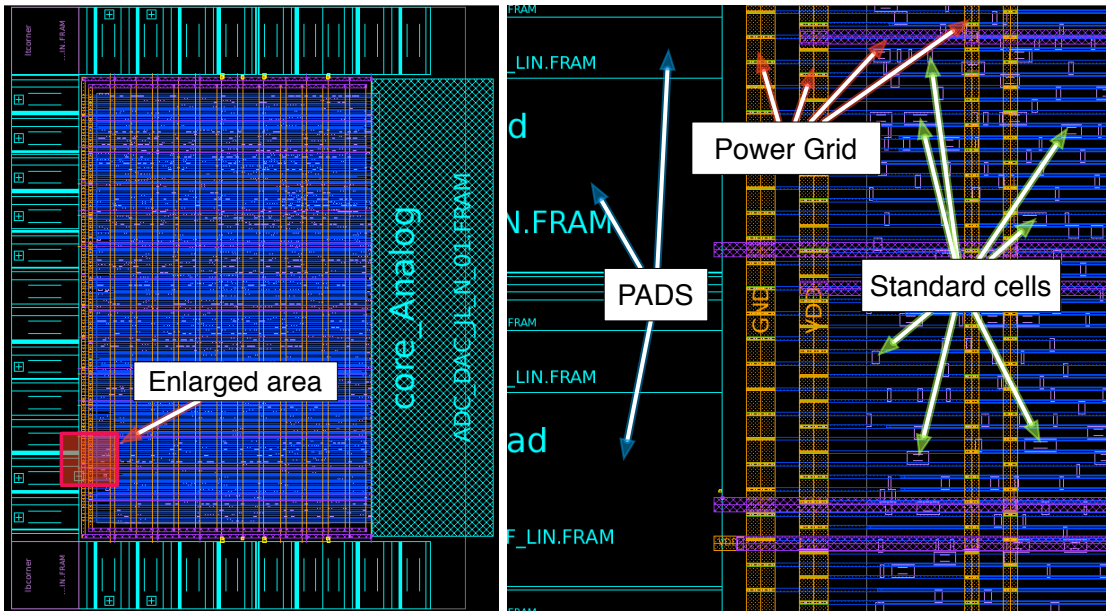

(a) Full floorplan (b) Zoom on the bottom left part

Figure 30: Floorplan of WIDEMACV1 chip

4.6.7 *Layout operations*

The last step necessary for building the proposed mixed signal ASIC chip was to perform final layout operations. Standard cells provided in the design kit are only partial implementation for IP reasons. This is why replacing the links to the standard cellw with the provided "inner-view" must not be done. Replacement of every cell provided in the design kit or elsewhere by the founder has to be kept as a link. However, the analog blackbox for which all the blackbox models have been issued can replace the simplified black box that stood for it in all the automatic steps. Considering that the FRAM view of this analog cell model did specify the locations of ports correctly, every signal entering and leaving this black box fits to the actual analog design. Analog power supply provided by the pads implemented specifically has been connected manually to the analog block, and a final DRC check is performed.

GDS files are issued and sent to the foundry company, or to a Multi Project Wafer (MPW) operator. These entities do perform the cell replacement, and add other foundry specific postprocessing. The final design is sent back to the designer for verification, and is included in a mask set for production.

4.7 ASIC PROOF OF CONCEPT

4.7.1 *Implementation details*

The two main applications targeted for WiDeCS protocol are SHM and indoor localization. However, determining the position of a node by using relative distance

between nodes does require a nanosecond scale synchronization in order to reach meter-scale distance evaluation. A FPGA implementation, along with 500 MHz ADC and DAC only allow synchronization errors down to 20 ns between nodes with OFDM modulation, and 5 ns with IR-UWB modulation.

An ASIC implementation allows to obtain the best performances attainable. Moreover, the ASIC form is power efficient because we do only implement the needed parts. The proposed mixed signal ASIC demonstrator, named WIDEMACV1, is a 1x1 mm ASIC designed in 65nm CMOS from ST Microelectronics. It contains a 2 GHz 2-bit DAC, a 4 GHz 6-bit flash ADC, and a digital logic containing an IR-UWB transmitter, an IR-UWB receiver, the fixed slot TDMA MAC with WiDeCS and Wireless Deterministic Localization (WiDeLoc) services. Debug modules and I/Os have been designed and implemented in the digital logic to reduce the number of required pads. The 1x1 mm chip does allow a limited number of pads on its pad ring. In this case, the analogue part of the chip does require its own RF pad design in order to reach its best performances. The WIDEMACV1 chip is detailed in figures 31 and composed of two major parts: the analogue circuit, and the digital logic part.

4.7.1.1 *Analogue circuit*

The analogue part of the WIDEMACV1 chip contains the 4 Gsps 6bit ADC, the 2 Gsps 2bit DAC, and a clock signal divider to transform a 4 GHz clock source into the different clock signals required in the circuit. A custom logic counter circuit generates the clocks necessary for sampling, and for code conversion. The resulting 4 GHz, 2 GHz, and 1 GHz are fed to different stages of the temperature to binary encoder. The remaining 500 MHz clock is provided as the clock source to the digital logic part. This analogue circuit has been designed by ChipYards on behalf of the LAAS CNRS. In order to use this analogue circuit alongside the synthesized RTL logic, I have developed models at different levels including a VHDL behavioral model, a timing and load ".db" model for Design Compiler synthesis, and a FRAM cell tile for Place and Route (PR) in Synopsys ICC. The analogue part of the circuit is designed to consume 40 mW at 4 GHz clock frequency.

4.7.1.2 *Digital logic*

The digital logic implements the IR-UWB transmitter, an IR-UWB receiver, the fixed slot TDMA MAC with WiDeCS and WiDeLoc services. This part is developed in VHDL language.

The setup implemented in the WIDEMACV1 chip is a 500 Mbps data-rate over 2GHz bandwidth IR-UWB physical layer connected with the 5 slots TDMA MAC layer, which includes Synchronization and ToF estimation. The TDMA frame has a fixed 16s cycle time, and a beacon is transmitted by a master node every 16s. The frame size is also fixed in design to 192 bits. This size is chosen to have a better control on transmission time, and on the effect of clock drift on reception performances. The WiDeCS implementation performs time-stamping of the entering and leaving frames with the 500 MHz digital clock. A top level file connects it to the analogue

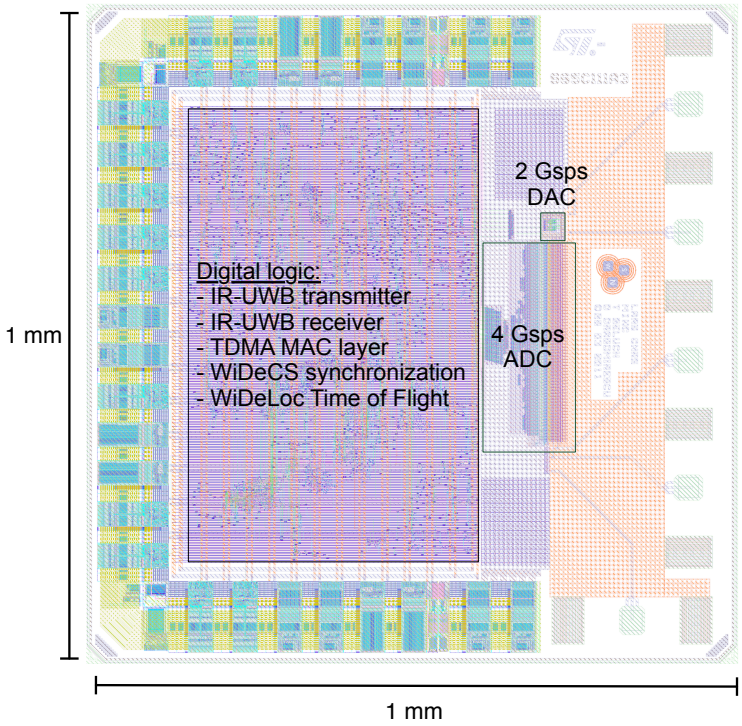

(a) layout description

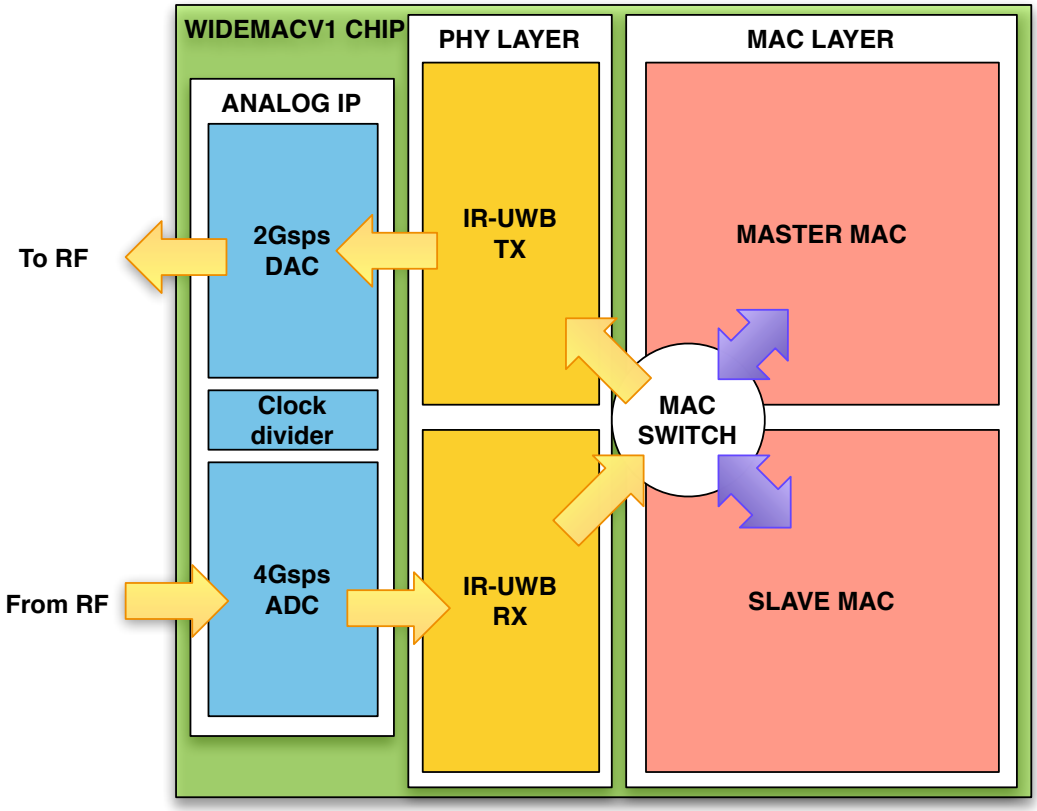

(b) block diagram

Figure 31: WIDEMACV1 chip

ADC, DAC and clock divider. The analogue part occupying a whole third of the chip size, is taken into account during the whole synthesis and PR process. Owing to limitations in the number of pads, modules have been implemented around the system to provide measurement capabilities while keeping a reasonable number of pads. Among these modules, the data checker is composed of a pseudo-random sequence generator to feed the data input of the MAC layer with data to send. On the receiver side, the data received by the slave node is compared with the expected data, and a single bit output shows the status of the last data received. Another module is used to serialize data provided by the chip concerning the estimated ToF. Owing to such modifications, the number of required debug pads has fallen from more than 50 pads to 7. The downside is that the data obtained through this method is harder to compute and to analyze.

The whole VHDL coded system has been synthesized for a 500 MHz digital clock frequency. The resulting RTL, after PR, has a power consumption of less than 8mW at 500 MHz clock frequency. The core occupation is under 39% and the chip is clearly pad-limited, i.e. the chip could be smaller if the number of pads was reduced.

4.7.2 *Measurement setup and results*

This section describes the test and measurement setup designed for characterizing the proposed proof-of-concept named WIDEMACV1. Considering the proposed system architecture, multiple different tests are necessary to characterize the system correctly. Indeed, the baseband is composed of:

- an ADC and a DAC for interfacing the analogue RF front-end with the digital logic baseband
- an IR-UWB transmitter and an IR-UWB receiver as the physical layer
- the WiDeCS TDMA MAC layer including a synchronization and a ToF evaluation algorithms

Each of these parts has to be verified individually in order to analyze the source of potential problems. The following figures 32 and **??** represent the two major test-benches designed for testing the chip with the most exhaustive test protocol. Both make use of the same Printed Circuit Board (PCB) test board designed for test efficiency.

The first tests run on the WIDEMACV1 chip are aimed at checking the correct behavior of the chip in transmit state using the setup presented in fig 32. Tested parts include the transmitting IR-UWB modulator included in the physical layer, the DAC analogue part, and a sub-part of the MAC layer whose goal is to regularly send the TDMA frame beacon.

In order to perform this test, the chip is correctly setup using the dedicated jumpers. A power supply providing 3 voltages: 1.2V VDD for powering the digital part, 1.2V VDDA for the analogue part, and 2.5V VDDE for the pads. A frequency synthesizer is used to provide the high speed 4 GHz clock signal. Other clocks are

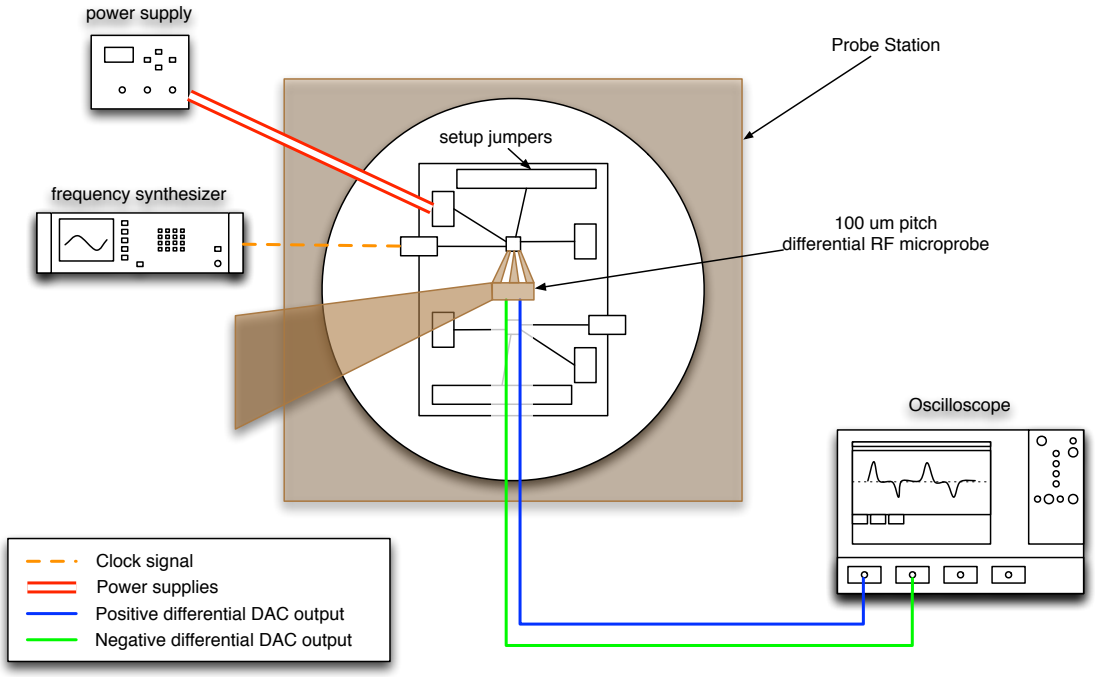

Figure 32: Probe station setup for transmitted signal analysis

derived inside the chip for digital logic, and DAC functioning. Most of the pads on the chip are bonded to the PCB. However, the inputs of the ADC and the output of the DAC remain unconnected. This is done in order to leave clean pads for landing the differential RF probe without risking short circuits. Using this differential probe, the positive and negative parts of the differential DAC's output are connected to a LeCroy SDA 813Zi high bandwidth oscilloscope [64]. It is then possible to analyze the transmitted pulses in both time and frequency domains.

The figure 33a shows a frame beacon being sent by the master node on the network. The second sub-figure (33b) is a zoom of the same frame for measuring time-domain related parameters. The first parameter that can be measured is the data-rate. In this implementation, each pulse represents a bit being transmitted. The measured chip-time, representing the time between two pulses is of 2 ns. The corresponding data-rate is then 500 Mbps. An other parameter which can be extracted from this measurement is the peak output power. The measured amplitude is 600 mV. Considering that the scope has a 50 input impedance, the peak output power is then $P = U \times I = \frac{U^2}{R} = \frac{0.6^2}{50} = 7.2mW = 8.57dBm$

The same scope allows a spectrum analysis of the transmitted signal. The figure 34 displays the spectrum analysis of the same signal as above. In this figure, it is possible to determine the occupied bandwidth, as well as the PSD. The measured first harmonic bandwidth is a 2.0GHz bandwidth from DC to 2 GHz. Other harmonics

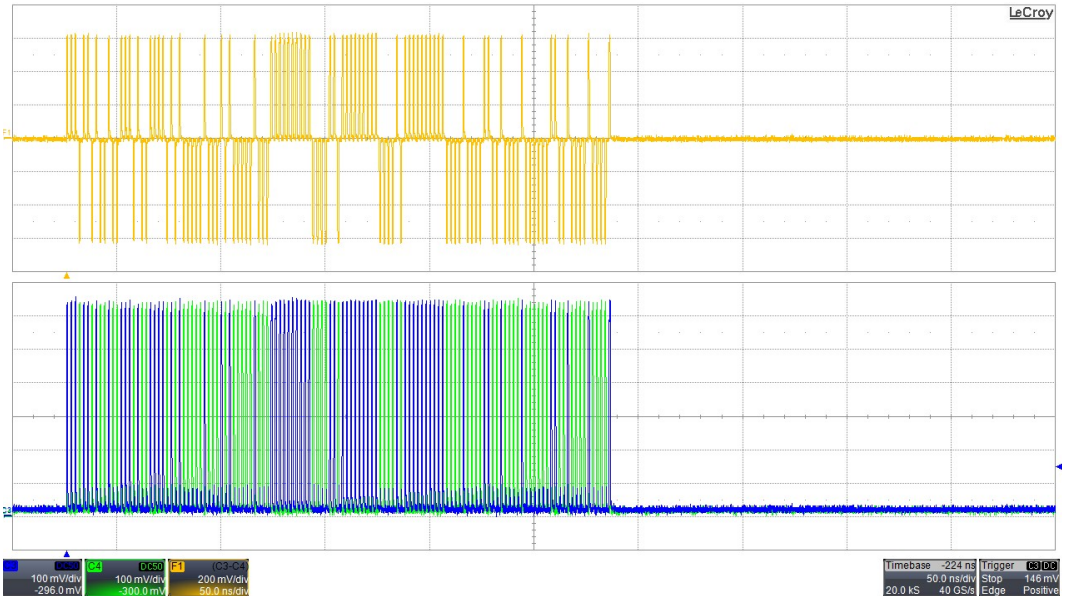

(a) Full frame

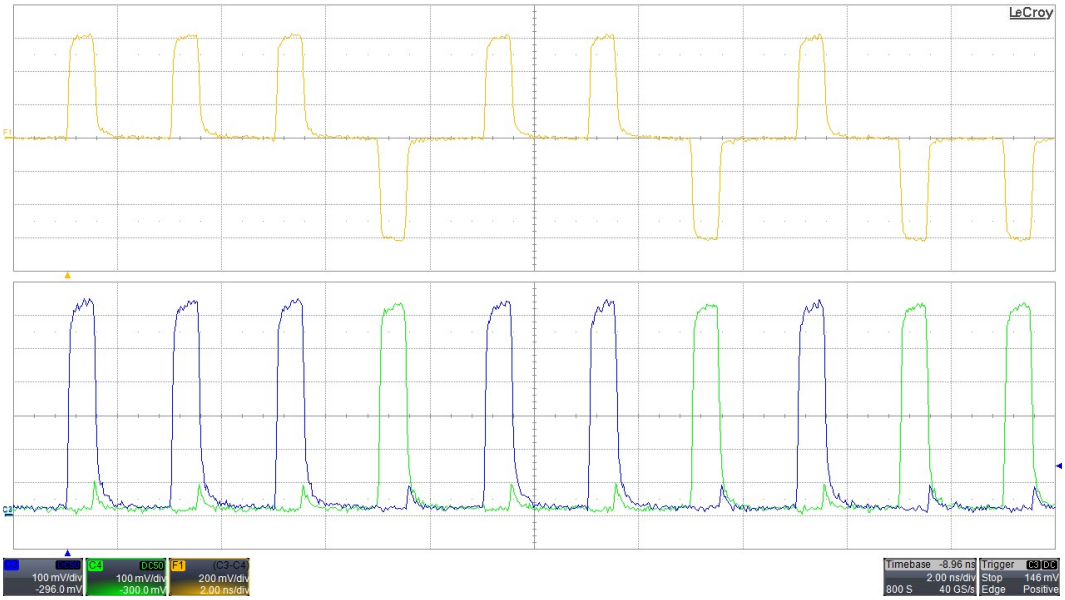

(b) Zoom on a portion of the frame

Figure 33: Time domain DAC output of WIDEMACV1, scope display

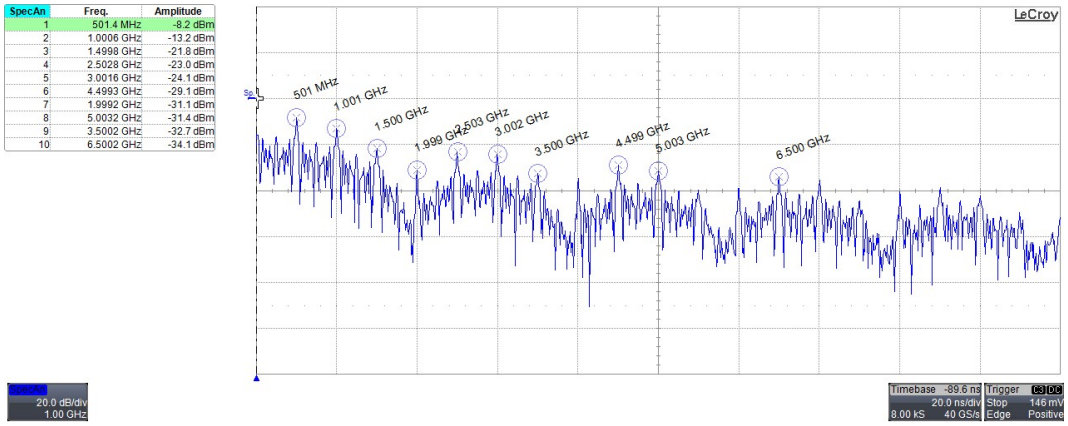

Figure 34: Spectrum analysis of WIDEMACV1, scope display

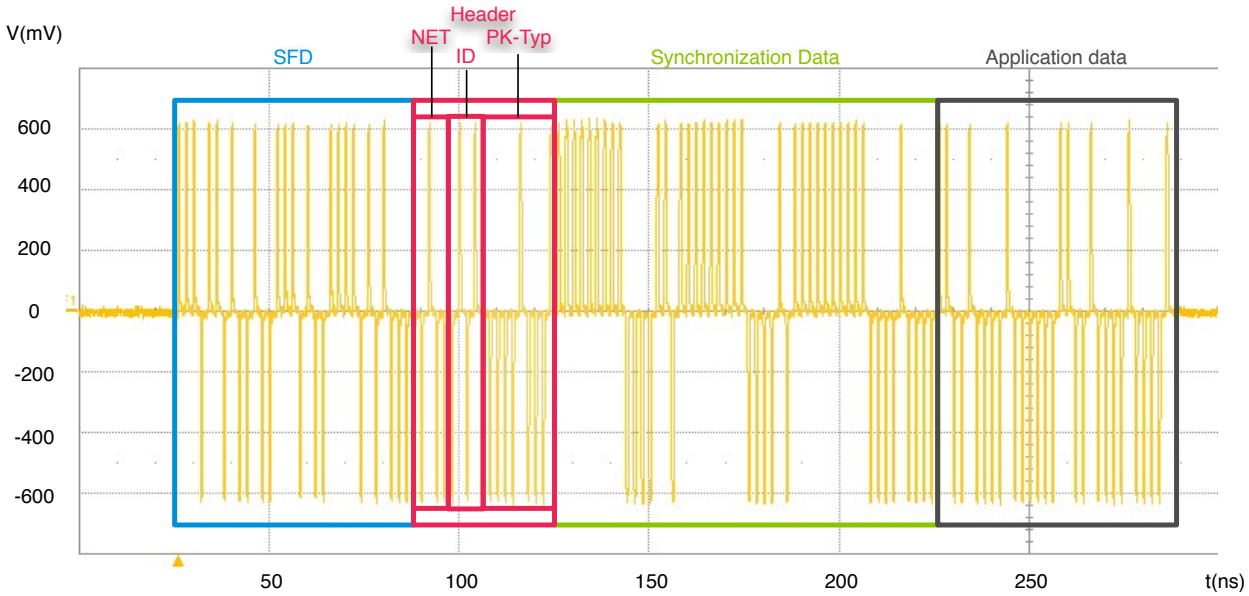

Figure 35: Details of a data transmission occuring in a time slot

remain unfiltered at the output of this chip, and should be filtered in order to comply with UWB regulations. The measured PSD does not exceed -8.2dBm/MHz and has the usual IR-UWB spectrum shape. The peak output power is reached when a pulse is transmitted. The raw power emitted at the output of the baseband chip is 8.57dBm. However, due to the folding effect of the DAC component, this power is spread over many harmonics of the target band. Filtering then has to be performed either between the baseband and the RF front-end, or inside the RF front-end.

Details of a frame transmitted by the master node of a pico-net in its dedicated time slot are shown in figure 35. 31 SFD pulses are used for detection and PHY level synchronization. Nodes are identified through a 4 bit NET-ID allowing 16 pico-nets to exist in the same network and a 4 bit node ID which also determines the time-slot allocated to this specific node. The synchronization data is sent in 16 bit signed format for each slave node. The application data is the last data included in this sample frame. FEC and security issues are not taken into account

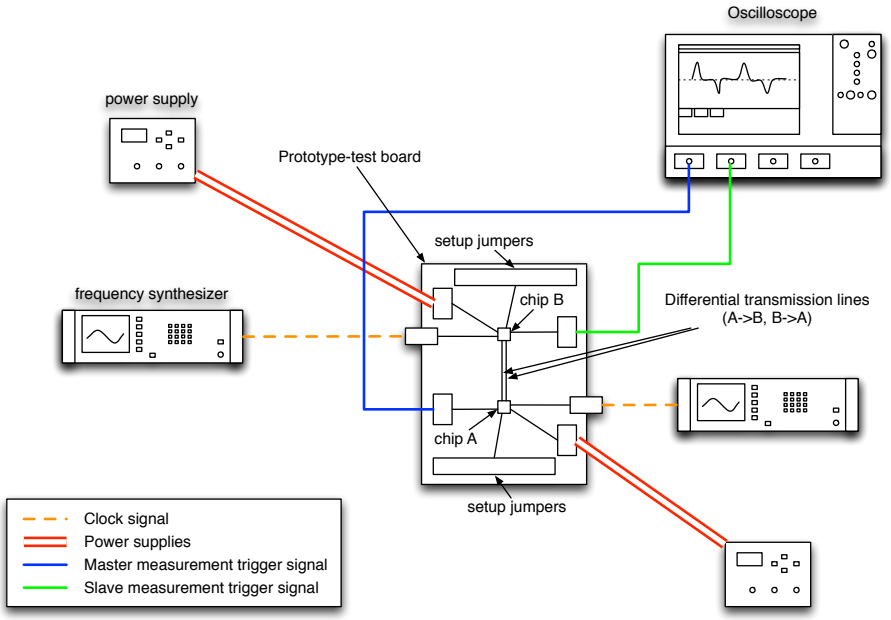

Figure 36: Setup for full connectivity check including PHY TX and RX, MAC, synchronization and localization

in this demonstrator, and are expected to double the frame length due to strong requirements in terms of BER.

The figure **??** shows the "face to face" test setup designed for testing the MAC layer with its synchronization and ToF estimation services. This setup uses a specifically designed PCB board as detailed in figure 37. This board is designed with a 180° rotational symmetry around its center point in order to allow two chips mounted on it to be completely independent from one another except for the transmission line for communication. The top of this figure shows a schematic of a chip's connections, and the bottom part is a picture of the same design. Power supplies are provided to each chip separately through a specific 2.54 mm 2-row header. VDD is the power supply for digital logic and ranges between 0.9 V and 1.2 V. VDDA supplies analog logic, and has a narrover range of 1 V to 1.2 V. VDDE supplies the pads with 2.5 V. Inputs of the chip are connected to 3-pin jumpers allowing to either connect the input to a "0" state (GND) or to a "1" state (VDDE). These setup jumpers are present to define the MAC address (IDNode(1:0)), the Master/Slave status (IDNODE(2)), and the debug mode (Debug_mode(1:0) to be used. The debug mode selector is a 2 bit input and can be used to force the chip in specific debug modes such as Normal ({0,0}), ADC/DAC Loopback ({0,1}), and PHY loopback({1,0}). The possible test modes are detailed below, and their specific goals are explained.

Outputs of the chip, mostly for debug purpose in this case, are available on 2.54 mm header pins named "Debug outputs".

The direct test mode is used to check that the master node correctly sends a beacon frame, and that this beacon is correctly received by a slave node listening on the same channel. This is useful for determining BER of the transmission. The

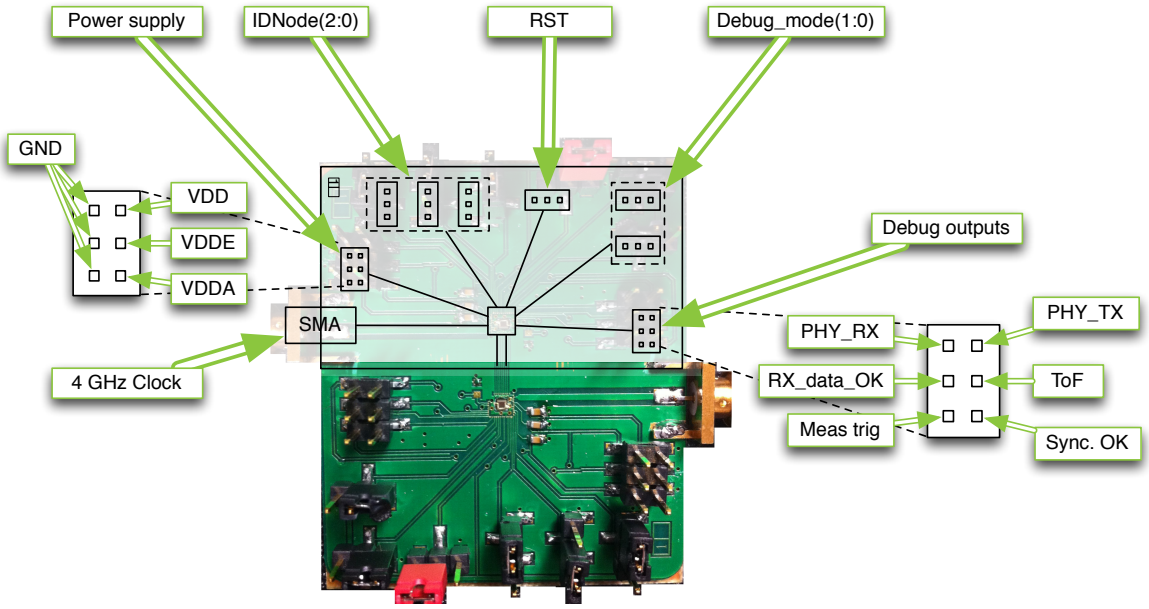

Figure 37: WIDEMACV1 test board

data sent on the channel is also output on the PHY_debug_TX output, and can be compared with the frame that is given to the receiving MAC layer. The BER resulting from the test conditions is then easily determined. In these test conditions, the tests designed to measure the BER were under dimensioned. This is due to ideal transmission between the transmitting baseband chip, and the receiving baseband chip. The transmission lines between these two nodes do not modify the signal transmitted. The receiver is then receiving an ideal pulse train with no delay spread. In this setup, the goal is then to check that every part of the baseband implicated in transmitting and receiving pulses is working accordingly to the design sent to fabrication.

This test mode will also be utilized in the future when the research team will succeed in connecting this baseband chip to the TX and RX RF front-end chips. Logging the TX and RX debug output will be the best solution to monitor the BER, and to improve our knowledge on the effects of the environment on 60 GHz IR-UWB wireless communications.

The "loopback" mode (fig. 38b) is used to determine the source of a potential problem in the ADC or in the DAC. If the signal sent by the Master node (on the right) is not retransmitted correctly by the right node functioning in loopback mode, then there is a problem between the ADC and the DAC. Determining which one of these two elements is defective is done by checking that the node sends correct beacon in master mode.

In the "full" test mode (fig. 38c), the nodes are configured with standard values. One node is setup as a master node, whereas the second one gets an ID Node and works in slave mode. During this test, the whole system is being tested, and informations about most of the used parts is available at the output. Due to the

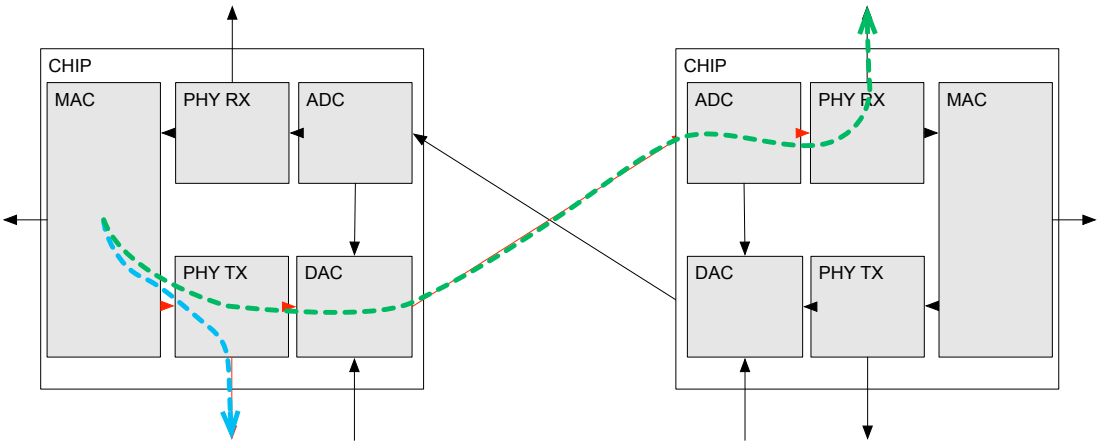

(a) “direct” test mode for TX and RX physical layers validation

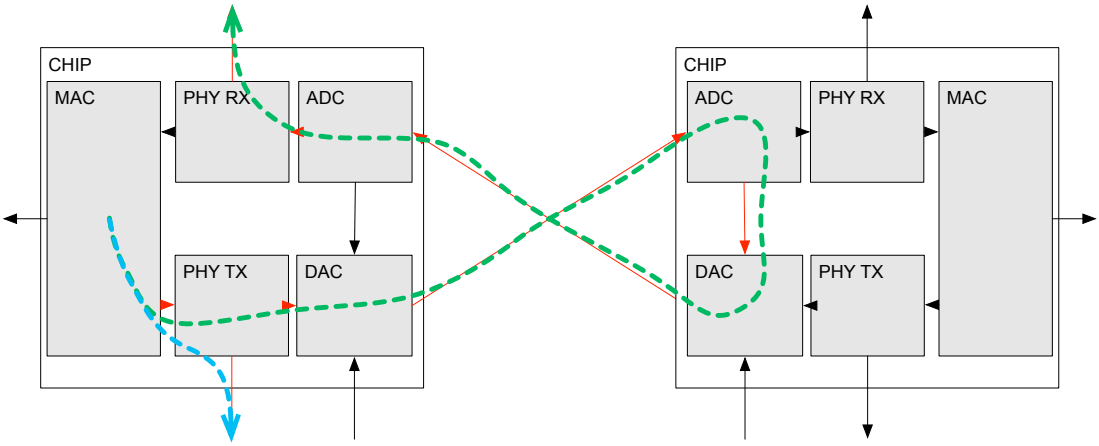

(b) “loopback” test mode for ADC/DAC validation

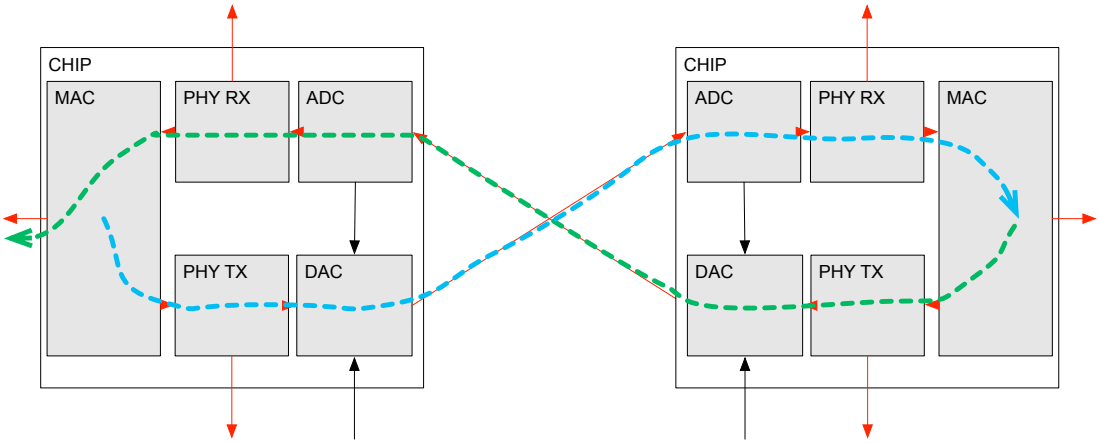

(c) “full” test mode for complete functionality validation

Figure 38: Face to face test modes

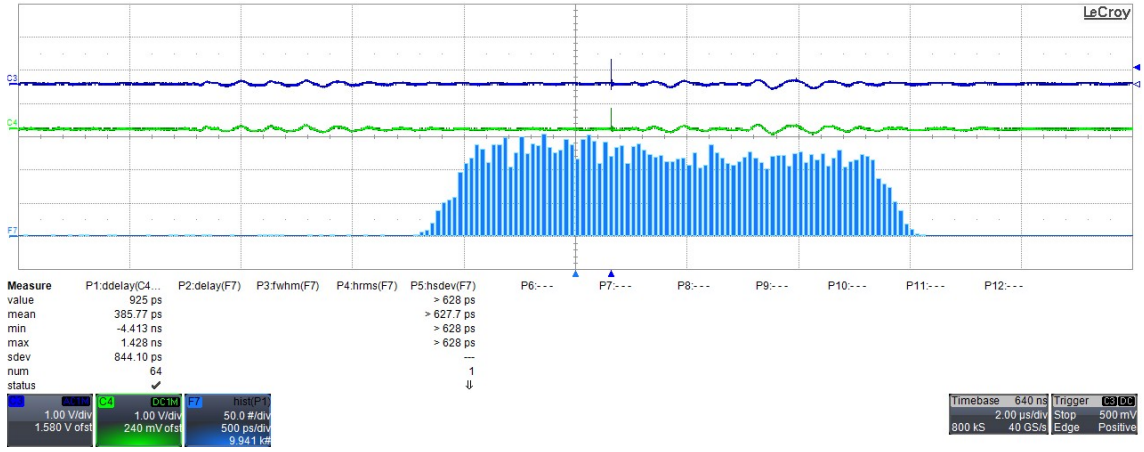

Figure 39: Histogram of delays between measurement triggers on master and slave nodes

limitation in the number of pads, the data input and outputs have been replaced by a pseudo-random generator for generating sensor data, and a value checker for comparing the received data with the values expected. Owing to this workaround, the 2x8 I/O pads that were necessary to check the correct data transmission are shrunk to one pad signaling wether or not the received data is conform with the expected one.

This test mode is also used to test the ToF evaluation, as well as the synchronization performances. In order to test synchronization between measurement triggers, the setup shown in fig. **??** is used. The measurement triggers generated by each of the two nodes are captured in the LeCroy SDA 813Zi, and the delay between those two triggers is measured repeatedly. A trend and a histogram of these delay is then computed in the scope, and displayed as in fig. 39.

Owing to the variety of test conditions tried with this test mode, the effect of clock related parameters on synchronization has been studied. Clock parameters such as frequency, drift and offset have been tuned, and their effect on the system's performances has been studied. Tests have been done with the "full" face to face test setup. Synchronization performances have been logged through their mean value, their standard deviation, and the maximum error measured. Mean value is rarely the most representative value in error analysis, because such trigger delays are often in a gaussian distribution around the real value. The standard deviation gives a more realistic information about this gaussian, and the maximum error gives a information about a possible loss of synchronization.

These parameters, and the resulting effect are detailed below:

- Clock frequency: Considering the explanations given in chapter 3, The WiDeCS synchronization scheme should provide a better synchronization with a greater sampling frequency. Tuning the clock frequency aims at checking this assumption. For this purpose, the clock frequencies have been tuned from 600 MHz to 4 GHz. During the test, power supply values have been adapted to make the chip work at high frequencies.

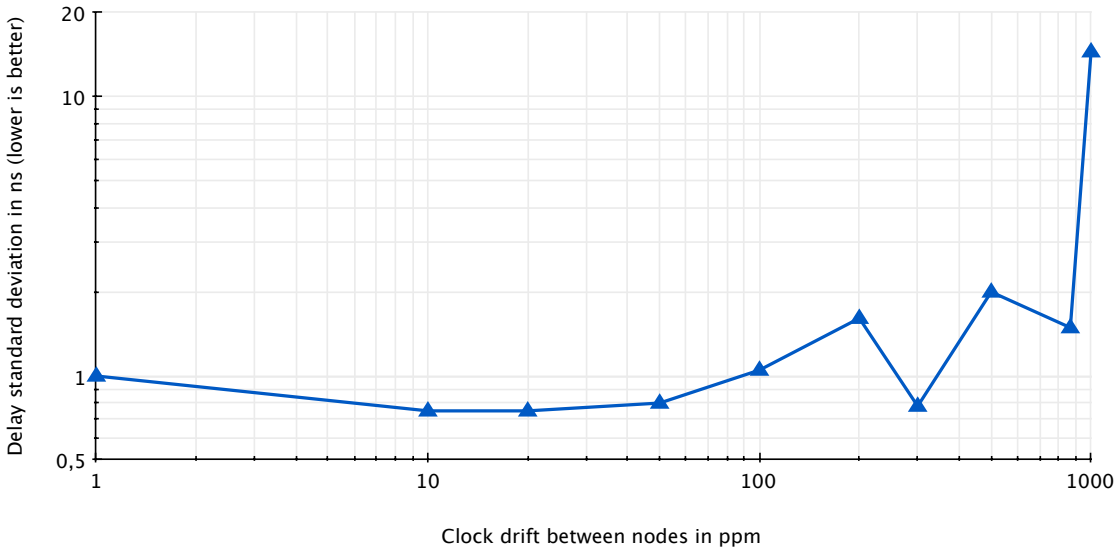

Figure 40: Synchronization stability versus clock drift between nodes (@3GHz base clock frequency)

- Clock drift: In a real world context, nodes do never have the exact same clock source. Owing to the number of clock sources and to their respective frequency stability, the clocks provided to the nodes are drifting from one another. In order to test the resilience of the physical layer, the MAC protocol and the WiDeCS scheme, we tune the 2 frequency synthesizers with a growing drift between them.

The resulting synchronization performances have been summed up in the table 4.

These results confirm the link between the clock frequency and the attainable synchronization error. The digital part, which is using a 500 MHz divided clock, should allow frequencies up to 4.5 GHz according to the synthesis reports. However, the chip stops working at frequencies higher than 4.1GHz. This seems to be due to the clock frequency divider. The divider causes calibrated delays between rising edges of the different generated clocks.

The resilience to clock drift has been tested for this system with the clock frequency providing the best efficiency in terms of synchronization: 3 GHz. The figure 40 shows that the synchronization error grows with the clock drift. However, the resulting error is always reasonable when compared to the state of the art, and does not reach unacceptable values. The maximum absolute error attained during tests was 45 ns with a 1000 ppm clock drift which is very unlikely to be encountered with usual clock sources such as quartz or MicroElectroMechanical Systems (MEMS) based oscillators. With a 500ppm clock drift between two node, the nodes do synchronize with an absolute delay under 10 ns (7.5 ns @ 3 GHz $\pm$ 500 ppm).

The last information we could get out of this full test is the power consumption when the system is operating. It is necessary to perform this measurement simultaneously with performance tests in order to take into account the lowest necessary power supply voltage applied to the chip. The values listed in table 4 are the lowest values allowing the system to work at its best performances. These

Test parameters				Test results						
F_{clk}(MHz)	F_{clk}(ppm)	VDD (V)	VDDA (V)	I(VDDA) (mA)	I(VDD) (mA)	P_{tot}(mW)	t_{mean}(ns)	t_{stddev}(ns)	t_{max}(ns)	Min EPP
50	0	1	1	8.6	0.069	8.665	178	122	320	1390 pJ/bit
100	0	1	1	8.7	0.141	8.826	88	61	160	706 pJ/bit
200	0	1	1	9	0.272	9.258	45	30	80	370 pJ/bit
400	0	1	1	10.4	0.537	10.091	19.9	14.2	40	218 pJ/bit
800	0	1.1	1	12.5	1.179	13.685	8.5	6.7	20	137 pJ/bit
1000	0	1.1	1	13.5	1.473	14.95	5.7	4.5	16	120 pJ/bit
1600	0	1.2	1	16.3	2.564	19.36	5	2.9	10.1	96.8 pJ/bit
2000	0	1.2	1	18.2	3.19	22	3.8	2.3	8	88 pJ/bit
2500	0	1.2	1	20.5	3.98	25.22	1.09	0.945	3.4	80.7 pJ/bit
3000	0	1.3	1.1	26.2	5.2	35.42	1.18	0.75	2.8	94.5 pJ/bit
3000	10	-	-	-	-	-	3.34	1	5.45	-
3000	20	-	-	-	-	-	3.34	0.75	2.9	-
3000	50	-	-	-	-	-	3.56	0.8	3.35	-
3000	100	-	-	-	-	-	3.45	1.05	3.85	-
3000	200	-	-	-	-	-	3.68	1.61	5.7	-
3000	300	-	-	-	-	-	3.78	0.78	3.3	-
3000	500	-	-	-	-	-	9.1	2	7.5	-
3000	866	-	-	-	-	-	12.68	1.49	5.55	-
3000	1000	-	-	-	-	-	29.5	14.5	41.5	-
3100	0 [a]	1.2	1.2	28.7	5.64	41.21	2.81	0.127	3.11	105 pJ/bit
3100	0 [a]	1.2	1.2	-	-	-	1.60	1.60	5.54	-
3500	X[b]	1.3	1.2	31.7	5.95	45.78	2.73	0.64	2.35	105 pJ/bit
4000	X[b]	1.3	1.2	35.9	6.84	51.98	0.374	0.677	6.7	104 pJ/bit

Table 4: Performance with face to face setup

a These tests have been done with the same clock source shared between the nodes
b The synthesizers do not provide reliable ppm information above 3GHz

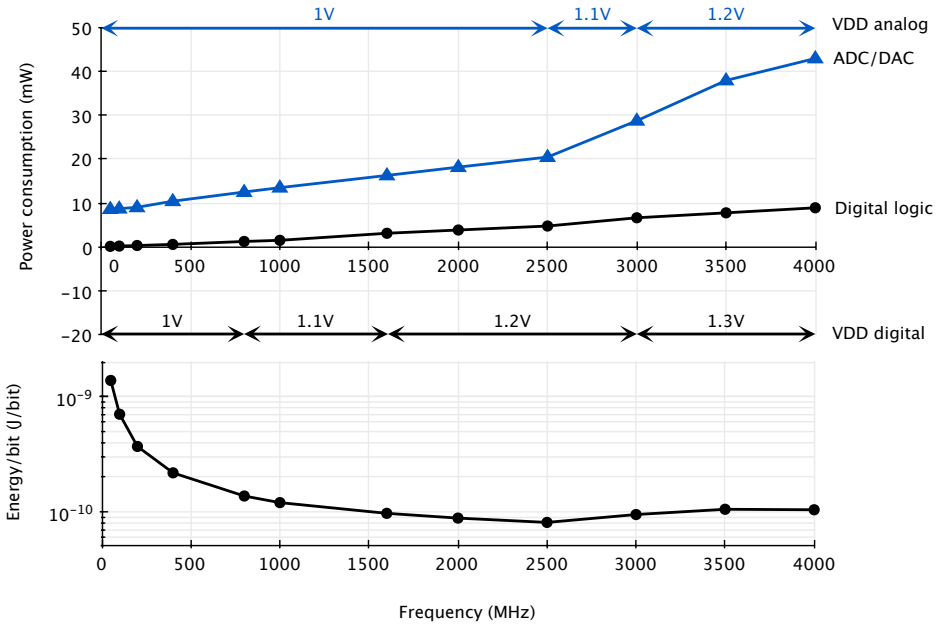

Figure 41: Power consumption versus clock frequency

power measurements have been compiled in the figure 41. The power consumption of the circuit evolves linearly with clock frequency. The rising rate is also function of the supply voltage. When operating at 2.5 GHz, the circuits only consumes 25.2 mW. This consumption rises to 52 mW at 4 GHz clock frequency. The second curve present in this graph shows the evolution of the system's efficiency versus clock frequency. The most efficient frequency is 2.5 GHz with an Energy Per Pulse (EPP) 81 pJ/bit for the entire baseband chip including ADC/DAC, PHY and MAC layers and synchronization and localization services. This can be compared with the state of the art in IR-UWB systems as in the table5. Publications about existing systems often describe only one part of the entire system, and do rarely include the MAC layer.

When compared with state of the art systems, the proposed system proposes high data-rate and good synchronization while keeping the lowest energy per bit, even when comparing the whole proposed SoC with state of the art receivers. The weakest point of this chip is its performances in distance evaluation. However, this can be improves through specific algorithms for better detecting the ToA with the same sampling rate.

4.8 CONCLUSION

This chapter has demonstrated an implementation of the WiDeCS and WiDeLoc protocols from hardware simulations to FPGA and ASIC implementation. The TDMA MAC layer performs its tasks correctly and sets a time domain multiplexing with limited

Ref.	Tech.	Freq.	Contents	Pulse rate	Sync. acc.	Sync. err range	Min EPP	Ranging acc.
Tamtrakarn et al. [96]	0.15μm FD-SOI CMOS	0-960MHz	RX only	25k	n.a.	n.a.	12000pJ	n.a.
Terada et al. [97]	0.18μm CMOS	0-960MHz	Transceiver	1M	n.a.	n.a.	4000pJ	2.5 cm
Lee et al. [66]	0.18μm BiCMOS	3-10GHz	RX only	100M	n.a.	n.a.	750pJ	n.a
Lachartre et al. [60]	0.13μm CMOS	4-5GHz	Transceiver	31M	n.a.	n.a.	1100nJ	30 cm
Mercier et al. [73]	90nm CMOS	3.5-4.5GHz	Digital BB	16M	1 ns	n.a.	300 pJ	30 cm
Daly et al. [34]	90nm CMOS	3.5-4.5GHz	RX only	16M	n.a.	n.a.	500pJ	30 cm
Zheng et al. [104]	0.18μm CMOS	3.1-5.5GHz	Full Baseband (w/o ADC)	1M	n.a.	n.a.	6220nJ	n.a.
Van Helleputte et al. [99]	0.13μm CMOS	0-960MHz	RX only	39M	n.a.	n.a.	108pJ	1.4 cm
This work (2GHz clock)	65nm CMOS	0-1GHz	Full Baseband	250M	3.8ns	$\pm$ 8ns	88pJ	est. 30 cm
This work(3GHz clock)	65nm CMOS	0-1.5GHz	Full Baseband	375M	1.18ns	$\pm$ 2.8ns	94.5pJ	est. 20 cm

Table 5: Comparison with state of the art UWB systems

overheads owing to WiDeCS synchronization protocol. Concerning measurement trigger synchronization, the measured trigger delays between master and clock nodes do rarely exceed 2-3 clock periods in an usual context.

The FPGA demonstrator, working with a UWB OFDM PHY layer, has a measurement trigger error under 60 ns for 98% of the measurements. This is mostly due to unrecovered data losses on the wireless channel. However, the 50 MHz bandwidth would not allow much more than 20ns trigger delay in a best case scenario.

The WIDEMACV1 chip working at 3GHz base clock generates a 3 ns period digital clock. In this case, the resulting trigger error range of 2.8 ns is very good compared to the clock period. The performances attained by the WIDEMACV1 chip are encouraging considering that this prototype is a proof of concept for the technologies included inside the chip. Perspectives for this system include power reduction techniques to reduce the power consumption owing to a power switching policy based on the knowledge the system has about slot allocation. Power switching would allow a substantial reduction of the power consumption of the DAC, the ADC, and even the RF front-end which has a power-up setup time under 20 ns.

An other perspective for this system is to build a SoC using the proposed baseband as an IP peripheral to the Advanced Microcontroller Bus Architecture (AMBA) Advanced High-performance Bus (AHB) or Wishbone system bus. The SoC implementation has many advantages. Among them, the most interesting one is the network protocol stack which would allow more complex routing policies. Such system would open the way to innovative routing protocols taking advantage of the synchronization capabilities of the demonstrated system.

GENERAL CONCLUSION

The work presented in this thesis focused on improving performance at different layers of the radio interface of a Wireless Sensor Network (WSN) node. Such improvement gained in amplitude with some choices and assumptions being made at the beginning of the research work. We chose to work on high data-rate WSNs with critical need for high reliability synchronization and localization services. A cross layer system, designed for Constant Bit Rate (CBR) transmission of data has been developed, and services for ranging and synchronization named WideLoc and WideCS have been designed, tested and implemented. The proposed communication system is based on an Impulse Radio UltraWide Band (IR-UWB) modulation technique, which has been modified from the work previously performed in the research team. A Time Division Multiple Access (TDMA) multiplexing is used as the main MAC scheme, and works with a cluster tree network architecture. Thanks to the cross-layer design of this system, services such as synchronization and ranging have been specifically designed and implemented alongside the MAC layer. These services do take advantage of the cross-layer architecture to determine the Time of Flight (ToF) through Time of Departure (ToD) and Time of Arrival (ToA) measurement at the time the first effective bit of data leaves the PHY layer of the transmitting node, and enters the PHY layer of the receiving node. Such nanosecond scale time-stamping capabilities do dramatically improve the synchronization performance. Moreover, the TDMA period used for Medium Access Control (MAC) is also used as a refresh period for synchronization and ranging. Owing to these techniques, the synchronization between the nodes is kept as precise as possible for long experimentations, while keeping a very fast response to changes in the propagation time in case of nodes moving away from or towards each other.

Simulations with a HDL simulator show synchronization error below two ADC clock periods, and ToF accuracy of 1 clock period. Considering that this system is designed for clock frequencies of 500 MHz, 2 GHz, and 4 GHz, this gives a prospective synchronization error below 2 ns in any case, and a ToF precision of 0.25 ns, leading to 15 cm of attainable ranging precision.

The other axis of work in this thesis is the optimization at the hardware level through an efficient implementation. The proposed cross-layer system has been implemented on FPGA development boards, and shows promising results. Synchronization over the wireless link shows measurement trigger delays below 60 ns for 95% of the measurements with a 125 MHz clock.

In order to improve performance, as well as to reduce the power consumption, an ASIC implementation has been realized, and a specific ASIC design flow has been set-up in order to build a mixed signal custom SoC in the ST Microelectronics 65nm CMOS technology. The goal of this ASIC was to demonstrate a low power SoC including a radio interface for IR-UWB communications in a high data-rate context.

A test PCB board has been designed for testing different aspects of the system such as two way communication, TDMA network initialization, synchronization, ranging, and energy consumption. Different testing processes have been developed using the same PCB test board for reducing costs, and improving QoR.

The fabricated ASIC is designed to function with an external clock source ranging from 500 MHz to 4 GHz. It allows a data-rate of 500 Mbps with a 4 GHz clock

source for a power consumption of 52 mW, or 104 pJ/bit. Best efficiency and synchronization performance are attained for a clock frequency of 3 GHz. The resulting data-rate is 375 Mbps, and the synchronization error is as low as 1.18 ns with a maximum error of 2.8 ns.

Perspectives for this work are possible at multiple levels of the design. A way of improving the MAC protocol is to build a more flexible protocol taking into account the arrival of new nodes into an existing network, as well as the release of TDMA slots when the corresponding node leaves the network. The implementation of a routing protocol on top of the proposed system is also a lead to improving the overall behavior in changing environments, while keeping a low complexity at low levels, and bringing the network intelligence to nodes with access to a reliable power source.

Another lead of improvement is related to the ASIC implementation, and addresses concerns about reducing the system's power consumption. The work presented in this thesis was designed with energy saving methods in mind. Independent blocks and service modules have been developed, and may be powered ON and OFF through a power management unit. This module is still under work, and may lead to extremely low power consumption by shutting down the RF systems between two data exchanges for example.

The path that lead to the work presented in this thesis began 6 years ago, and implied the work of many persons in the research team. Yet, to achieve the main goal for our research team, other people will have to continue the work.

RÉSUMÉ EN FRANÇAIS

GENERAL INTRODUCTION

Les avancées récentes dans la conception de dispositifs MEMS ainsi que dans les technologies sas fil ont ouvert la voie vers de nouvelles techniques de mesure. Habituellement, les capteurs sont déployés loin de l'électronique de traitement, et necessitent un traitement du signal lourd pour extraire les données pertinentes du bruit. De plus, les capteurs conventionnels sont souvent connectés individuellement aux conditionneurs, et causent des coûts supplémentaires pour leur déploiement. Les réseaux de capteurs consistent en un grand nombre de noeuds sensitifs communicants qui travaillent ensemble pour détecter et mesurer les évènements physiques, puis pour les traiter et transmettre des informations.

Ces fonctionnalités ont causé l'utilisation des réseaux de capteurs dans des domaines très variés. Des systèmes sont par exemple déjà utilisés en opération militaire avec notamment le remplacement de certains champs de mine par des réseaux de capteurs sans fil. D'autres applications, comme la surveillance de santé des structures (SHM) sont en cours de développement, notammment pour le controle des voies ferrées, des autoroutes, etc.. Plus récemment, de nouvelles applications sont devenues des sujets de recherche active, et requièrent l'échange continu de grandes quantités de données ainsi qu'un déclenchement synchrone des prises de mesure, pour effectuer des mesures de vibrations par exemple. De tels besoins ne peuvent être résolus par des techniques de communication actuelles.

Le travail présenté dans cette thèse vise à concevoir une architecture de système sur puce (SoC) pour une utilisation dans un réseau de capteurs sans fil. Les améliorations de l'état de l'art visées se situent dans la conception croisée (Cross-layer) de l'interface réseau, ainsi que dans l'implémentation d'une preuve de concept fonctionnelle de système sur puce mixte démontrant les fonctionnalités de l'interface réseau conçue. L'interface « Cross-layer » proposée comprend une couche MAC adaptée au besoin de la mesure sans fil, et implémente une couche réseau UWB impulsionnelle conçue par Aubin Lecointre . Des services innovants sont également proposés pour la synchronisation des mesures. Concernant l'implémentation sur puce ASIC, le démonstrateur proposé a été conçu pour conserver les meilleures performances possibles avec une consommation minimale.

La première partie de cette thèse décrit les applications possibles pour les réseaux de capteurs sans fil, ainsi que l'état de l'art les concernant. Le chapitre 1 traite du contexte des réseaux de capteurs et de leurs applications. Le chapitre 2 traite de l'utilisation des techniques UWB dans ces réseaux, ainsi que de l'état de l'art de ces technologies UWB. La deuxième partie est concentrée sur les travaux de conception et d'implémentation réalisés. Le chapitre 3 décrit la structure du système proposé, et propose un protocole de synchronisation de noeuds dénomé WiDeCS. Le dernier chapitre propose deux implémentations de ce système, ainsi qu'un protocole de test spécifique au démonstrateur ASIC.

2

INTRODUCTION AUX COMMUNICATIONS DANS LES RÉSEAUX DE CAPTEURS SANS FIL

Les réseaux de capteurs sans fil sont des systèmes composés de capteurs intelligents embarqués avec des fonctionnalités de transmission sans fil de données et une part variable d'autonomie. Ces éléments, communicant entre eux sans fil, ont souvent des fonctions de récupération et agrégation de mesures vers un point de chute, des fonctionnalités de mesures hétérogènes de grandeurs de types différents, ou même de mouvement par exemple. Ce chapitre décrit quelques unes des applications possibles pour les WSNs choisis pour leur avancée technologique, ou pour leur intérêt dans le travail présenté dans cette thèse. Les modes de communication sans fil sont ensuite étudiés dans une deuxième section. La dernière section décrit deux services pour les réseaux de capteurs sans fil qui ont été ciblés dans cette thèse : la synchronisation des mesures, et des méthodes de localisation.

2.1 APPLICATIONS POSSIBLES

Les réseaux de capteurs ne sont pas limités par des contraintes imposant un standard unique. Ce domaine comprend en effet tout système composé de noeuds doués de capacités de mesure, et communicant entre eux dans le but d'effectuer une tache. Des applications possibles pour ces systèmes peuvent être trouvées dans tous les domaines de la vie courante.

- Applications pour la défense et la sécurité : Dans le milieu de la défense et de la sécurité, les réseaux de capteurs permettent l'amélioration des connaissances liées à l'environnement, mais également liées aux moyens humains et matériels. Ils permettent par exemple de détecter des intrusions dans des zones protégées et peuvent remplacer des champs de mines par des systèmes de détection d'intrusions. Dans un contexte de contrôle des moyens, l'installation de réseaux de capteurs dans les véhicules ou sur les personnes peuvent permettre le contrôle de leur santé [3].

- Applications industrielles : De nombreux domaines industriels peuvent tirer avantage des réseaux de capteurs, de la gestion d'inventaire au contrôle de santé des bâtiments, en passant par le test industriel. Les mondes de l'aéronautique et du spatial par exemple, sont de grands consommateurs de tests, de prise de mesure et d'essais. Le remplacement des appareils de mesure actuels par des réseaux de capteurs disposés directement sur la surface d'un avion est étudié actuellement par plusieurs grands avionneurs, et permettrait d'améliorer la fiabilité de ces tests ainsi que leur coût.

- Applications pour la santé : Dans le domaine de la santé, ils visent principalement à améliorer la connaissance et le suivi des paramètres vitaux des patients ou à leur identification et localisation.
- Applications pour l'écologie : Les réseaux de capteurs utilisés pour des applications de contrôle de l'environnement permettent pour la plupart de surveiller de vastes zones, et de détecter des changements généralisés ou locaux même de faible ampleur.
- Applications pour le grand public: Le grand public est également concerné par les avancées liées aux réseaux de capteurs. Les voitures de demain seront probablement en réseau afin de mieux gérer les encombrements routiers, mais aussi effectuer des portions de trajet de manière automatique.

2.2 COMMUNICATIONS POUR LES WSN EN ENVIRONNEMENT INDUSTRIEL

Les réseaux de capteurs, par la diversité des applications possibles, ne peuvent être adressés tous par la même technologie de communication. Certains de ces réseaux nécessiteront des grandes portées et n'auront qu'un besoin en débit limité, où d'autres conserveront des portées limitées à quelques mètres ou dizaines de mètres, mais pourront transmettre beaucoup de données. On peut ainsi dégager deux grandes familles d'interfaces de communication sans fil utilisables pour les réseaux de capteurs.

2.2.1 *Communications à bas débit*

Les communications sans fil permettant aux WSNs d'atteindre des grandes portées sont souvent utilisées de manière très sporadique dans le temps, afin de limiter les couteux échanges de données. De nombreuses optimisation de la consommation entrent en jeu, telles de longues périodes de sommeil, et des rendez vous réguliers pour les échanges de données entre noeuds.

IEEE 802.15.4-2006 est de par son utilisation massive le standard actuel pour la communication dans les réseaux de capteurs [13]. Ce standard définit plusieurs couches PHY et MAC faible consommation pour la transmission de données sans fil. Plusieurs contextes sont décrits, proposant soit des portées courtes jusqu'à 10m, soit des portées jusqu'à 2km, tout en permettant des débits jusqu'à 250kbps.

2.2.2 *Communications à haut débit*

L'utilisation de techniques de communication à haut débit est, bien que consommatrice d'énergie, parfois inévitable dans certains contextes. Des mesures rapides de quelques kech/s prises en simultané sur plusieurs dizaines de noeuds permettent en effet des corrélations dans le temps et dans l'espace. Or de telles mesures requièrent des réseaux pouvant faire transiter plus de 10Mbps de données applicatives. Les

standards IEEE 802.11 décrivant les différentes générations de WiFi, permettent aujourd'hui de faire transiter jusqu'à 7Gbps dans certaines configurations multi-antennes [4]. Cependant, la grande longévité de ce standard et les choix techniques successifs ont rendu toute implémentation complexe, ce afin conserver une rétro-compatibilité. Cette complexité, ajoutée à des algorithmes de codage complexes, rend la consommation de ces technologies élevée.

Dans la dernière décennie, les technologies de fabrication de circuits intégrés ont permis d'augmenter les fréquences de fonctionnement, et ainsi d'utiliser des bandes de largeur plus grande. Cela a permis une'augmentation des débits, comme dans le standard ECMA 368 (WiMedia). Cependant, d'autres implémentations de plus faible complexité ont été proposées afin de répondre à d'autres besoins comme la mesure [53], ou également pour les WSNs. Le travail présenté dans cette thèse utilise pour la couche PHY des technologies IR-UWB présentées par Aubin Lecointre dans sa thèse et étudiées au chapitre 2.2. Lesquelles ont été modifiées afin de supporter des mesures de temps de vol (ToF).

2.2.3 *Protocoles MAC à économie d'énergie*

Depuis le début des années 2000, et l'augmentation de l'intérêt porté aux réseaux de capteurs sans fils, de nombreuses recherches ont été menées sur l'augmentation de la durée d'activité de ces réseaux. De grands efforts de recherche ont ainsi été portés sur une couche stratégique pour atteindre ce but: le contrôle d'accès au médium (MAC). Les pistes principales explorées pour réduire la consommation des réseaux ont visé à réduire trois sources de surconsommation : La perte de données, par exemple en raison de collision ou de manquement de rendez-vous. L'activation inutile de l'électronique de réception pendant laquelle le noeud consomme de l'énergie, mais ne reçoit rien car personne ne transmet. Une trop grande complexité contrebalance un gain éventuel en qualité par un cout énergétique trop grand. Plusieurs protocoles MAC ont ainsi été conçus, et ont proposé des solutions diverses à ces problématiques. Les protocoles optimisés pour l'évitement de collision , comme le S-MAC [59], son successeur le T-MAC [98] et également le B-MAC [59] implémentent un protocole basé sur l'écoute du canal avant transmission CSMA couplée avec des temps de sommeil en cas d'inactivité. De tels protocoles sont bien adaptés à des réseaux de composition variables et d'adaptent aux entrées et sorties. Cependant leurs optimisations énergétiques sont limitées en efficacité. D'autres protocoles, à planification comme le LEACH [52, 59] ou le TRAMA [85], initient un multiplexage temporel du canal (TDMA), et permettent d'optimiser les périodes d'écoute de chaque noeud. L'inconvénient de ces protocoles est principalement lié à une latence à l'entrée d'un nouveau noeud dans le réseau. Pour finir, plusieurs protocoles hybrides, adaptés à des situations particulières ont vu le jour. Le protocole DMAC [70], par exemple est optimisé pour l'accumulation de données vers un point de chute unique.

De nombreuses couches MAC existent donc à destination des réseaux de capteurs. Cette multiplicité a permis l'émergence de protocoles spécialisés en fonction du type de réseau à construire.

2.3 SERVICES POUR LES WSNS

2.3.1 *Synchronisation d'horloge et de prise de mesures*

Comme expliqué précédemment, les protocoles à planification sont plus appropriés pour des échanges réguliers de données en raison la prévisibilité de l'occupation du canal. Les protocoles de synchronisation fonctionnent principalement autour de mesures de date de transmission et de réception de paquets de données afin de déterminer les délais causés par le temps de transmission de la donnée (ToF) entre l'application émettrice et l'application destinataire de la donnée. Des mesures de ce délai, couplées à des calculs statistiques permettant de réduire les incertitudes, la performance de synchronisation dépend donc principalement de la variance de ces délais, et de la qualité du calcul. Des protocoles adaptés à des réseaux filaires ont ainsi été développés, puis améliorés pour mieux traiter les latences au niveau MAC comme pour le IEEE 1588 PTP. Cependant, le contexte des réseaux sans fil ne permet pas les mêmes optimisations. Des protocoles simples de datation de trame ont donc été utilisés dans un premier temps afin de caler à 32us près des horloges entre elles sur une communication sans fil (Ping et al. [83]). Des techniques similaires, basées sur la transmission d'une balise de référence (RBS), permettent la synchronisation de plusieurs esclaves entre eux comme montré par PalChaudhuri et al. [80], Maroti et al.[72] et améliorent la précision à 1.5us. Plus récents, d'autres protocoles, plus proches de ceux utilisés sur les réseaux filaires, capturent des temps de vol et sur une base statistique déduisent l'erreur de correction à compenser. Cette dernière technique, dont une variante atteignant une précision de 600ns a été proposée par Cooklev et al. [33]. Les plus précis de ces protocoles basent leur performance sur l'hypothèse que le temps de vol est stable, et que les noeuds sont statiques [30]. La difficulté est donc de proposer un protocole alliant performance de synchronisation absolue, et rapidité d'adaptation au mouvement.

2.4 CONCLUSION

Ce chapitre a démontré en quoi les réseaux de capteurs peuvent être une solution viable dans de nombreuses situations, du contrôle de l'environnement, à la localisation des membres d'une escouade militaire. Cependant, apporter une solution à tous ces champs d'applications n'est possible qu'avec une large palette de technologie, dont seulement certaines pourront etre adaptées à l'application visée. Bien que plusieurs technologies soient disponibles dans le cas des réseaux à bas débit, aucune technnologie ne répond à ce jour à la problématique de l'instrumentation sans fil. Cette thèse adresse donc cette problématique en proposant une bande de base qui résout deux points de blocage que sont les débits atteignables, et la synchronisation des prises de mesure.

3

ULTRALARGE BANDE ET RÉSEAUX DE CAPTEURS SANS FIL

3.1 INTRODUCTION AUX COMMUNICATIONS ULTRALARGE BANDE (UWB)

L'Ultralarge Bande est une technologie radio qui vise à occuper une bande passante extrêmement large afin de moduler un signal radio. L'utilisation d'une telle bande passante ouvre de nouvelles possibilités pour les communications sans fil, et apporte une complexité spécifique. Parmi ces spécificités, la principale est la densité spectrale de puissance (PSD)autorisée qui est très basse pour éviter les interférences avec d'autres systèmes utilisant des bandes étroites comprises dans la bande occupée par la modulation UWB. La faible PSD émise autorisée, souvent de l'ordre de -43dBm/MHz fait que la PSD reçue est souvent a peine plus grande que le niveau de bruit ambiant. Par ailleurs, les modulations UWB possèdent une propriété liée au domaine temporel : une large bande de fréquence permet de moduler de très courts évènements temporels. Cette différence entre bande étroite et bande large est illustrée dans la figure 42. Plusieurs techniques de modulation ont été proposées, et permettent de tirer avantage des spécificités de l'UWB pour servir des objectifs divers. Il est en effet possible d'utiliser un canal UWB comme un ensemble de bandes étroites orthogonales. Les modulations MB-OFDM utilisées dans des standards comme le IEEE 802.11ad (WiGig 60GHz), ECMA 368 (Wimedia 3-10GHz)[37, 51] sont utilisées sur des largeurs de bande jusqu'à 1.7GHz pour transmettre jusqu'à 7Gbps de données sur 5m [82, 16]. Une autre utilisation possible d'une telle largeur de spectre est la réduction de consommation et leur utilisation dans les réseaux de capteurs. Le besoin de puissance de transmission est limité dans son ampleur en raison des limitations règlementaires, mais également dans sa durée. Il est alors possible de réveiller les composants réseau que pendant de très courtes périodes de temps, et ainsi économiser de l'énergie. La radio UWB impulsionnelle, par exemple, est une technique de modulation, détaillée en 3.2, qui est basée sur la transmission d'impulsions de durée de l'ordre de la nanoseconde, avec une période pouvant aller de 4 ns à quelques microsecondes [41, 94, 24]. Le standard IEEE 802.15.4a-2011, décrivant des interfaces à faible consommation et faible débit, a ajouté une telle modulation et porte le débit maximal pour ce standard à 39Mbps. Quelque soit la raison principale pour utiliser les technologies UWB, les particularités temporelles de cette technologie en font un très bon support pour des services de synchronisation et mesure de distance.

Les autorités de régulation ont pour la plupart autorisé l'utilisation non-licenciée de deux bandes pour des modulations UWB. Une première, située entre 3.1GHz et 10.6GHz est autorisée souvent en partie par les différentes autorités avec des niveaux d'émission souvent inférieurs à -41.3dBm/MHz. La deuxième bande UWB traitée dans cette thèse se situe entre 57GHz et 66GHz. Les niveaux de pertes élevés

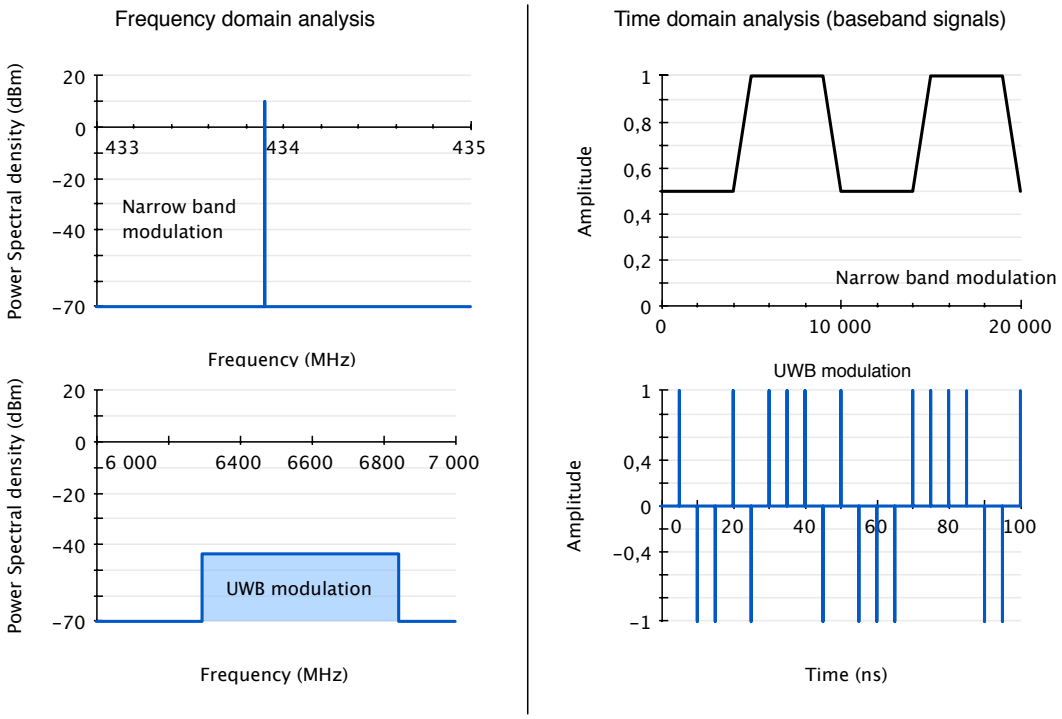

Figure 42: Comparaison bande étroite / UWB

dans ces bandes de fréquences permettent des niveaux d'émission plus élevés que dans la bande précédente de l'ordre de 13dBm/MHz max en Europe par exemple.

3.2 IR-UWB

3.2.1 *Principes et techniques de modulation*

La radio ultralarge bande impulsionnelle est basée sur l'émission de courtes impulsions à des intervalles définis. Cette concentration dans le temps de la transmission d'énergie donne à ces modulations un fort ancrage dans le domaine temporel. Les multi trajet, par exemple, sont perçus par le récepteur comme des échos des impulsions reçus plusieurs fois au niveau du récepteur (voir figure 43). Les techniques de modulation des impulsion existant peuvent etre combinées afin d'augmenter le débit au cout cependant d'une complexité accrue des récepteurs. Parmi ces modulations, des modulations comme le PPM, ou modulation par position de l'impulsion permet de définir plusieurs slots possible, et à coder l'information dans le choix du slot utilisé. D'autres modulations modifient elles la forme de l'impulsion et codent l'information dans l'amplitude de celle ci (ASK), ou dans la phase donnée à l'impulsion (BPSK). Cette dernière méthode permet, hors combinaison de modulations, d'obtenir les débits les plus élevés, ainsi que le meilleur BER possible. Le temps nécessaire entre deux impulsions peut être limité à l'étalement des échos sur le canal, et cette méthode ne souffre pas des perturbations pouvant causer des variations dans l'amplitude du signal reçu. Le standard IEEE 802.15.4a, qui

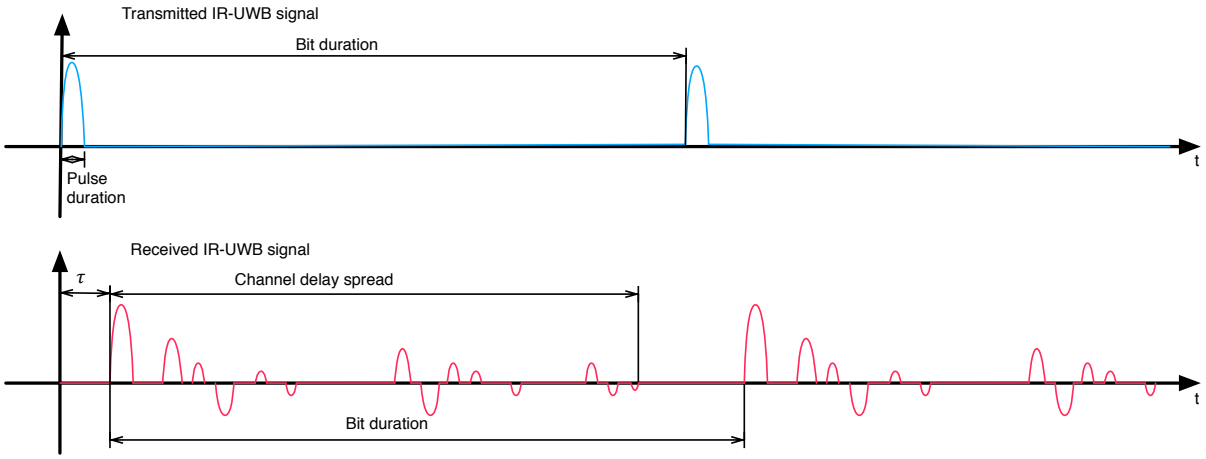

Figure 43: Etalement des échos sur l'IR-UWB

décrit la première interface standardisée pour l'IR-UWB, utilise une combinaison de modulation BPSK et de PPM. Cette combinaison permet de communiquer avec des dispositifs très peu complexes, ne décodant que la modulation PPM, mais également de tirer profit des controles d'erreur implémentés sur la modulation BPSK.

3.2.2 *IEEE 802.15.4a, la standardisation d'une modulation IR-UWB*

La révision a du standard IEEE 802.15.4 apporte comme principal ajout une modulation IR-UWB utilisable dans un contexte de réseau sans fil personnel. Les débits prévus dans ce standard sont compris entre 110kbps et 27.24Mbps [15] sur des distances jusqu'à 10m [12]. De plus, les contextes d'utilisations de ce standard impliquent l'utilisation de noeuds à fonctionnalité réduite (RFD) et de noeuds à fonctionnalité pleine (FFD). Cela implique donc une hétérogénéité des noeuds prise en compte dans les protocoles de contrôle d'accès au médium. Cette hétérogénéité se transcrit également par des modulations, codages et protocoles obligatoires, alors que d'autres implémentations plus performantes mais plus couteuses sont proposées en option. Au niveau de l'utilisation des fréquences, des canaux de 500MHz sont proposés dans la bande de 3.1-10.6GHz, certains d'entre eux pouvant être joints en canaux de 1.3GHz. La densité spectrale de puissance autorisée est de -41.3dBm. Les couches PHY proposées peuvent utiliser une unique modulation PPM dans un objectif de réduction des couts et de la consommation. Cependant, une modulation plus complexe, croisant le PPM et le BPSK permet de transmettre simultanément un bit de donnée dans la modulation PPM, ainsi qu'un bit de codage convolutionnel dans la modulation BPSK. Un message ainsi transmis par un composant supportant la modulation hybride peut donc être reçu correctement par un composant ne supportant que la modulation PPM obligatoire. Les avantages liés au code convolutionnel transmis dans la modulation BPSK seront donc perdus. De la même manière, plusieurs moyens de contrôle d'accès au medium sont proposés dans le standard. Une transmission sur un principe MAC ALOHA est proposée comme fonctionnalité obligatoire, alors que des protocoles plus complexes permettent d'augmenter les

performances en mettant en place un multiplexage temporel (TDMA) géré par un coordinateur de réseau personnel (PAN). Des fonctionnalités d'écoute de porteuse (Carrier Sense - CS) permettent également de détecter la présence d'une trame TDMA existante, et de ne pas la perturber par exemple. Ce standard présente donc une implémentation très adaptative de réseau de capteurs basés sur une modulation IR-UWB. Les exigences de débit et de simplicité traitées dans cette thèse ne sont cependant pas traitées dans une seule implémentation, et rendent le système complet trop complexe à mettre en oeuvre dans le contexte de remontée de données de mesure. De plus, à ce jour, aucune implémentation de cette révision du standard n'est disponible commercialement.

3.2.3 *Implémentations faible consommation de transceivers IR-UWB*

Depuis l'ouverture des bandes libres pour des communications UWB par les différentes autorités régulatrices, de nombreuses recherches ont porté sur la conception d'interfaces de communication IR-UWB à basse consommation. Ces paragraphes visent à donner un aperçu des techniques les plus remarquables proposées. Les émetteurs IR-UWB ont pour principale caractéristique la génération dans un temps très court d'impulsions électriques. Ce principe de fonctionnement transforme de manière générale la structure même de l'émetteur, en rendant possible le remplacement des mixers, amplificateurs, et autres oscillateurs contrôlés en tension par d'autres blocs. Des générateurs d'impulsion analogiques ont par exemple été conçus en utilisant des fonctions dérivatives sur des signaux numériques [89, 68, 69]. D'autres implémentations, permettant des modulations BPSK, utilisent des mixeurs pour construire des impulsions gaussiennes en exploitant leur comportement transitoire [102, 20]. Bien que ces implémentation principalement analogiques proposent pour la plupart des consommations très basses, ainsi que des dimensions réduites, beaucoup de taches liées à la formation des paquets et à la synchronisation des récepteurs sont considérées comme étant réglées au niveau supérieur. D'autres implémentations proposées, principalement numériques, proposent également des fonctionnalités comme la reconfiguration de la forme d'impulsion et d'amplitude. Certaines implémentations numériques utilisent par exemple des chaines d'inverseurs pour créer des impulsions de longueur très faible [93, 78, 101]. L'autre méthode principale pour former des impulsions est de les générer numériquement, puis d'utiliser un DAC rapide [63, 62]. Cette dernière méthode, bien que nécessitant un travail supplémentaire au niveau du design du DAC, permet une reconfiguration à la volée de la forme d'impulsion. Les récepteurs, d'un autre coté, peuvent également être rangés par la proportion d'électronique numérique les composant. Des implémentations analogiques de récepteurs, ne fournissant qu'une information binaire en sortie, ont été proposés dès 2006 [96]. Depuis, plusieurs implémentations de récepteurs utilisant un front-end analogique spécifique couplé à une partie numérique ont été proposées notamment au MIT par l'équipe de Prof. Chandrakasan [73, 34]. La consommation de ces composants a ainsi été réduite par pas successifs pour atteindre la centaine de picoJoules par impulsion en 2010 [99].

4

CONCEPTION CROISÉE D'UN SYSTÈME DE COMMUNICATIONS UWB POUR WSN

4.1 VUE SYSTÈME ET CONCEPTION CROISÉE

Les besoins exprimés précédemment n'ont pas été atteints par des méthodes de conception classiques comme le modèle OSI. Ces méthodes sont développées pour des applications génériques, et ne s'adaptent que de manière marginale à des applications très spécifiques. La solution proposée résout ces problèmes en utilisant la conception croisée de l'interface réseau, de la tête RF aux services de synchronisation de prise de mesure. Comme montré dans la figure 44, des services standards du réseau comme la couche MAC ou la couche PHY peuvent être interrogés directement par des services annexes comme la synchronisation. L'intérêt est ici de réduire les délais inconnus dans les différentes couches du réseau, en interrogeant directement la couche responsable de la détection d'un paquet par exemple. De plus, le résultat de cette synchronisation est réintroduit dans la gestion de la trame TDMA au niveau de la couche MAC afin d'optimiser les temps de garde, et d'éviter les doublons de fonctionnalité. De telles optimisations ont permis de proposer un protocole de synchronisation de mesure - WiDeCS [**?**] - couplé à une couche MAC spécifique permettant la mise en réseau de capteurs afin de remonter des données vers un point de chute unique décidé au moment de la conception du réseau.

4.2 COUCHE MAC À MULTIPLEXAGE TEMPOREL

La couche MAC est basée sur du TDMA en raison principalement du déterminisme naturel de ce contrôle d'accès. Les moments et temps de parole sont maitrisés par un coordinateur. Par extension, un retard ou une avance sur ce temps de parole, couplé à une estimation du temps de propagation du paquet permet de déterminer une désynchronisation de l'horloge du noeud concerné, et ainsi agir sur la correction à appliquer. Dans un souci de simplification de l'implémentation de ces interfaces, la couche MAC TDMA proposée est implémentée en affectation fixe des slots. Chaque noeud voit son adresse et son slot affecté avant l'allumage des noeuds et du réseau.

4.3 OPTIMISATIONS DANS LA COUCHE PHYSIQUE IR-UWB

Les besoins en synchronisation très précise émis par les utilisateurs du monde aéronautique et spatial impliquent des besoins au niveau des couches physiques du réseau. Le système proposé est basé sur une modulation radio impulsionnelle IR-UWB et encode l'information dans la phase de l'impulsion (BPSK) proposée et implémentée par Aubin Lecointre [61]. Des impulsions positives ou négatives sont

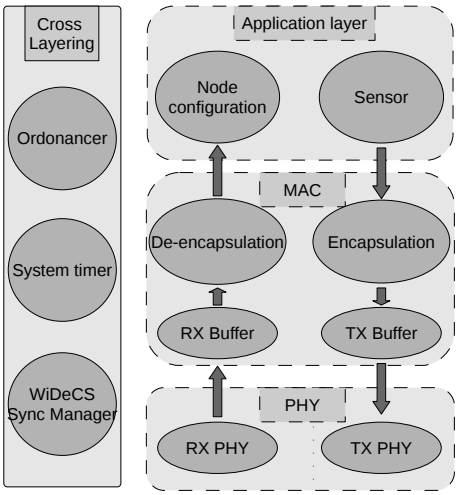

Figure 44: Système proposé

émises, puis décodées dans le récepteur. L'émetteur forme le paquet en ajoutant un délimiteur de début de trame (SFD), transforme les informations binaires en formes d'impulsions correspondantes ayant une largeur de bande proportionnelle à la fréquence de fonctionnement (2GHz de bande pour un fonctionnement à 4GHz), puis les transmet à la couche RF. Du coté du récepteur, plusieurs détecteurs d'impulsion travaillent en parallèle, et transmettent la valeur reçue la plus probable en fonction de l'amplitude et de la phase du signal mesuré. Ces informations sont ensuite compilées dans un détecteur / décodeur Rake qui détecte la séquence du SFD dans les valeurs détectées, puis déclenche un système de vote entre les différents multi-trajets. La valeur la plus probable de chaque bit est ainsi votée parmi les voies ayant déclenché sur la séquence SFD, et est transmise à la couche MAC. Les modifications apportées à cette couche physique on consisté à dater précisément les moments de départ du premier bit de donnée efficace de la couche PHY émettrice (hors SFD), ainsi que le moment d'arrivée de ce même premier bit à l'entrée de la couche PHY réceptrice (après le SFD). De telles mesures peuvent etre prise au top près d'une horloge à 4GHz en raison fonctionnement très rapide des étages les plus bas niveau de cette couche PHY. Le comportement temporel de la communication UWB permet en effet des événements, dont la durée est de l'ordre de la nanoseconde, lors de transmission sur une bande passante de 1GHz.

Les différentes couches du réseau ont donc été conçues ou adaptées afin de tirer les meilleures performances dans l'objectif de proposer une interface à haute performance de synchronisation et faible consommation.

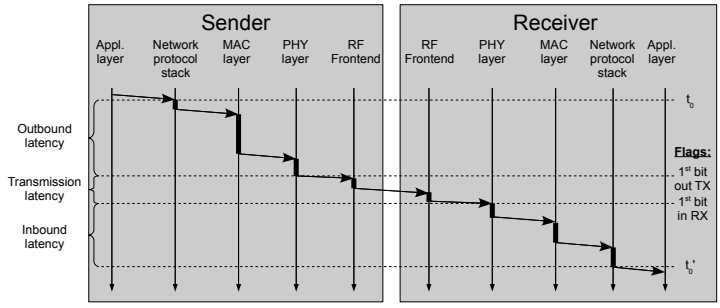

Figure 45: Délais successifs lors d'une transmission d'information sur un réseau sans fil

4.4 SERVICES CROSS-LAYER : UNE SYNCHRONISATION OPTIMISÉE

La raison principale des difficultés existant dans la synchronisation des horloges dans les réseaux de capteurs est située au niveau des délais inconnus. Un message est en effet passé de couche en couche pour être successivement encapsulé par ces dernières, et pour être émis sur le canal en respect du contrôle d'accès choisi. Ces couches de l'interface réseau génèrent des délais retardant l'émission du paquet, puis sa mise à disposition après réception chez le destinataire comme montré en figure 45. Ces délais, possédant une part variable d'aléatoire, réduisent la précision atteignable concernant la mesure du temps de vol (ToF) qui est le véritable délai à identifier. Les modifications énoncées précédemment aidant, WiDeCS récupère les dates d'émission et de réception du premier bit de donnée utile tant à sa sortie de la couche PHY émettrice, qu'à l'entrée dans la couche PHY réceptrice. Ce faisant, les calculs effectués sur ces datations sont soumis aux délais liés au DAC, aux têtes RF, à l'ADC et au temps de vol. La variabilité des délais dans les convertisseurs de même que dans les têtes RF étant de l'ordre de la gigue des horloges utilisées, elle se trouve de l'ordre de la dizaine de picosecondes, et n'est pas mesurable par un échantillonnage à la nanoseconde.

Le processus de synchronisation de WiDeCS se déroule en deux étapes : La première étape, de pré-synchronisation, permet d'initialiser le réseau, et de faire en sorte que les noeuds esclaves transmettent leurs paquets dans leurs slots respectifs. Pour cela, le coordinateur envoie régulièrement le marqueur de début de trame, en spécifiant à l'intérieur de celui ci l'identifiant du sous réseau créé. Les esclaves, en écoute permanente, se synchronisent simplement en faisant coïncider le début de la trame tel que reçu avec leur début de cycle. Une fois cette étape effectuée, les esclaves commencent à émettre des informations dans leur slot. La deuxième étape consiste à affiner la précision de la synchronisation par la mesure de retards : l'esclave mesure le retard entre le moment prévu pour la réception d'un paquet du maitre et sa réception effective, ainsi qu'entre le moment prévu pour sa propre transmission, et le moment où cette dernière a été effectuée.

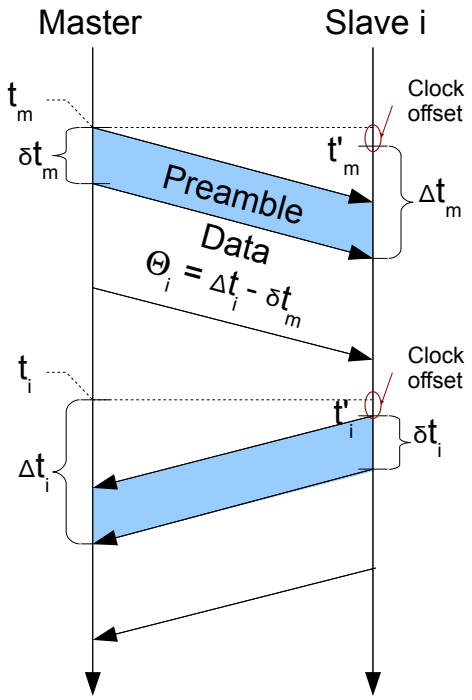

Figure 46: Echange d'informations de délais

Du coté du maitre, ces mesures sont effectuées pour chacun des esclaves présents sur le sous-réseau. Par la suite, le décalage des horloges entre les noeuds est calculé selon l'équation 4.2 appliquée aux mesures prises comme dans la figure 46.

$$\Delta t_{clk} = \frac{(\Delta t_i + \delta t_m) - (\delta t_i + \Delta t_m)}{2} \tag{4.1}$$

$$\Delta t_{clk} = \frac{\Theta_i - (\delta t_i + \Delta t_m)}{2} \tag{4.2}$$

Une étude des sources d'erreur dans la mesure, et de leur amplitude a permis de borner l'incertitude dans le retard estimé à +-2 périodes d'horloge de datation. Par ailleurs, l'implémentation de ce protocole au sein même de la couche MAC le rend extrêmement réactif, l'évolution du temps de vol étant compensée à l'échange de données suivant.

5

DÉMONSTRATEURS RÉALISÉS AUTOUR DE L'UWB ET WIDECS

5.1 APPLICATIONS CIBLES

Deux applications cibles ont été choisies comme support de démonstration pour les travaux effectués dans cette thèse :

5.1.1 *Système pour le controle de santé des structures aéronautiques*

Les premières applications ciblées concernent le contrôle de santé des structures (SHM) appliqué aux avions. Depuis quelques années de nouveaux avions faisant de plus en plus appel aux matériaux composites ont été conçus, comme les Boeing 787 ou Airbus A350. Avec l'utilisation de plus en plus massive de composite, de nouvelles contraintes et types de défauts sont apparus, et ont comme caractéristique d'être rarement visibles à l'oeil nu. Des techniques de vérification de la santé des structures ont donc été mises au point, et peuvent faire appel à des matrices de sondes disposées à des distances de 20-50cm. Des corrélations sont faites entre les mesures prises en même temps et permettent entre autres de localiser les défauts, et parfois d'en évaluer la gravite. Le réseau de mesure doit donc synchroniser les prises de mesure sur plusieurs sondes en simultané, puis rapatrier toutes les données vers un centre de traitement. A ce jour, aucun système de mise en réseau sans fil ne permet d'obtenir ni les besoin en terme de débit de données, ni en terme de synchronisation. Par ailleurs, des contraintes énergétiques sont ajoutées et sont liées à une installation possible sur les parois extérieures. La question de l'économie fait donc partie de l'équation à résoudre dans ce cas.

5.1.2 *Radio tactique impulsionnelle UWB pour communication et localisation en intérieur*

Une autre application, plus proche du domaine militaire, pourrait également profiter des innovations et développements de cette thèse. La problématique de la localisation des soldats et matériels est d'un intérêt stratégique pour l'évitement de tirs amis, ainsi que pour les centres de commandement. A ce jour, plusieurs techniques de localisation en extérieur existent et sont utilisées de concert. Cependant, la progression des personnes à l'intérieur de bâtiments ou de caves fait perdre cet avantage stratégique dans le cas de guérilla par exemple. Le deuxième démonstrateur technologique s'applique donc à participer à la résolution de ce problème, et à apporter une solution d'évaluation des distances par mesure du temps de vol. Cette technologie utilisant les modulations UWB et le protocole WiDeCS, un échange d'information entre les noeuds est également possible pour d'autres desseins. La

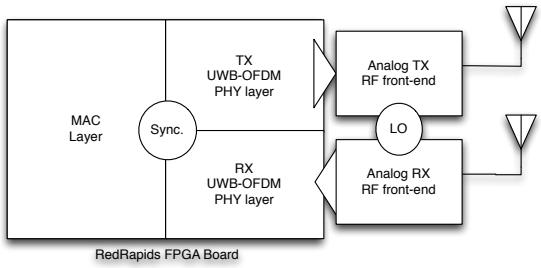

Figure 47: Schema bloc du démonstrateur

portée prévue est de l'ordre de 10m, et l'objectif ici est de synchroniser au mieux les noeuds afin d'obtenir une évaluation la plus fiable du temps de vol des paquets. La faible sensibilité des protocoles et modulations utilisées est également necessaire à une bonne évaluation de la distance entre les noeuds.

5.2 SIMULATION MATÉRIELLE

Des simulations au niveau matériel ont permis de vérifier la fonctionnalité et les performances des protocoles développés. Le banc de test virtuel développé implémente les circuits développés en VHDL synthétisable, et un modèle de canal prenant en compte l'atténuation et des délais de propagation variables. Les simulations menées sur ce banc virtuel ont montré une erreur de synchronisation de mesure inférieure à 3 tops d'horloge sur des délais de propagation de plusieurs dizaines de nanosecondes, correspondant à plus de 10m de distance dans l'application militaire. De la même manière, l'algorithme de calcul du temps de vol a réalisé un sans faute en se calant très rapidement après un changement de temps de propagation.

5.3 DÉMONSTRATEUR FPGA

Le démonstrateur sur FPGA est conçu pour l'application de surveillance des structures mécaniques. Ce démonstrateur est constitué d'une bande de base implémentée sur FPGA, et connectée à un ADC et à un DAC embarqués sur la carte FPGA. Une tête RF simple, est constituée d'un assemblage de circuits connectorisés type Mini-Circuits effectuant la translation de fréquence vers 6.8GHz. Une tête RF de réception, composée de la même façon, fait la translation inverse. La bande de base implémentée dans le FPGA est composée d'une couche MAC TDMA avec WiDeCS, et d'une couche PHY OFDM développée par Julien Henaut. Cette couche PHY a également été modifiée afin de capturer les dates de départ et d'arrivée des paquets dans la bande de base. L'ensemble de ces blocs est assemblé selon le schéma blocs de la figure 47.

Les tests effectués sur ce démonstrateur ont été mené avec deux noeuds complets se faisant face à 5m de distance. Un enregistrement de l'erreur de déclenchement

de prise de mesure au cours du temps permet d'évaluer les performances, tant au niveau de la communication que du protocole de synchronisation. Ces mesures montrent une erreur de synchronisation des deux noeuds inférieure à 6ons pour une horloge de 120MHz. L'écart constaté avec les simulations est dû à l'absence de correction d'erreur dans le démonstrateur, pouvant causer des corrections erratiques en cas d'erreur dans la transmission.

Ce démonstrateur FPGA a donc permis la preuve du concept de la couche MAC TDMA à slot fixe et de l'algorithme de synchronisation WiDeCS. Cependant, les performances nominales avec une couche PHY IR-UWB sont atteintes pour des fréquences de fonctionnement entre 2GHz et 4GHz. Un démonstrateur ASIC fut donc necessaire pour assurer la montée en fréquence.

5.4 PREUVE DE CONCEPT ASIC

L'objectif de ce démonstrateur était, à terme, une intégration en système sur puce de l'ensemble du noeud comprenant les interfaces capteur, l'intelligence embarquée sur microcontrôleur, la bande de base, et également la tête RF. La technologie de fonderie utilisée pour la conception du démonstrateur de bande de base a donc été guidée par les besoins en technologie au niveau de la tête RF vers une technologie CMOS 65nm de chez ST.

Le démonstrateur de bande de base complète, nommé WIDEMACV1, est un ASIC de 1x1mm fabriqué en CMOS 65nm chez ST. Il est composé d'une partie analogique effectuant une conversion A/N à 4Gech/s et une conversion N/A à 2Gech/s. Un circuit de gestion d'horloge permet de router une horloge à 4GHz en entrée, et de la diviser pour fournir une horloge à 500MHz au circuit numérique. Le circuit numérique, de son coté, est composé de la couche PHY complète IR-UWB décrite précédement, et de deux couches MAC, la maitre et l'esclave, qui sont changeable au démarrage. Les protocoles WiDeCS pour la synchronisation, et WiDeLoc pour l'évaluation de temps de vol sont implémentés dans ces deux couches MAC. Une surcouche d'adaptation de signaux permet de limiter le nombre d'E/S numériques à 12, et ainsi respecter la contrainte de taille pour l'ASIC.

Pour concevoir une telle preuve de concept fonctionnelle sur ASIC en CMOS 65nm, il a également fallu concevoir un processus adapté à la conception de circuits mixtes pouvant utiliser les librairies numériques fournies par le fondeur. Le design de puce ainsi conçu a pu etre fabriqué et est présenté en figure 48.

De nombreuses contraintes ayant forcé la conception d'une puce spécifique, tant au niveau des fréquences d'horloge, qu'au niveau des entrées et sorties de déboggage, il a également été necessaire de concevoir un banc de test spécifique. Ce banc de test, permettant le montage seul ou face à face de deux puces, propose des alimentations séparées, de même que des entrées et sources d'horloges séparées également. Les puces sont reliées sur cette carte de sorte que la sortie UWB de l'une entre dans l'entrée de l'autre, et vice versa. Les conditions de test appliquées

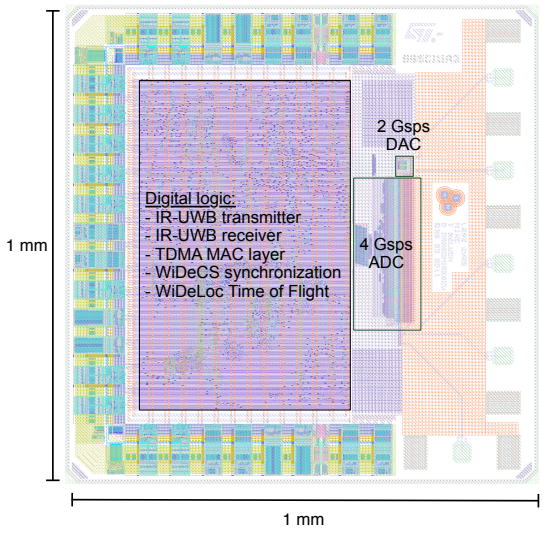

Figure 48: WIDEMACV1 - vue CAO

à ces puces ont donc consisté à faire varier des paramètres comme les fréquences de fonctionnement, les tensions d'alimentation, les réglage d'adresse, et le passage en mode déboggage. Ces essais ont permis de vérifier dans un premier temps la fonctionnalité annoncée de cette bande de base, et de démontrer que la fréquence de fonctionnement de 4GHz peut etre atteinte et permettre des débits jusqu'à 500Mb/s. L'erreur de synchronisation de prise de mesure, inférieure à 2.8ns dans 95% des cas, reste correcte et inférieure à 6ns quand les horloges ont une dérive relative de 500ppm. La consommation totale mesurée en fonctionnement est de 48mW, ce qui rapporté à la consommation pour un bit transmis et recu revient à 94.5pJ/bit.

5.5 CONCLUSION

Ce chapitre a montré plusieurs démonstrateurs réalisés dans le cadre de cette thèse, allant progressivement des simulations matérielles, vers une puce ASIC implémentant l'ensemble des travaux réalisés. En comparaison des simulations matérielles, les performances du système ASIC, bien que placé dans des conditions favorables, atteint une précision de synchronisation inférieure à la période de l'horloge numérique. Les perspectives pour ce système incluent des efforts supplémentaires sur la réduction de consommation, notamment par des techniques de power gating, qui permettrait de couper l'alimentation des blocs inutilisés. D'autres perspectives consistent également à intégrer ce baseband réalisé comme périphérique d'un bus standard sur un SoC, permettant ainsi son interfaçage avec un processeur type ARM Cortex M. Cela permettrait d'augmenter les reconfigurations possibles, et de faire effectuer des taches au plus près du capteur.

CONCLUSION GÉNÉRALE

Le travail présenté dans cette thèse visait à améliorer les performances des interfaces radios pour réseaux de capteurs. Pour ce faire, deux contextes particuliers des domaines aéronautique et militaires ont été visés. Pour répondre aux besoins de ces applications, un concept de bande de base a été proposé. Cette bande de base implémente une couche PHY en radio impulsionnelle UWB, une couche MAC spécifique, et des services de synchronisation de prises de mesure WiDeCS, et dévaluation de temps de vol WiDeLoc. Plusieurs démonstrateurs ont été conçus et fabriqués, et ont permis de démontrer des performances au delà de létat de lart, notamment au niveau de la synchronisation qui a atteint une erreur de synchronisation inférieure à 3ns sur le démonstrateur ASIC. La consommation énergétique de cette bande de base est également inférieure à létat de lart, avec 94.5pJ/bit pour lASIC avec une horloge à 3GHz. Des perspectives damélioration de ce concept se situent principalement dans lintégration de celle ci dans un système sur puce complet pouvant à terme réaliser seul les taches dacquisition, de traitement et de transmission des mesures pour des réseaux de mesure.

Part III

APPENDIX

A

FPGA IMPLEMENTATION FLOW

A.1 INTRODUCTION

The following FPGA development and implementation flow has been designed and improved for some parts from multiple sources. Among them, the first one to serve as a basis for this flow is Daniela Dragomirescu's graduate level VHDL for FPGA course.

Considering the ASIC implementation being the ultimate objective for this thesis work, the FPGA implementation flow is a step towards this objective. This is why the flow describes herebelow is lacking some optimizations regarding specific delays on I/Os and performace adjustements. The FPGA design and implementation flow is then performed as in figure 49. This document details these steps, as well as conditions for considering a step successful in the order given in figure 49.

A.2 HDL CODING, AND IP BLOCKS IMPLEMENTATION

Most of the design tasks are performed by coding algorithms and DSP implementations in the VHDL language. This language presents many advantages for building circuits. However, it posesses one major drawback. Among the listed advantages, the most interesting is a stringent syntax. Owing to this property, VHDL helps in designing reliable circuits with a low probability of undetected errors. Other advantages include signal types, processes, STD_logic and STD_ulogic types for taking into account all the possible values of a signal in a chip. The major drawback of VHDL, on the other side, is the fact that most of the code compilers and synthesizers are taking Verilog language as the primary input. VHDL code is often pre-analyzed and pre-compiled before processing the other steps, thus reducing the overall performance.

Considering its advantages and drawbacks, VHDL language remains very useful for rapid prototyping new algorithms and circuit designs. Errors are raised earlier in the process, and help gaining time in debugging. After reading a course on VHDL coding, one can design a working chip. This section aims at providing useful tips at whoever knows how to code in VHDL, but wants to improve the quality of results.

A.2.1 *Conditions*

The *if* condition is often overused by newcomers to VHDL programming. The way the designer writes a similar algorithm does drastically change the attainable performance.

As an example, the following three VHDL processes are correct in their syntax. However, the implementation resulting from a synthesis of each one of them depends on the number of possible misinterpretations of the code by the compiler.

```
if_only : process(clk)
        variable c : integer;
begin
        if (rising_edge(clk)) then
                if (rst_n = '0') then   -- reset low
                        a <= 1; -- signal init (Integer)
                        b <= 3; -- signal init (Integer)
                        c := 2;
                else
                        if (a = 3) then    -- if 1
                                c := c+1;
                        end if;
                        if (b = 5) then    -- if 2
                                a <= a-1;
                        end if;
                        if (c = 10) then          -- if 3
                                b <= 1;
                                a <= 2;
                        end if;
                end if;
        end if;
end process;
```

This code will be sequentially interpreted during simulation, and the affectation of variable c will be performed before testing it in the next if statement. However, many synthesizers do generate RTL logic with a random behavior for this specific code. In this case, it is advised to avoid using variables in the code, and to avoid consecutive if statements that may be entered in the same pass.

A better choice would be to use the elsif statement.

```
if_elsif : process(clk)
begin
        if (rising_edge(clk)) then
                if (rst_n = '0') then   -- reset low
                        a <= 1; -- signal init (Integer)
                        b <= 3; -- signal init (Integer)
                        c <= 2; -- signal init (Integer)
                else
                        if (a = 3) then    -- if 1
                                c <= c+1;
                        elsif (b = 5) then      -- if 2
                                a <= a-1;
                        elsif ((c = 10) or ((c = 9) and (a = 3)) then   -- if
                            3
                                b <= 1;
```

```
                                a <= 2;
                        end if;
                end if;
        end if;
end process;
```

The behavior of this process is the same as the previous writing in simulation. However, this writing helps the synthesizer in optimizing the RTL implementation, and avoid random behavior.

A.2.2 *Signal versus variable*

The difference between signals and variables is a concept I think is hard to aprehend for students who are used to develop only sequential computer code. However, a simple recommendation can help in better determining wether to use a signal or a variable when coding in VHDL. A signal will be used to store an information and make it accessible to every process in its module. The signal's value accessed when reading it in a process is the value the signal had at the begining of the execution of the process. On the other side, when setting a signal's value in a process, it will be actually set only at the end of this process, and will take the latest value given in the process. The hardware implementation of a signal is then a simple register setting the value at the clock edge, and making it accessible.

On the other side a variable is set inside a process, and is accessible from the process itself. In the process, the value is directly set and accessible with the same constaints as in a computer code. However, the impementation of a variable requires a latch for every write access to it in the process, and then slows the process proportionnally to the number of affectations to the same variable it contains.

To conclude on signal versus variable, a signal shall be used everytime it is possible, even if some supplementary coding is required because of the delay caused by its late affectation.

A.2.3 *On-chip buses*

Tri-state implementations of buses are widely used in communication between chips. These buses do indeed require a limited number of transmission lines to be routed on the PCB, and then reduce the cost in terms of routing complexity. However, tri-state cells are extremely rare in the ASIC world, and do require more complex implementation than usual latches and gates. For these reasons, most of the on-chip buses are based on an arbiter distributing the right to transmit data to and from modules connected to it and routing this data from the transmitter of the data to its recipient. Among the most used on-chip buses, we can count ARM AMBA bus collection, which includes APB bus for low speed peripherals, AHB bus for high speed peripherals and medium speed memory, and AXB which is the fastest bust present in AMBA 3 specification. An other bus, more used in the academic context, is the WishBone bus. This open-source bus proposed by

OpenCores is very similar to the AHB bus implementation, and provides similar performance.

A.2.4 *chip's input / outputs*

The I/Os of the top level shall follow these requirements, in order to avoid signal type modification during synthesis. Following these requirements also keeps a match between the I/Os of the different architectures of the chip, from the behavioral VHDL, to the backannotated placed and routed chip's model.

The main rule is to only use STD_logic and STD_ulogic signal types, along with their respective vector variants STD_logic_vector and STD_ulogic_vector. Using this only signal type for all the I/Os of the top module will ensure constant interfaces for the chip, and will keep the testbench matched to the implementation.

A.3 BEHAVIORAL SIMULATION

The functionnal simulation is aimed at verifying the correct functioning of a synthesizable HDL coded chip. For this task, non synthesizable models of peripherals, and communication channels are developed to match the real working environment for the future chip.

Once this is done, the chip's HDL model, as well as the peripheral and environment models are connected in a testbench, and are fed with the planned input signals such as a correct clock, a reset signal, and other application related I/Os. Notice that models for the implemented IP blocks either have to be compiled along with the behavioral model of the circuit, or be pre-compiled and hard linked inside the simulator's configuration files (i.e. synopsys_sim.setup)

Simulation is performed using Synopsys VCS simulator. This choice has been made to keep the same simulator for both the FPGA implementation flow, and the ASIC implementation flow. VCS allows Unified Power Format (UPF) low power description format for specifying power zones with specific power supply levels, power gating, and other Dynamic Voltage and Frequency Scaling (DVFS) functionalities.

VHDL simulation in VCS is performed through the three following command lines, considering VCS is correctly setup and added to the system's PATH.

```
vhdlan -full64 -debug -nc -vhdl08 -w {library} {src-files}
vcs -full64 -debug -nc {top level}
./simv -gui
```

Debuging the algorithm implementation can be performed by checking the functioning of the behavioral model in simulation, and correcting the code accordingly.

A.4 SYNTHESIS

Once the behavioral simulation gives satisfying results responding to all the requirements, the next step is to synthesize the implementation by using a standard cell library from the chosen design kit. Pre-synthesized IP do often require a specific design kit for synthesis on a specific FPGA.

Synthesizers such as Synopsys Synplify do make use design constraint files for specifying the location of the FPGA pads linked to every I/O pad of the top level. These files do also specify the different clocks present in the system, specific delays may also be included when peripherals do posess specific requirements in terms of setup time for example. Synplify's advised file format is *.sdc for Synopsys Design Constraints. These design constraints also include pad assignment for every port of the top level module, as well as parameters such as power level delivered by each pad, and potential buffers required.

Synthesis is then performed through a Graphical User Interface (GUI), and results in a RTL logic implementation ready for place and route steps, or for istrumentation step. Other outputs of the synthesis process include power, occupation and timing reports, along with a post-synthesis simulation model. Post synthesis operation is similar to the behavioral model simulation. However, in this case, it is necessary to compile the design-kit model libraries for the simulator to have access to the functioning of every implemented gate, latch, or pad.

A.5 PLACE AND ROUTE

The place and route step is run after a successful place and route, confirmed with post-synthesis simulation and/or formal verification.

This step results in a BIT file ready to be programmed on the FPGA. Other ouput formats include MCS format for programming the FPGA content in a flash memory which is run at every powerup of the FPGA and loaded at this time.

A.6 IN SYSTEM DEBUGGING

In-system debugging is achieved through FPGA instrumentation and monitoring softwares. Two different softwares have been used in this work, mostly for bug related reasons. These softwares, Chipscope from Xilinx, and Identify from Synopsys, work by first instrumenting a synthesized module and then running the FPGA in monitored mode. Istrumentation requires specifying the clock signal, monitored signals, trigger equations, ad well as memory depth. Owing to these parameters, complementary RTL logic is implemented in the synthesized modules, adds memory for storing signal value history, and adds a communication block for transmitting data to the computer software.

Once this instrumentation is done, a synthesized file is issued, ready for continuing the flow through place and route operations.

When running an instrumented design, waveforms are issued every time a trigger event occurs in the FPGA.

In system debugging then allows to check the behaviour of a digital design in its real operation context. In this work, this step was necessary because of the lack of models concerning the ADC used for digitizing the baseband signals in the receiver.

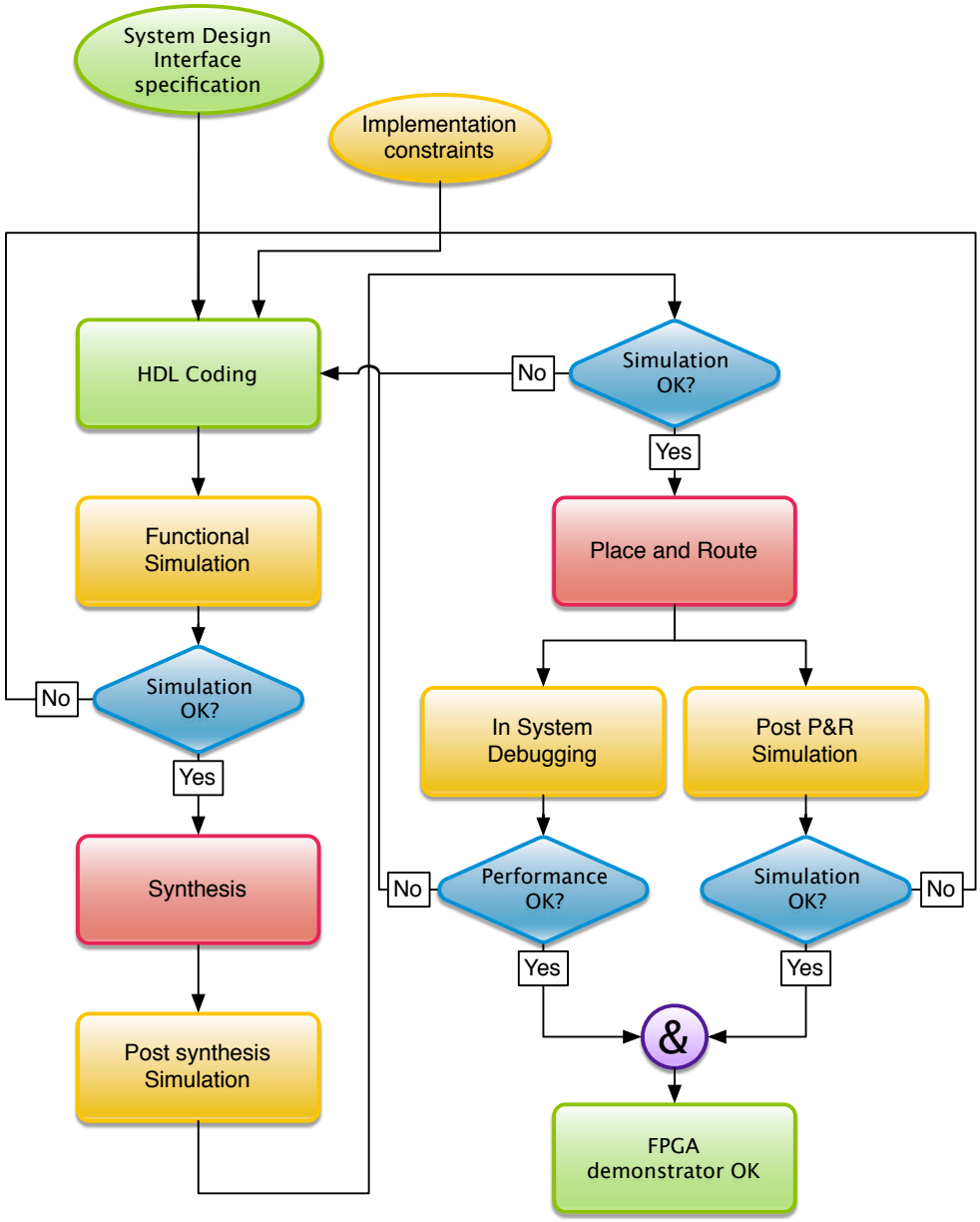

Figure 49: FPGA Flow

BIBLIOGRAPHY

[1] Technology | WirelessHD, . URL http://www.wirelesshd.org/about/technology/.

[2] ZigBee Alliance, . URL http://www.zigbee.org/.

[3] Structural Health Monitoring Company | MD7 Digital SHM System, PZT based SHM, CNT based SHM, . URL http://www.metisdesign.com/structural-health-monitoring-company.html.

[4] 802.11-2012, . URL http://ieeexplore.ieee.org/xpl/articleDetails.jsp?tp=&arnumber=6178212&contentType=Standards&refinements%3D4294965216%26sortType%3Ddesc_p_Publication_Year%26searchField%3DSearch_All%26queryText%3D802.11.

[5] ZigBee Home Automation, . URL http://www.freescale.com/webapp/sps/site/overview.jsp?code=ZIGBEE_HOMEAUTOMATION#.

[6] A parameter study of stripline-fed Vivaldi notch-antenna arrays. *IEEE Transactions on Antennas and Propagation*, 47(5):879–886, May 1999.

[7] 802.11b-1999/Cor 1-2001, 2001.

[8] On the distribution of the peak-to-average power ratio in OFDM signals. *IEEE Transactions on Communications*, 49(2):282–289, 2001.

[9] 50.2-71 GHz realignement. 66(15):7402–7408, January 2001.

[10] IEEE 1588 standard, 2004.

[11] US Code of Federal Regulation (CFR). October 2004.

[12] IEEE Standard for Information Technology - Telecommunications and Information Exchange Between Systems - Local and Metropolitan Area Networks - Specific Requirements. - Part 15.1: Wireless Medium Access Control (MAC) and Physical Layer (PHY) Specifications for Wireless Personal Area Networks (WPANs). *IEEE Std 802.15.1-2005 (Revision of IEEE Std 802.15.1-2002*, page 0, 2005.

[13] 802.15.4-2006, 2006.

[14] IEEE Std 1451.5, 2007.

[15] IEEE Standard for Information Technology - Telecommunications and Information Exchange Between Systems - Local and Metropolitan Area Networks - Specific Requirement Part 15.4: Wireless Medium Access Control (MAC)

and Physical Layer (PHY) Specifications for Low-Rate Wireless Personal Area Networks (WPANs). *IEEE Std 802.15.4a-2007 (Amendment to IEEE Std 802.15.4-2006*, pages 1–203, 2007.

[16] 802.15.3c-2009, 2009.

[17] Wireless Universal Serial Bus Specification 1.1 , September 2010.

[18] 802.15.4-2011, 2011.

[19] United States of America. FCC Code of Federal Register (CFR).

[20] D Barras, G von Bueren, W Hirt, and H Jaeckel. A multi-modulation low-power FCC/EC-compliant IR-UWB RF transmitter in 0.18-μm CMOS. *Radio Frequency Integrated Circuits Symposium, 2009. RFIC 2009. IEEE*, pages 69–72, 2009.

[21] T Baykas, Chin-Sean Sum, Zhou Lan, Junyi Wang, M A Rahman, H Harada, and S K Communications Magazine IEEE Kato. IEEE 802.15.3c: the first IEEE wireless standard for data rates over 1 Gb/s. *Communications Magazine, IEEE*, 49(7), 2011.

[22] T. Beluch, D Dragomirescu, and R Plana. A sub-nanosecond Synchronized MAC-PHY Cross-layer design for Wireless Sensor Networks. *Ad Hoc Networks*, 2012.

[23] Thomas Beluch, Daniela Dragomirescu, Florian Perget, and Robert plana. Cross-Layered Synchronization Protocol for Wireless Sensor Networks. In *Networks (ICN), 2010 Ninth International Conference on*, pages 167–172, 2010.

[24] R Blazquez, P P Newaskar, F.S Lee, and A.P Chandrakasan. A baseband processor for impulse ultra-wideband communications. *Solid-State Circuits, IEEE Journal of*, 40(9):1821–1828, 2005.

[25] T Borr, J Juyon, and E Tournier. A both Gaussian and sinusoidal phase-to-amplitude converter for low-power ultra-high-speed direct digital synthesizers. In *New Circuits and Systems Conference (NEWCAS), 2011 IEEE 9th International*, pages 5–8, 2011.

[26] J V Capella, A Bonastre, J J Serrano, and R Ors. 2009 International Conference on Wireless Networks and Information Systems. In *2009 International Conference on Wireless Networks and Information Systems (WNIS)*, pages 395–398. IEEE.

[27] D Cassioli, M.Z Win, F Vatalaro, and A.F Molisch. Low Complexity Rake Receivers in Ultra-Wideband Channels. *Wireless Communications, IEEE Transactions on*, 6(4):1265–1275, 2007.

[28] Matteo Ceriotti, Luca Mottola, Gian Pietro Picco, Amy L Murphy, Stefan Guna, Michele Corra, Matteo Pozzi, Daniele Zonta, and Paolo Zanon. *Monitoring heritage buildings with wireless sensor networks: The Torre Aquila deployment*. IEEE Computer Society, April 2009.

[29] C C Chao, W Y Jen, Y P Chi, and B Lin. Inderscience Publishers - Log In - Resource Secured. *International Journal of Electronic . . .*, 2007.

[30] Q.M Chaudhari, E Serpedin, and K Qaraqe. On Minimum Variance Unbiased Estimation of Clock Offset in a Two-Way Message Exchange Mechanism. *Information Theory, IEEE Transactions on*, 56(6):2893–2904, 2010.

[31] Pedro Cheong, Ka-Fai Chang, Ying-Hoi Lai, Sut-Kam Ho, Iam-Keong Sou, and Kam-Weng Tam. A ZigBee-Based Wireless Sensor Network Node for Ultraviolet Detection of Flame. *IEEE Transactions on Industrial Electronics*, 58 (11):5271–5277.

[32] B Chowdhury and R Khosla. RFID-based hospital real-time patient management system. *. . . Science*, 2007.

[33] T Cooklev, JC Eidson, and A Pakdaman. An Implementation of IEEE 1588 Over IEEE 802.11b for Synchronization of Wireless Local Area Network Nodes. *Instrumentation and Measurement, IEEE Transactions on*, 56(5):1632–1639, 2007.

[34] Denis C. Daly, Patrick P. Mercier, Manish Bhardwaj, Alice L. Stone, Zane N. Aldworth, Thomas L. Daniel, Joel Voldman, John G. Hildebrand, and Anantha P. Chandrakasan. A Pulsed UWB Receiver SoC for Insect Motion Control. In *Ieee Journal of Solid-State Circuits*, pages 153–166. MIT, Cambridge, MA 02139 USA, 2010.

[35] J Dederer, B Schleicher, A Trasser, T Feger, and H Schumacher. A fully monolithic 3.1-10.6 GHz UWB Si/SiGe HBT Impulse-UWB correlation receiver. In *Ultra-Wideband, 2008. ICUWB 2008. IEEE International Conference on*, pages 33–36, 2008.

[36] Michael J Dunn. Global Positioning System Directorate Systems Engineering & Integration Interface Specification IS-GPS-200, March 2012.

[37] ECMA International. Standard ECMA-368, December 2008. URL http://www.ecma-international.org/publications/standards/Ecma-368.htm.

[38] ECMA International. Standard ECMA-387. *ECMA-international*, pages 1–302, December 2010.

[39] Jeremy Elson, Lewis Girod, and Deborah Estrin. Fine-grained network time synchronization using reference broadcasts. *SIGOPS Operating Systems Review*, 36(SI), December 2002.

[40] C.C Enz, A El-Hoiydi, J.-D Decotignie, and V Peiris. WiseNET: an ultralow-power wireless sensor network solution. *Computer*, 37(8):62–70, 2004.

[41] J R Fernandes and D Wentzloff. Recent advances in IR-UWB transceivers: An overview. In *Circuits and Systems (ISCAS), Proceedings of 2010 IEEE International Symposium on*, pages 3284–3287, 2010.

[42] R.J Fontana and S J Gunderson. Ultra-wideband precision asset location system. In *2002 IEEE Conference on Ultra Wideband Systems and Technologies*, pages 147–150. IEEE.

[43] R.J Fontana, E Richley, and J Barney. Commercialization of an ultra wideband precision asset location system. In *Ultra Wideband Systems and Technologies, 2003 IEEE Conference on*, pages 369–373, 2003.

[44] Saurabh Ganeriwal, Ram Kumar, and Mani B Srivastava. Timing-sync protocol for sensor networks. In *SenSys '03: Proceedings of the 1st international conference on Embedded networked sensor systems*. ACM Request Permissions, November 2003.

[45] A Genser, C Bachmann, C Steger, J Hulzink, and M Berekovic. Low-Power ASIP Architecture Exploration and Optimization for Reed-Solomon Processing. In *Application-specific Systems, Architectures and Processors, 2009. ASAP 2009. 20th IEEE International Conference on*, pages 177–182, 2009.

[46] P.J Gibson. The Vivaldi Aerial. In *Microwave Conference, 1979. 9th European*, pages 101–105, 1979.

[47] I Guvenc and Chia-Chin Chong. A Survey on TOA Based Wireless Localization and NLOS Mitigation Techniques. *Communications Surveys & Tutorials, IEEE*, 11(3):107–124, 2009.

[48] I Guvenc, Z Sahinoglu, and P V Orlik. TOA estimation for IR-UWB systems with different transceiver types. *IEEE Transactions on Microwave Theory and Techniques*, 54(4):1876–1886.

[49] J Halamka. Early experiences with positive patient identification. *Journal of Healthcare Information Management*, 2006.

[50] Tyler Harms, Sahra Sedigh, and Filippo Bastianini. Structural Health Monitoring of Bridges Using Wireless Sensor Networks. *IEEE Instrumentation & Measurement Magazine*, 13(6):14–18.

[51] Ghobad Heidari. *WiMedia UWB*. Technology of Choice for Wireless USB and Bluetooth. Wiley, January 2009.

[52] W R Heinzelman, A Chandrakasan, and H Balakrishnan. Energy-Efficient Communication Protocol for Wireless Microsensor Networks. In *HICSS33: Hawaii International Conference on System Sciences*, page 10. IEEE Comput. Soc.

[53] J Henaut, D Dragomirescu, and R Plana. FPGA Based High Date Rate Radio Interfaces for Aerospace Wireless Sensor Systems. *Systems, 2009. ICONS '09. Fourth International Conference on*, pages 173–178, 2009.

[54] Shu-Chiung Hu, You-Chiun Wang, Chiuan-Yu Huang, and Yu-Chee Tseng. Measuring air quality in city areas by vehicular wireless sensor networks. *Journal of Systems and Software*, 84(11), November 2011.

[55] Yi Huang, Yang Lu, H Chattha, Xu Zhu, I Hewitt, and S Hussain. UWB antennas for radio positioning systems. *Antennas and Propagation, 2009. EuCAP 2009. 3rd European Conference on*, pages 3779–3782, 2009.

[56] J Kannisto, T Vanhatupa, M Hannikainen, and T.D Hamalainen. Software and hardware prototypes of the IEEE 1588 precision time protocol on wireless LAN. *Local and Metropolitan Area Networks, 2005. LANMAN 2005. The 14th IEEE Workshop on*, page 6, 2005.

[57] Tufan Karalar and Jan Rabaey. An RF ToF Based Ranging Implementation for Sensor Networks . In *2006 IEEE International Conference on Communications*, pages 3347–3352. IEEE.

[58] Simarpreet Kaur and Leena Mahaj. Power Saving MAC Protocols for WSNs and Optimization of S-MAC Protocol. *International Journal of Radio Frequency Identification & Wireless Sensor Networks*, page 1, 2011.

[59] Miguel A Labrador and Pedro M Wightman. *Topology control in wireless sensor networks*. with a companion simulation tool for teaching and research. Springer Verlag, 2009.

[60] D Lachartre, B Denis, D Morche, L Ouvry, M Pezzin, B Piaget, J Prouvee, and P Vincent. A 1.1nJ/b 802.15.4a-compliant fully integrated UWB transceiver in 0.13μm CMOS. In *Solid-State Circuits Conference - Digest of Technical Papers, 2009. ISSCC 2009. IEEE International*, pages 312–313, 2009.

[61] A Lecointre, D Dragomirescu, and R Plana. Largely reconfigurable impulse radio UWB transceiver. *Electronics Letters*, 46(6):453–U102, 2010.

[62] A Lecointre, D Dragomirescu, and R Plana. Largely reconfigurable impulse radio UWB transceiver. *Electronics Letters*, 46(6):453–455, 2010.

[63] Aubin Lecointre, Daniela Dragomirescu, and Robert plana. Design and Hardware Implementation of a Reconfigurable Mostly Digital IR-UWB Radio. *Romanian Journal of Information Science and Technology*, 11(4):295–318, 2008.

[64] LeCroy. WaveMaster® 8 Zi-A Series Datasheet. URL http://cdn.lecroy.com/files/pdf/lecroy_sda_8_zi-a_datasheet.pdf.

[65] C P Lee and J P Shim. An exploratory study of radio frequency identification (RFID) adoption in the healthcare industry. *European Journal of Information Systems*, 2007.

[66] F.S Lee, R Blazquez, B.P Ginsburg, J.D Powell, M Scharfstein, D.D Wentzloff, and A.P Chandrakasan. A 3.1 to 10.6 GHz 100 Mb/s Pulse-Based Ultra-Wideband Radio Receiver Chipset. In *Ultra-Wideband, The 2006 IEEE 2006 International Conference on*, pages 185–190, 2006.

[67] Xinrong Li. Performance study of RSS-based location estimation techniques for wireless sensor networks. In *Military Communications Conference, 2005. MILCOM 2005. IEEE*, pages 1064–1068. IEEE, 2005.

[68] Dayang Lin, B Schleicher, A Trasser, and H Schumacher. A SiGe HBT low-power pulse generator for impulse radio ultra-wide band applications. In *Ultra-Wideband (ICUWB), 2010 IEEE International Conference on*, pages 1–4, 2010.

[69] Dayang Lin, B Schleicher, A Trasser, and H Schumacher. Si/SiGe HBT UWB impulse generator tunable to FCC, ECC and Japanese spectral masks. *Radio and Wireless Symposium (RWS), 2011 IEEE*, pages 66–69, 2011.

[70] Gang Lu, B Krishnamachari, and C S Raghavendra. An Adaptive Energy-Efficient and Low-Latency MAC for Data Gathering in Wireless Sensor Networks. In *18th International Parallel and Distributed Processing Symposium, 2004.*, pages 224–231. IEEE.

[71] S Mandal, D Saha, and T Banerjee. A neural network based prediction model for flood in a disaster management system with sensor networks. In *2005 International Conference on Intelligent Sensing and Information Processing, 2005.*, pages 78–82. IEEE.

[72] Miklós Maróti, Branislav Kusy, Gyula Simon, and Ákos Lédeczi. The Flooding Time Synchronization Protocol. In *SenSys*, pages 39–49. Baltimore, MD, USA, 2004.

[73] P.P Mercier, M Bhardwaj, D.C Daly, and A.P Chandrakasan. A 0.55V 16Mb/s 1.6mW non-coherent IR-UWB digital baseband with $\pm$1ns synchronization accuracy. In *Solid-State Circuits Conference - Digest of Technical Papers, 2009. ISSCC 2009. IEEE International*, pages 252–253, 2009.

[74] MicroChip. Microchip MiWiTM Wireless Networking Protocol Stack. URL http://ww1.microchip.com/downloads/en/AppNotes/AN1066%20-%20MiWi%20App%20Note.pdf.

[75] A.F Molisch, K Balakrishnan, D Cassioli, C C Chong, S Emami, A Fort, J Karedal, J Kunisch, H Schantz, and U Schuster. IEEE 802.15. 4a channel model-final report. *IEEE P802*, 15(04):0662, 2004.

[76] A.F Molisch, K Balakrishnan, D Cassioli, Chia-Chin Chong, S Emami, A Fort, J Karedal, J Kunisch, H Schantz, and K Siwiak. A comprehensive model for ultrawideband propagation channels. In *Global Telecommunications Conference, 2005. GLOBECOM '05. IEEE*, page 6, 2005.

[77] E Montón, J F Hernandez, J M Blasco, T Hervé, J Micallef, I Grech, A Brincat, and V Traver. Body area network for wireless patient monitoring. *IET Communications*, 2(2):215, 2008.

[78] D Morche, F Hameau, D Lachartre, G Masson, C Mounet, M Pelissier, D Helal, L Smaini, and D Belot. Digital Radio Front-End for High Data Rate Impulse UWB System. In *Electronics, Circuits and Systems, 2006. ICECS '06. 13th IEEE International Conference on*, pages 788–791, 2006.

[79] Y Q Ni, Y Xia, W Y Liao, and J M Ko. Technology innovation in developing the structural health monitoring system for Guangzhou New TV Tower. ... *Control and Health Monitoring*, 2009.

[80] S Palchaudhuri, A.K Saha, and D.B Johnsin. Adaptive clock synchronization in sensor networks. *Information Processing in Sensor Networks, 2004. IPSN 2004. Third International Symposium on*, pages 340–348, 2004.

[81] A.S Paul and E.A Wan. RSSI-Based Indoor Localization and Tracking Using Sigma-Point Kalman Smoothers. *Selected Topics in Signal Processing, IEEE Journal of*, 3(5):860–873, 2009.

[82] E Perahia, C Cordeiro, Minyoung Park, and L.L Yang. IEEE 802.11ad: Defining the Next Generation Multi-Gbps Wi-Fi. In *Consumer Communications and Networking Conference (CCNC), 2010 7th IEEE*, pages 1–5, 2010.

[83] S Ping. Delay measurement time synchronization for wireless sensor networks. *Intel Research*, 2003.

[84] G Rahmatollahi, M Guirao, S Galler, and T Kaiser. Position estimation in IR-UWB autonomous wireless sensor networks. *Positioning, Navigation and Communication, 2008. WPNC 2008. 5th Workshop on*, pages 259–263, 2008.

[85] Venkatesh Rajendran, Katia Obraczka, and J J Garcia-Luna-Aceves. Energy-efficient collision-free medium access control for wireless sensor networks. In *SenSys '03: Proceedings of the 1st international conference on Embedded networked sensor systems*. ACM Request Permissions, November 2003.

[86] Red Rapids. *Channel Express 365 datasheet*.

[87] Rhode&Schwartz. RTO Digital Oscilloscopes product page.

[88] Hans G Schantz. A real-time location system using near-field electromagnetic ranging. In *2007 IEEE Antennas and Propagation International Symposium*, pages 3792–3795. IEEE, 2007.

[89] B Schleicher, J Dederer, and H Schumacher. Si/SiGe HBT UWB impulse generators with sleep-mode targeting the FCC masks. In *Ultra-Wideband, 2009. ICUWB 2009. IEEE International Conference on*, pages 674–678, 2009.

[90] C.E Shannon. Communication in the Presence of Noise. In *Proceedings of the IRE*, pages 10–21, 1949.

[91] S Shiwei Zhao, P Orlik, A.F Molisch, H Huaping Liu, and J Jinyun Zhang. Hybrid Ultrawideband Modulations Compatible for Both Coherent and Transmit-Reference Receivers. *Wireless Communications, IEEE Transactions on*, 6(7):2551–2559, 2007.

[92] P Silva, M Paralta, R Caldeirinha, J Rodrigues, and C Serodio. Traceme — indoor real-time location system. *Industrial Electronics, 2009. IECON '09. 35th Annual Conference of IEEE*, pages 2721–2725, 2009.

[93] L Smaini, C Tinella, D Helal, C Stoecklin, L Chabert, C Devaucelle, R Cattenoz, N Rinaldi, and D Belot. Single-chip CMOS pulse generator for UWB systems. *Solid-State Circuits, IEEE Journal of*, 41(7):1551–1561, 2006.

[94] L Stoica, S Tiuraniemi, I Oppermann, and H Repo. An ultra wideband impulse radio low complexity transceiver architecture for sensor networks. In *Ultra-Wideband, 2005. ICU 2005. 2005 IEEE International Conference on*, pages 55–59, 2005.

[95] Bharath Sundararaman, Ugo Buy, and Ajay D Kshemkalyani. Clock synchronization for wireless sensor networks: a survey. *Ad Hoc Networks*, 3:281–323, 2005.

[96] A Tamtrakarn, H Ishikuro, K Ishida, M Takamiya, and T Sakurai. A 1-V 299/spl mu/W Flashing UWB Transceiver Based on Double Thresholding Scheme. *VLSI Circuits, 2006. Digest of Technical Papers. 2006 Symposium on*, pages 202–203, 2006.

[97] T Terada, S Yoshizumi, M Muqsith, Y Sanada, and T Kuroda. A CMOS ultra-wideband impulse radio transceiver for 1-Mb/s data communications and +/- 2.5-cm range finding. In *Ieee Journal of Solid-State Circuits*, pages 891–898. Keio Univ, Dept Elect & Elect Engn, Yokohama, Kanagawa 2238522, Japan, 2006.

[98] Tijs van Dam and Koen Langendoen. An adaptive energy-efficient MAC protocol for wireless sensor networks. In *SenSys '03: Proceedings of the 1st international conference on Embedded networked sensor systems*. ACM Request Permissions, November 2003.

[99] N Van Helleputte, M Verhelst, W Dehaene, and G Gielen. A Reconfigurable, 130 nm CMOS 108 pJ/pulse, Fully Integrated IR-UWB Receiver for Communication and Precise Ranging. *Solid-State Circuits, IEEE Journal of*, 45(1):69–83, 2010.

[100] Nick Van Helleputte and Georges Gielen. A 70 pJ/Pulse Analog Front-End in 130 nm CMOS for UWB Impulse Radio Receivers. In *Ieee Journal of Solid-State*

Circuits, pages 1862–1871. Katholieke Univ Leuven, ESAT MICAS, B-3001 Leuven, Belgium, 2009.

[101] David D Wentzloff and Anantha P Chandrakasan. A 47pJ/pulse 3.1-to-5GHz All-Digital UWB Transmitter in 90nm CMOS. In *Solid-State Circuits Conference, 2007. ISSCC 2007. Digest of Technical Papers. IEEE International*, pages 118–591, 2007.

[102] D.D Wentzloff and A.P Chandrakasan. Gaussian pulse Generators for subbanded ultra-wideband transmitters. *Microwave Theory and Techniques, IEEE Transactions on*, 54(4):1647–1655, 2006.

[103] Jinyun Zhang, Philip V. Orlik, Zafer Sahinoglu, Andreas F. Molisch, and Patrick Kinney. UWB Systems for Wireless Sensor Networks. *Proceedings of the Ieee*, 97(2):313–331, 2009.

[104] Y.J Zheng, S.-X Diao, C.-W Ang, Y Gao, F.-C Choong, Z Chen, X Liu, Y.-S Wang, X.-J Yuan, and C.H Heng. A 0.92/5.3nJ/b UWB impulse radio SoC for communication and localization. In *Solid-State Circuits Conference Digest of Technical Papers (ISSCC), 2010 IEEE International*, pages 230–231, 2010.